Spring 1990

New approaches to fiber optic chemical sensors for ions

Marian Frances McCurley
University of New Hampshire, Durham

Order Number 9027434

New approaches to fiber optic chemical sensors for ions

McCurley, Marian Frances, Ph.D.

University of New Hampshire, 1990

U·M·I

300 N. Zeeb Rd.
Ann Arbor, MI 48106

NEW APPROACHES TO FIBER OPTIC CHEMICAL SENSORS FOR IONS

BY

MARIAN F. MCCURLEY
A.B., College of the Holy Cross, 1984

DISSERTATION

Submitted to the University of New Hampshire
in Partial Fulfillment of
the Requirements for the Degree of

Doctor of Philosophy

in

Chemistry

May, 1990

This dissertation has been examined and approved.

Dissertation director, W. Rudolf Seitz
Professor of Chemistry

Christopher F. Bauer
Associate Professor of Chemistry

Howard R. Mayne
Assistant Professor of Chemistry

Richard P. Johnson
Associate Professor of Chemistry

Donald C. Sundberg
Professor of Chemical Engineering

4.5.90
Date

DEDICATION

to my mother, for teaching me that I have choices and supporting me in the ones I have made,

to my brother and sisters for keeping me humble,

to Ed for being the wind beneath my wings,

and in memory of my father - Dad, thank-you for your gentle strength, quiet love and constant support. You are never far from my heart.

ACKNOWLEDGEMENTS

I thank Dr. W. Rudolf Seitz, your support, encouragement and advice have transformed a naive young student into a wiser yet not jaded scientist.

I thank the chemistry faculty, especially Dr. Sterling Tommellini and Dr. Christopher Bauer for their guidance in my years at UNH.

I wish to thank my fellow graduate students both past and present for making my time here an enjoyable one.

I would like to express my gratitude to John Grady for running the EPR spectra and Dr. N. Dennis Chasteen for helping in their interpretation. I would also like to thank Dr. Andersson at the University of Uppsala for donating a sample of immobilized TED for comparison with the commercial samples.

I am grateful to Art Anderson in the Physics Machine Shop for his expertise in the construction of instrumentation developed in this research.

This research was supported in part by a National Science Foundation Grant CHE85-02061.

TABLE OF CONTENTS

LIST OF TABLES

LIST OF FIGURES

ABSTRACT

NEW APPROACHES TO FIBER OPTIC CHEMICAL SENSORS
FOR IONS
by

Marian F. McCurley

University of New Hampshire, May, 1990

Two problems of current fiber optic chemical sensors (FOCS) were addressed in this research. First, an immobilized ligand was characterized as a possible reagent for detecting anions selectively. Second, a new approach to fiber optic chemical sensing based on polymer swelling was demonstrated.

The immobilized reagent explored for selective detection of anions is marketed as tris(carboxymethyl)ethylenediaminediacetic acid (TED). Characterization of this reagent showed that it is actually a mixture of ligands with ethylenediaminediacetic acid (EDDA) being the major species. Conclusive evidence was found in the EPR spectra. Several model ligands including a sample of TED from a private source were compared to the commercial product. EPR spectrum of the commercial reagent most resembled the EDDA spectrum. Theoretical and experimental capacities and conditional complexation constant of "immobilized ligand" for Cu(II) were measured

and found to be consistent with this interpretation.

A new type of sensor based on polymer swelling coupled to optical displacement was demonstrated. Two commercially available bead polymers, Dowex 50W and SP Sephadex served as reagent phases for sensing ions. When the sensor is placed into an ionic solution the bead contracts. This brings a reflector in contact with the bead closer to the end of the fiber or fibers such that the intensity of the reflected light reaching the detector changes. Response is both rapid, on the order of seconds, and reversible. Both reagents detect a change in concentration of ions in solution, but the sensor based on SP Sephadex is more sensitive. Total change in the normalized reflected intensity at 400 nm for Dowex 50W is 48% and for SP Sephadex is 93%. Dynamic range was 0.100 to 1.0 M for Dowex 50W and 0.001 to 0.1 for SP Sephadex.

A CM Sephadex bead polymer serves as a sensor for pH. Response is both reversible and rapid. Relative intensity changes are on the order of 10% for a pH change of 1.0 unit at 0.01 M ionic strength. An ionic strength of 0.1 reduces the response due to the change in pH.

Parameters which affect the performance of the sensors include number of fibers employed, degree of crosslinking of the bead, bead diameter and salt type.

CHAPTER I

INTRODUCTION

Introduction

Fiber optic chemical sensors (FOCS) or optrodes make it possible to couple a laboratory based spectrometer to a remote sampling site. A number of FOCS have been developed; these are described at great length in several reviews,[1-5] which detail the mechanics of optical fibers, the manner in which FOCS are categorized and the various types of conventional optrodes that have been developed.

The majority of FOCS involve an immobilized reagent phase. These sensors are based on changes in the absorbance, luminescence or reflectance of the immobilized reagent due to interaction with an analyte. A sensor with an immobilized reagent phase not only couples the spectrometer to the sample but also interacts chemically with the sample making it possible to detect analytes that are not amenable to direct spectroscopic measurement. A typical FOCS with an immobilized reagent phase is shown in Figure 1.1. The typical FOCS is composed of three subsystems: electrical, optical and chemical, which need to be coupled together. The electrical subsystem includes the source, detector and recorder. The optical fiber or fibers and the method from or separating the source radiation from the

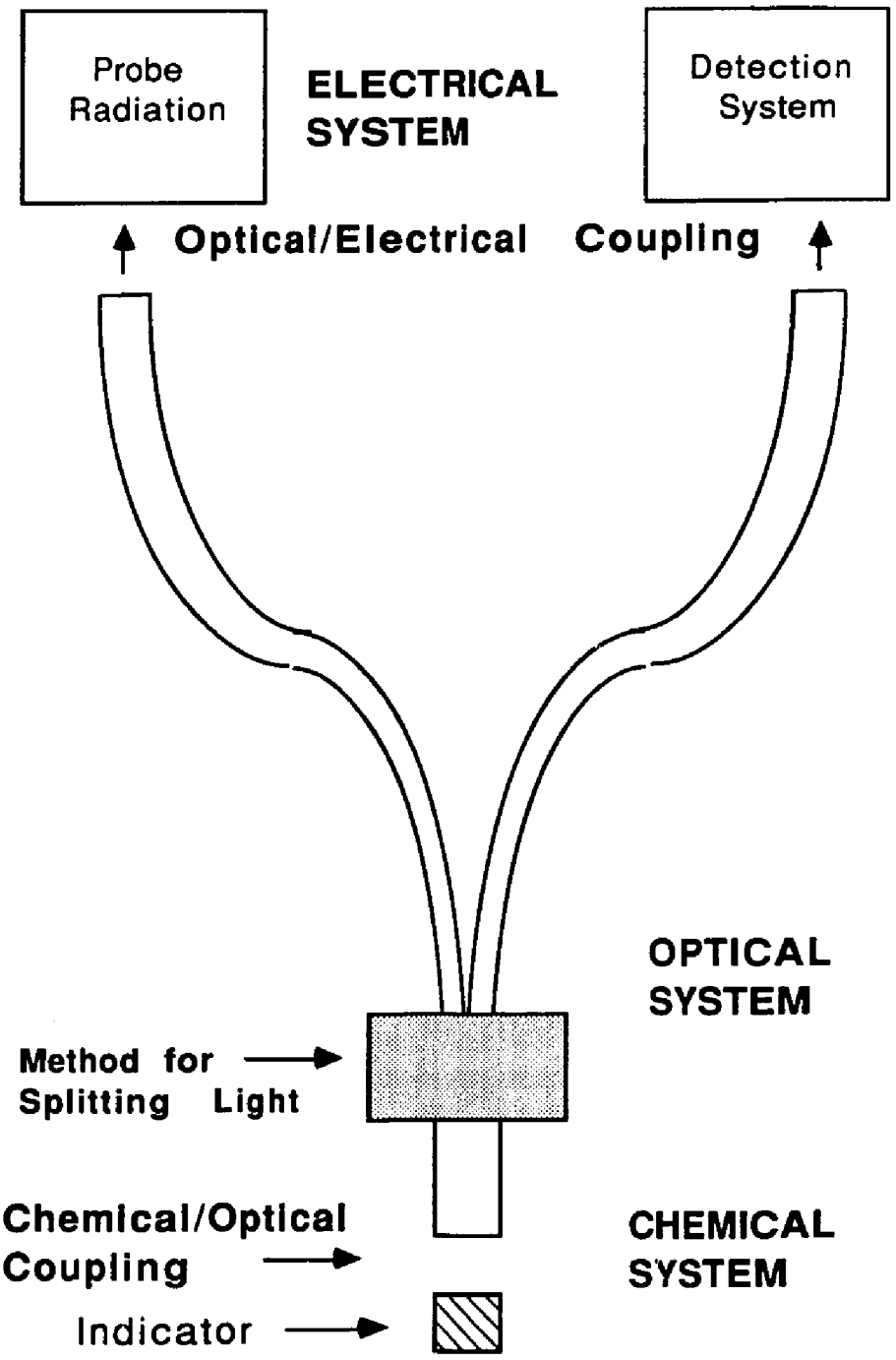

Figure 1.1: Fiber optic chemical sensor subsystems

light carried to the detector comprise the optical subsystem. The chemical subsystem is the immobilized reagent. The optical/electrical coupling is typically accomplished with a photomultiplier tube. The chemical and optical subsystems are coupled via a change in the fluorescence, absorbance or reflectance of the immobilized reagent.

While FOCS are likely to become the preferred alternative for many analytical measurements, the ideal FOCS has yet to be developed. The characteristics of an ideal FOCS include the following. The sensor should be rugged enough to withstand the abuses of the hostile environment presented by real samples and would not be subject to photodecomposition or leaching. Also, the FOCS should be a remote device that allows the spectrometer to remain in the protected environment of the laboratory. Third, the sensor should be inexpensive. This is essential if the probe is to be marketed and cost effective. Fourth, the sensor should be based on a technology generic enough such that it could sense many different types of analytes. Fifth, the sensor should be easily miniaturized so that perturbation of the sample is minimized. Sixth, the sensor should be selective for a specific analyte with little interference from other analytes. And finally, the sensor should be sensitive enough to be practical. The scientific community has concentrated their efforts in the areas of selectivity and

sensitivity virtually ignoring the other five qualities.

The goals of this research were twofold. The first was to develop a new approach to detecting anions selectively. The second was to demonstrate a new approach to sensing designed to overcome the limitations of current FOCS.

Anion Sensors

Anion FOCS have several potential applications which include monitoring water supplies to insure the proper concentration of F^- and Cl^-,[6,7] analyzing body fluids for Cl^- in vivo or in vitro[8] and detecting toxic species such as CN^- in industrial effluents.[9]

Four approaches to anion sensing have been described in the literature. The first approach is based on a redox reaction. Sulfide is determined based on its ability to reduce phenolindo-2,6-dichlorophenol (2,6-dichlorophenolindophenol, DIP) from the blue azoquinoid form into the colorless leuco form. The reagent is regenerated by oxidation with oxygen.[10] The second approach is based on halide quenching of fluorescence from an immobilized cationic fluorophor. The response is reversible but not selective. Sensitivity follows the order I>Br>Cl.[11] The third approach involves ion pairing. The ionophore is a pentacoordinate Al(III) complex. Response is selective but response times are long. Reagent leaching is also a problem.[12]

In the fourth approach anion sensing is based on ligand exchange. For example, anions, specifically halides, may displace fluorescein from silver fluoresceinate, thus allowing the fluorescein anion to fluoresce. Since the reagent is consumed, the reaction is irreversible. Sensitivity depends on the affinity of the halide for Ag(I) and follows the order I>Br>Cl.[13] In a second example, sulfide is determined based on its ability to displace dithiofluorescein from immobilized complexes with silver nitrate and with o-hydroxmercuribenzoic acid. Release of dithiofluorescein results in a reduction in reflectance of the immobilized reagent. The reaction is irreversible but the indicator may be regenerated.[10] Fluoride has been sensed using immobilized lanthanide complexes of alizarin complexone. Fluoride displaces water from the lanthanide ion, causing a shift in the reflectance spectrum of the immobilized complex. Selectivity is based on the affinity of lanthanide for fluoride.[14]

The approach investigated in this research for selective detection of anions involved the immobilized chelating ligand, tris(carboxymethyl)ethylenediamine. The selectivity is based on the formation constants of the Cu(II) complex of the ligand with anions.

Sensors Based on Polymer Swelling

A critical limitation of current FOCS is the need for immobilized indicator dyes. While these dyes allow the

sensor to be both selective and sensitive, they have several limitations. They absorb in either the UV or visible region of the spectrum often requiring expensive instrumentation to get an observable signal. The necessity of using UV or visible light limits the remoteness of the device, because Rayleigh scattered light increases with the fourth power of the frequency of the radiation, severely attenuating the signal at shorter wavelengths. They tend to photodecompose, which limits the ruggedness of these sensors. Changing from one analyte to another requires a new dye and usually means that the wavelength of the measurement has to be changed.

The FOCS that is the subject of this dissertation employs an immobilized reagent phase but is not based on any of the methods described in the literature. It overcomes the limitations of the immobilized indicator dyes by simply not using them. Instead, it incorporates polymer swelling and optical displacement into a single sensor. While these two concepts are not recent inventions, a fiber optic chemical sensor based on the union of these two concepts is a revolutionary idea. Interaction of the analyte with the polymer causes it to swell or shrink. This moves the reflector changing the intensity of light that gets reflected through the optical fiber to the detector.

The polymers employed in the sensor in this research are rugged. They are stable up to a few hundred degrees Celsius and are not subject to photodecomposition or

leaching. Since no dyes are required, near infrared radiation may be used. The optical fibers developed by the communications industry are inexpensive and highly transparent to near infrared radiation. Light can travel through the optical fibers for distances up to 50 km with little attenuation. Therefore, the sensor may operate as a remote device. The device is easily miniaturized, since it is based on reflected intensities and single or dual fiber measurements are readily made. The sensor is generic, since only the reagent phase is changed to sense a variety of analytes, including ions and neutral analytes. The instrument remains the same.

Sensors based on swelling have been described in the literature but the amount of swelling is determined electronically not by optical displacement. A humidity sensor developed by the Japan Auto Parts Industries Association is based on a blended paper of moisture swellable organic and electrically conductive fibers.[15,16] A hygrometer patented by the Sharp Corporation consists of 2 crosslinked C fibers that are imbedded in a piece of moisture sensitive plastic. The electrical resistance is measured.[17] A hygrometer developed by Katsushige Yamashita uses a moisture swellable organic polymer containing an electrolyte.[18] An oil sensor based on swelling was developed by Nitto Electric Industrial Co., Ltd. but again the detection was electronically based.[19]

Conclusion

The characterization of tris(carboxymethyl) ethylenediamine appears in Chapter 2. The theory of polymer swelling and optical displacement is detailed in Chapter 3. The instrumentation is described in Chapter 4. The development of the optical subsystem, the instrumentation for measuring the optical displacement of a reflector due to swelling of the polymer follows in Chapter 4. Sensors for ion concentration based on the crosslinked polymer beads Dowex 50W and SP Sephadex are described in Chapter 5. A sensor for pH based on crosslinked CM Sephadex is described in Chapter 6. Conclusions and future work are described in Chapter 7.

CHAPTER II

CHARACTERIZATION OF "IMMOBILIZED TRIS(CARBOXYMETHYL)ETHYLENEDIAMINE"

Introduction

The immobilization of tris(carboxymethyl) ethylenediamine (TED) (also known as ethylenediaminetriacetic acid) on a carbohydrate support was first described in 1975.[20] The first step in the procedure is to react the carbohydrate with epichlorohydrin. The modified surface is then reacted with an excess of ethylenediamine. The final step is to react the immobilized ethylenediamine with monobromoacetic acid.

It was shown that the Ni(II) and Cu(II) complexes of immobilized TED could serve as stationary phases for separating proteins by ligand exchange, a technique christened immobilized metal-ion affinity chromatography.[20-22] This technique is now well established, with diverse applications reported in the literature.[23] Immobilized TED is commercially available from Pierce Chemical Company.

In addition to serving as a stationary phase for ligand exchange chromatography, immobilized TED is potentially useful for other analytical applications such as preconcentrating heavy metal ions for determination by other techniques. My interest in immobilized TED arises from the possibility of developing ligand-selective indicators for

optical sensing.

Although the interaction between immobilized metal-TED complexes and proteins has been described,[24] the immobilized ligand has yet to be completely characterized. Equilibrium constants for metal ion binding have not been measured, nor has the putative structure been confirmed. This chapter describes the characterization of the interaction between commercially available immobilized TED and Cu(II) by a variety of techniques including elemental analysis, metal-ion binding-capacity measurements and EPR spectroscopy. The results suggest that the commercial material is actually a mixture of ligands, the major component being ethylenediaminediacetic acid. In contrast, the EPR spectrum of the Cu(II) complex with an immobilized TED sample provided by Dr. L. Andersson was that expected for TED, indicating that the commercial material differs from the immobilized TED described in the literature.[20-22,24] Consequently, the commercial product will be referred to as the "immobilized ligand" or the gel.

Experimental

Apparatus

Nitrogen was determined with a Perkin-Elmer 240B Elemental Analyzer after the sample had been dried to constant weight at 120°.

An Orion Digital Ionalyzer/501 with an Orion combination glass pH electrode was used for acid/base

titrations. An Orion cupric ion electrode with an Ag/AgCl reference electrode was used in the potentiometric copper titrations.

UV-VIS absorption spectra were measured on a Shimadzu Bausch+Lomb Spectronic 200UV recording spectrophotometer.

Cu(II) was determined by atomic absorption with an Instrumentation Laboratory 951 AA/AE spectrophotometer with a Jarrell Ash copper hollow-cathode lamp at the manufacturer's recommended instrument settings.

An IBM Instruments EC220[1A] Stripping Voltammeter with SCE reference, Pt ring auxiliary and mercury thin film working electrodes was used for anodic stripping voltammetry.

Electron paramagnetic resonance (EPR) spectra were measured on a Varian E-4 spectrometer interfaced to a Digital Equipment Corporation MINC 11-23 computer.

Reagents

The "immobilized ligand" batch numbers 850510086 and 860617089, were purchased from Pierce Chemical Company. Batch number 850510089 was used in most experiments. In addition, Dr. Andersson sent us a sample of immobilized TED prepared in his laboratory.

Other reagents included nitrilotriacetic acid (NTA), ethylenediamine-N,N'-diacetic acid (EDDA), N-(2-hydroxyethyl) ethylenediaminetriacetic acid (HEDT) and

mercuric chloride from Aldrich Chemical Company, iminodiacetic acid (IDA) from Eastman Kodak, ethylenediaminetetraacetic acid (EDTA) and Cu(II) AA standard from Fisher Scientific, and 2-[N-morpholino]ethanesulfonic acid (MES) buffer from Sigma Chemical Company.

A 0.0103 M mercuric chloride solution was prepared by dissolving 0.0280 g of $HgCl_2$ in a small amount of dilute hydrochloric acid and diluting to 10.0 ml with distilled water. Phosphate buffer (pH = 7.0) was prepared by dissolving 5.38 g of sodium dihydrogen phosphate and 16.35 g of sodium monohydrogen phosphate in 1000 ml of distilled water. Acetate buffer (pH = 5.0) was prepared by combining 2.34 g of sodium acetate and 0.34 ml of glacial acetic acid and diluting to 200 ml with distilled water. MES buffer (pH = 5.48) was prepared by mixing 0.976 g of MES and 1.6 ml of 0.5 M sodium hydroxide and diluting to 100.0 ml with distilled water. Unless otherwise indicated, the pH 5.0 acetate buffer was used for all experiments.

Procedures

The "immobilized ligand" was prepared for all experiments, except the potentiometric acid-base titration, in the same manner. Initially the "immobilized ligand" was rinsed with two or three 10 ml portions of distilled water to remove the preserving solution in which it was stored. Next the gel was protonated by washing with two or three 10

ml portions of 1 M hydrochloric acid, followed by rinsing with 10 ml of distilled water and two or three 10 ml portions of buffer or sodium hydroxide solution, as appropriate. Between washings, the gel was suction-dried on a fritted glass filter.

Potentiometric titrations were performed by adding the titrant, a 9.360×10^{-3} M NaOH solution, via a buret into a stirred slurry of the "immobilized ligand" (4.4 g). The slurry for the acid-base titration was prepared by rinsing it first with 1 M HCl then rinsing it with distilled water. This experiment was performed in two halves. In the first half a small quantity of distilled water was used, so the initial pH of the slurry was acidic. In the second half the slurry was rinsed with distilled water until the pH was the same for both the rinse and the distilled water. Measurements were taken after each addition of titrant when the solution reached equilibrium.

In a similar manner potentiometric copper titrations were performed with a 1000 ppm Cu(II) titrant. Ionic strength was adjusted by adding 2.0 ml of a 5 M $NaNO_3$ solution to a 100 ml sample for an ionic strength of 0.1 and the pH was adjusted to pH 6.0 with HCl and NaOH.

Samples for atomic absorption analysis were prepared by equilibrating the "immobilized ligand" in buffer with 10.0 ml of 1000 ppm Cu(II) solution. The gel was subsequently rinsed with distilled water. The solution

containing unbound copper was combined with the washings and diluted to 100.0 ml with distilled water. Bound copper was removed from the gel by treating it with two 10 ml portions of 1 M hydrochloric acid. The "immobilized ligand" was neutralized with three 10 ml portions of buffer, which were then combined with the bound copper fraction. This mixture was diluted to 100 ml with distilled water. Both fractions were further diluted with buffer to ensure that the final concentrations were in the appropriate linear working range for copper. In all cases the supernatant was removed from the immobilized gel by passing it through a fritted glass filter. Samples were analyzed in triplicate and the absorbance of each sample was measured five times.

Anodic stripping voltammetry was performed on a slurry of 3.3 ml of the "immobilized ligand" diluted to 100.0 ml with pH 5.0 acetate buffer. The sample was dearated by bubbling nitrogen through the slurry. A blanket of nitrogen bathed the surface throughout the experiment. A 0.400 ml aliquot of 0.0103 M mercuric chloride was the source of the mercury film.[25] Successive 0.100 ml increments of a 100 ppm Cu(II) standard solution were added to the slurry and allowed to equilibrate for 10 minutes, with stirring. Copper was deposited during a period of 3 minutes at a potential of -1.000 V vs SCE, and then stripped at a scan rate of 20 mV/sec. Deposition and stripping were repeated three times for each addition of Cu(II). Between

additions of Cu(II), the mercury film on the electrode was removed and an additional 0.400 ml portion of 0.0103 M mercuric chloride was added.

Competition experiments involved successive additions of 0.120 M IDA to 3.3 ml of gel complexed with 1.000 mg of Cu(II) and buffered to pH 5.0, in a total volume of 51.0 ml. After each aliquot of IDA was added, the solution was equilibrated by stirring for 10 min. The fractions containing bound and free Cu(II) were removed and collected as described above. The concentration of Cu(II) was determined by atomic absorption.

UV-VIS spectroscopy was used in an attempt to determine the equilibrium constant for complexation of the "immobilized ligand" with Cu(II). The experiment involved 3.302 ml the "immobilized ligand" complexed with 1.000 mg Cu(II) (4.765 micromoles Cu(II) / ml wet gel) buffered to pH 5.0 with acetate buffer in a slurry with a total volume of 51.0 ml. A 0.3000 M IDA solution was added to the slurry in increments. After each aliquot the solution was allowed to equilibrate with stirring for 10 minutes. The sample was then centrifuged twice to separate the slurry from the supernatant. The absorbance of the supernatant at 223.5 nm was measured. The titration was performed a second time with IDA in the blank (acetate buffer). The second titration used 3.312 ml of the "immobilized ligand" complexed with 0.25 mg Cu(II) (1.188 micromoles Cu(II) / ml

wet gel) buffered to pH 5.0 with acetate buffer in a slurry with a total volume of 50.25 ml. The concentration of the IDA solution was 0.0750 M. In addition a direct titration of the "immobilized ligand" with Cu(II) was performed with 4.198 ml gel buffered to pH 5.0 with a total volume of 50.0 ml. A 1000 ppm Cu(II) solution was added in 100 microl increments.

EPR spectra were taken for 1.0 g "immobilized ligand" samples which had been equilibrated for 10 minutes, with stirring, with various amounts of 200 ppm Cu(II) standard solution. The slurries were buffered with acetate at pH 5.0 and 5.5 and with MES at pH 5.5. After equilibration with Cu(II) the slurry was transferred to an EPR tube and slowly frozen in a dry ice/acetone slush, then cooled in liquid nitrogen for the EPR measurement. Samples of Cu(II) equilibrated with other complexing agents were prepared similarly.

Results

Cu(II) Binding Capacity

Theoretical binding capacity. A theoretical Cu(II) binding capacity for the gel was determined by measuring the nitrogen content of the gel. This calculation was based on the manufacturer's suggested structure for the "immobilized ligand", shown in Figure 2.1, and assumes that one Cu(II) ion is bound per two nitrogen atoms. The "immobilized ligand" batch number 850510086 contained 0.875 % nitrogen,

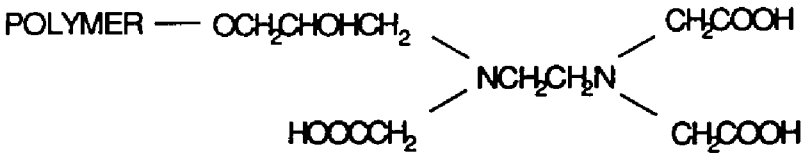

Immobilized TED

Figure 2.1: Structure for the "immobilized ligand" as suggested by Pierce Chemical Co.

which corresponds to 284 micromoles of Cu(II) per ml of dried gel. The density of the dried gel was found to be 0.91 g/ml. The "immobilized ligand" batch number 860617089 was found to contain 1.93 % nitrogen, which corresponds to 626 micromoles of Cu(II) per ml of dried gel. This batch also had a density of 0.91 g/ml.

In addition to the twofold difference in Cu(II) binding capacity, the two batches of the "immobilized ligand" differed greatly in their water content prior to drying. Batch number 850510086 lost 95.5 % of its total weight on drying, whereas batch number 860612089 lost only 77.0 %. Batch 860617089 thus has over an order of magnitude greater capacity for Cu(II) than does batch 850510086, if the capacity is based on the volume of wet gel.

Experimental binding capacity. Experimental Cu(II) binding capacities were measured for the "immobilized ligand" batch number 850510086 by both flame atomic absorption (AA) and anodic stripping voltammetry (ASV). The ASV titration was performed on samples buffered to pH 5.00 with acetate. The results are shown in Figure 2.2. The end-point was determined by extrapolating the two straight-line portions of the curve to the point where they intersect. This end-point corresponded to a capacity of 150 micromole of Cu(II) per ml of dried gel.

For volumes less than 1200 microl of added Cu(II) solution, the ASV experiment did not indicate a measurable

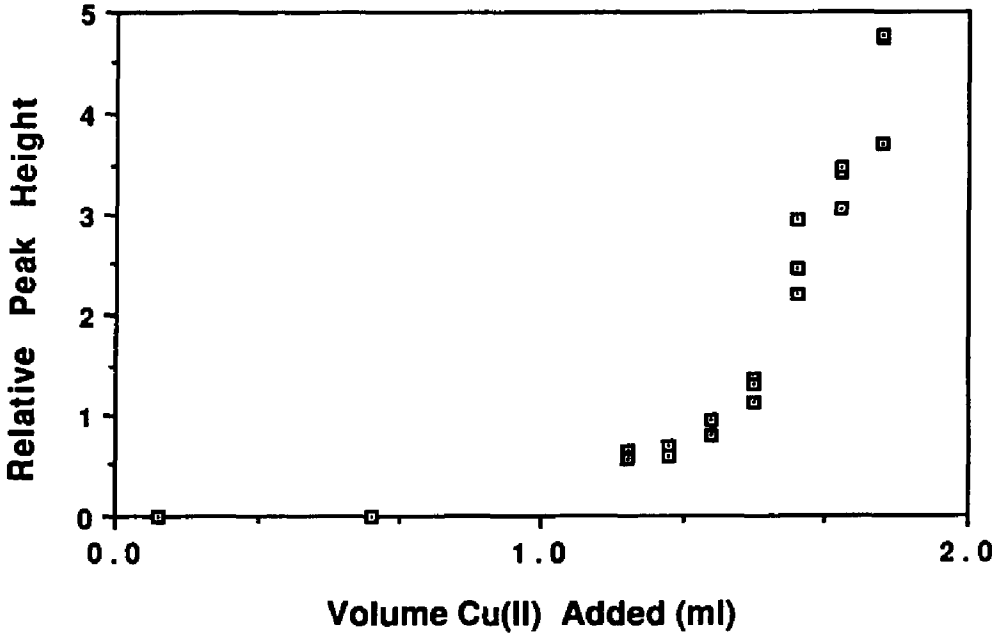

Figure 2.2: Anodic stripping voltammetry titration of the "immobilized ligand" with Cu(II) at pH 5.0

amount of free Cu(II). However, between 1200 and 1400 microl Cu(II) was observable, indicating that the Cu(II) binding equilibrium is not complete in this region.

The binding capacities measured by AA were 170 micromole of Cu(II) per ml of dried gel at pH 7.0 and 130 micromole of Cu(II) per ml of dried gel at pH 5.0.

Potentiometric titration. The potentiometric titration of the "immobilized ligand" with NaOH provides additional evidence that the ligand bound to the Fractogel surface is EDDA. The results of this experiment are shown in Figure 2.3.

There are two inherent problems in this titration. First, since the experiment was performed in two halves the two curves are overlapped. Error may be introduced in the placement of the two curves. Second, the washing procedure may cause some of the "immobilized ligand" to dissociate. Therefore, the initial form of the ligand is not known and quantitative conclusions such as the experimental capacity can not be drawn. However, information regarding the pKa's of the "immobilized ligand" appears to be consistent with the conclusion that the "immobilized ligand" is primarily EDDA.

There appear to be two breaks in the pH titration curve. Half-way between them the pH is approximately 6.7. This point should correspond to titrating the third proton of EDDA. The solution pKa for this proton is 6.72. It

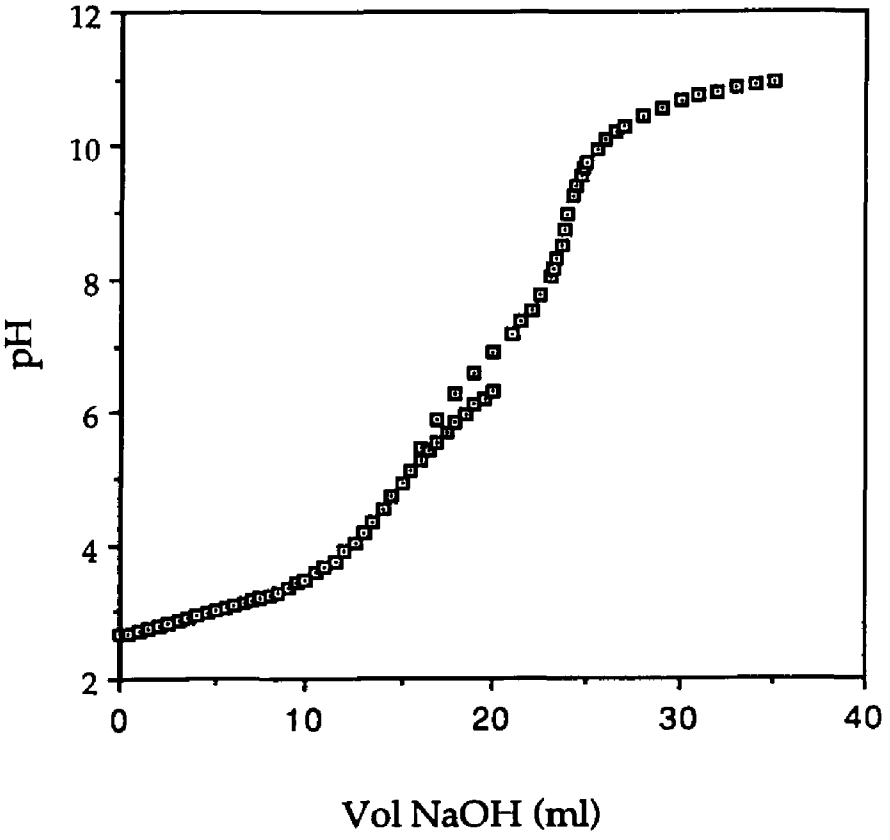

Figure 2.3: Potentiometric titration of the "immobilized ligand" with NaOH

could also include, however, the second proton for HEDT. The solution pKa for this proton is 5.37. While the observed midway point pH is between the pKa's for EDDA and HEDT, it is closer to the pKa for EDDA. This is consistent with interpreting the "immobilized ligand" as predominately EDDA. The acid dissociation constants for EDDA and HEDT are given in Table 2.1.

Complexation Constant

Initially, an attempt was made to determine the equilibrium constant for binding of Cu(II) to the "immobilized ligand" by potentiometric titration with Cu(II) monitored with a Cu(II) electrode. However, the response was sluggish, and satisfactory results were not obtained. Although Cu(II) electrodes respond to trace concentrations of free Cu(II) in the presence of dissolved Cu(II) complexes, this was not the case for the "immobilized ligand", which is in a separate phase.

Accordingly, the complexation constant was measured by a competition experiment. The procedure involved titrating the "immobilized ligand"-Cu(II) complex with iminodiacetic acid (IDA) at pH 5.0 and measuring the amount of Cu(II) removed by the IDA. Initially, an attempt was made to monitor the formation of the Cu(II)-IDA complex by UV-VIS spectroscopy. However, suspended particulates remained in the samples despite several attempts to remove them. The samples were decanted, filtered and centrifuged.

LIGAND	EXPRESSION	pKa
HEDT	H2L.H/H3L HL.H./H2L H.L./HL	2.6 5.37 9.81
EDDA	H3L.H./H4L H2L.H./H3L HL.H/H2L H.L./HL	1.66 2.37 6.72 9.69
IDA	H2L.H./H3L HL.H./H2L H.L./HL	1.82 2.61 9.34
		pKd
	M.2L./ML2 M.L./ML	5.97 10.57

Table 2.1: Equilibrium constants for formation of IDA-Cu(II) complexes and the acid-base dissociation constants for IDA, EDDA, HEDT

While centrifuging removed most of the suspended particles, those that remained interfered with the measurement giving inconclusive results. Consequently, atomic absorption spectroscopy was used to monitor the titration, since the clarity of the solution is not critical. An added benefit was that free IDA in solution does not interfere with the measurement. The results of this experiment are shown in Figure 2.4.

The conditional formation constant at pH 5.0 for Cu(II) complexation with the "immobilized ligand" was calculated to be 1.6×10^8. It is based on the point at which sufficient IDA has been added to complex half of the Cu(II). The calculation procedure has been described previously.[26] The main points are described below.

In the competition experiment the free ligand (IDA) competes for the metal ion Cu(II) complexed to the "immobilized ligand". The two ligands must have complexation constants of the same magnitude, and the free ligand must be in excess. The complexation constant for the "immobilized ligand" takes the form:

$$K_f = ML \,/\, L\,[M] \qquad 2\text{-}1$$

where K_f is the complexation constant for the "immobilized ligand", ML is the number of "immobilized ligands" associated with Cu(II), L is the number of "immobilized

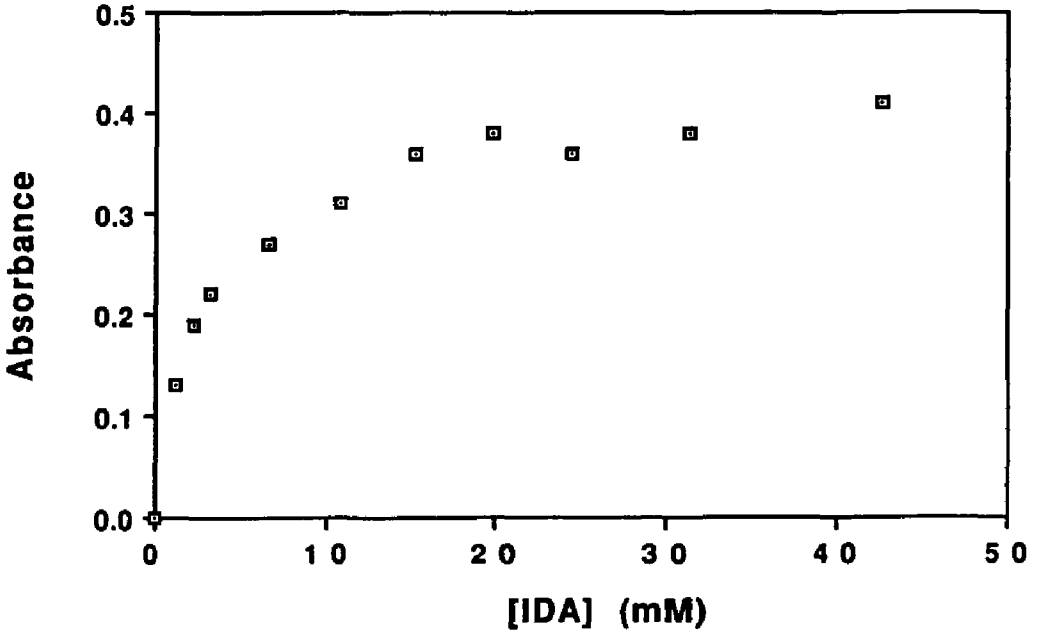

Figure 2.4: Competition titration of the "immobilized ligand" - Cu(II) complex with IDA at pH 5.0 monitored by atomic absoption spectroscopy

ligands" not associated with Cu(II) and [M] is the concentration of uncomplexed Cu(II) in solution.

When IDA is added to the solution, metal complexation by IDA and the acid-base characteristics of IDA need to be accounted for in the expression for the equilibrium constant for the "immobilized ligand" - Cu(II) complex. Since IDA reduces the free Cu(II) in solution, equation 2-1 can be modified by calculating beta, the fraction of free Cu(II) in solution:

$$\text{beta} = [M] \; / \; C_M \qquad 2\text{-}2$$

where [M] is the dissolved Cu(II) not associated with IDA and C_M is the total concentration of dissolved Cu(II) in all forms. When equation 2-2 is solved for [M] and substituted into equation 2-1 the following expression for the equilibrium constant is obtained:

$$K_f = ML \; / \; [L \; \text{beta} \; C_M] \qquad 2\text{-}3$$

Beta may be calculated from the following expression which also accounts for the acid-base characteristics of IDA:

$$\text{beta} = 1 \; / \; [1 + k_{f1} \; (\text{alpha} \; C_L) + k_{f1} \; k_{f2} \; (\text{alpha} \; C_L)^2] \qquad 2\text{-}4$$

where k_{f1} and k_{f2} refer to the equilibrium constants for

formation of IDA-Cu(II) complexes (these appear in Table 2-1), alpha is the fraction of IDA that is completely deprotonated at pH 5.0 (the acid-base dissociation constants used to calculate alpha also appear in Table 2-1) and C_L is the total concentration of IDA. It is assumed that the only metal ligand complexes which are important to consider are "immobilized ligand" - Cu(II) and IDA - Cu(II). This is reasonable since the experiments were carried out at pH 5.0 and the hydrolysis constants for the Cu(II) are small in comparison to the formation constants for IDA - Cu(II).

The absorbance due to Cu(II) shown in Figure 2.4 is proportional to the concentration of Cu(II) in solution. This concentration increases as IDA is added to the solution. At the point where absorbance has reached half its limiting value, half the Cu(II) has been removed from the "immobilized ligand". Consequently, at the half way point ML = L and expression 2-3 becomes:

$$K_f = 1 \; / \; [\text{beta } C_M] \qquad 2\text{-}5$$

The equilibrium constant for the "immobilized ligand" can be determined using calculated values of C_M and beta at the half way point. Beta at the half way point was determined graphically as shown in Figure 2.5. It was 4.47×10^{-5}. The value calculated for alpha at pH 5.0 was 4.55×10^{-5}. C_M was 1.4×10^{-4} M. The equilibrium constant

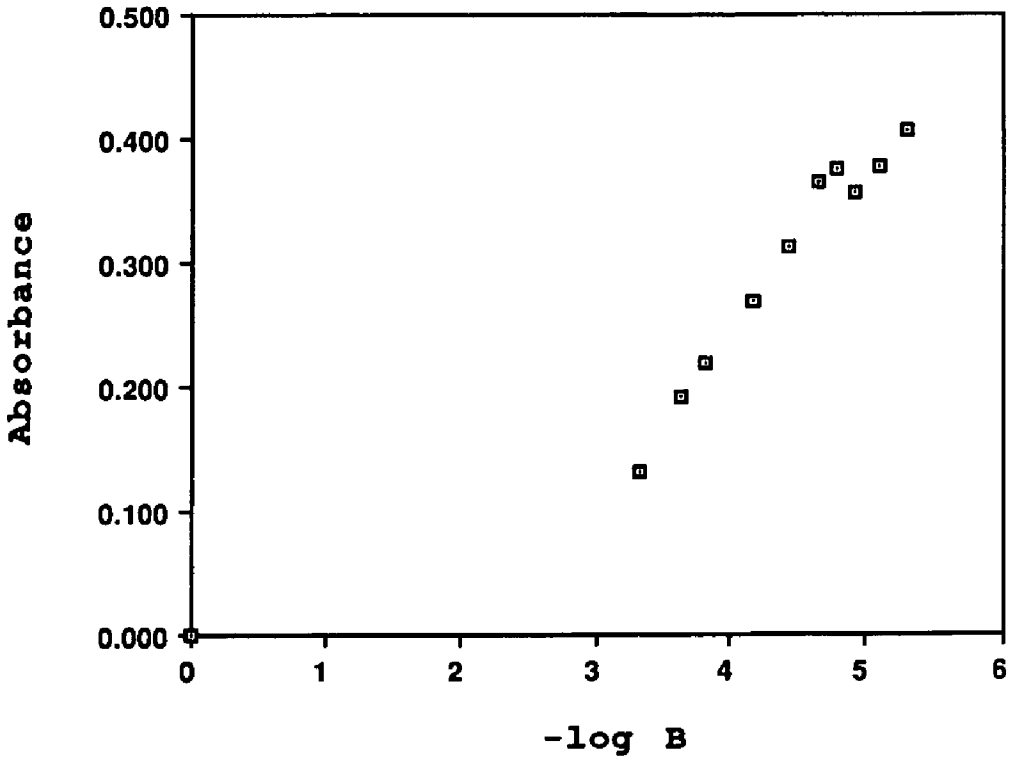

Figure 2.5: -log beta curve for the determination of beta at the mid-point in the competition titration

determined this way is a conditional constant, which depends on the acid-base characteristics of the "immobilized ligand".

EPR Spectra

EPR spectroscopy is an effective tool for elucidating the structure of Cu(II) complexes.[27] Cu(II) is paramagnetic. Complexation of Cu(II) changes the environment around the Cu(II) which affects the fine structure of the EPR signal. Figure 2.6 shows EPR spectra for batch 860617089 of the "immobilized ligand" containing 60 % and 100 % of the theoretical capacity for Cu(II), and also for the Cu(II) complex of the immobilized TED provided to us by Dr. Anderssen. The EPR spectrum for the Cu(II) complex of batch 850510086 is not shown but was identical to the spectrum for batch 860617089. The spectra for the "immobilized ligand"-Cu(II) complex were compared with spectra for Cu(II) complexes with a series of model ligands, including EDDA, HEDT, EDTA, NTA and IDA. Figure 2.7 shows the spectra of the model complexes, and Figure 2.8 shows the structure of the ligands as well as the structure proposed by Pierce for the "immobilized ligand". The EPR spectrum of Cu(II)-EDDA most closely resembles the EPR spectrum of the commercial "immobilized ligand"-Cu(II) complex. The spectrum for the immobilized TED provided by Dr. Anderssen is very similar to the spectrum of Cu(II)-HEDT.

The spectrum of HEDT indicates that two species are

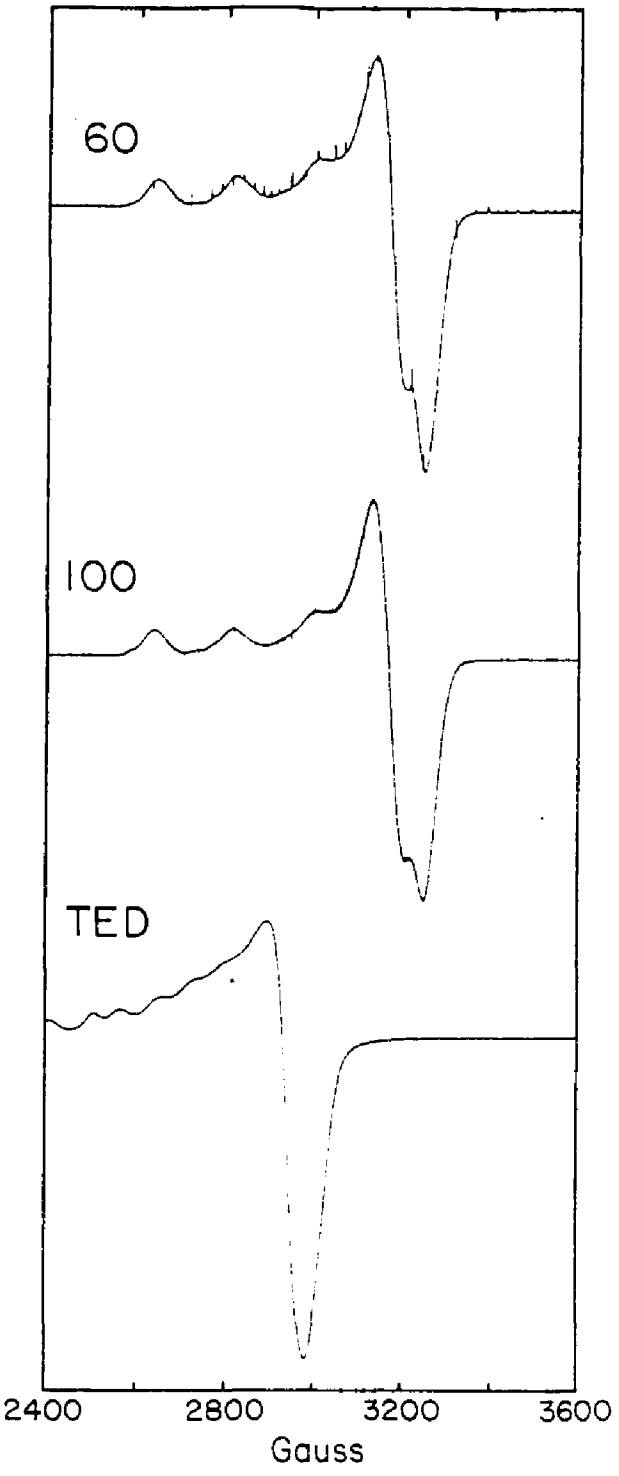

Figure 2.6: Electron paramagnetic resonance (EPR) spectra for Cu(II) complexed with the "immobilized ligand" from Pierce Chemical Co. and Dr. Anderssen

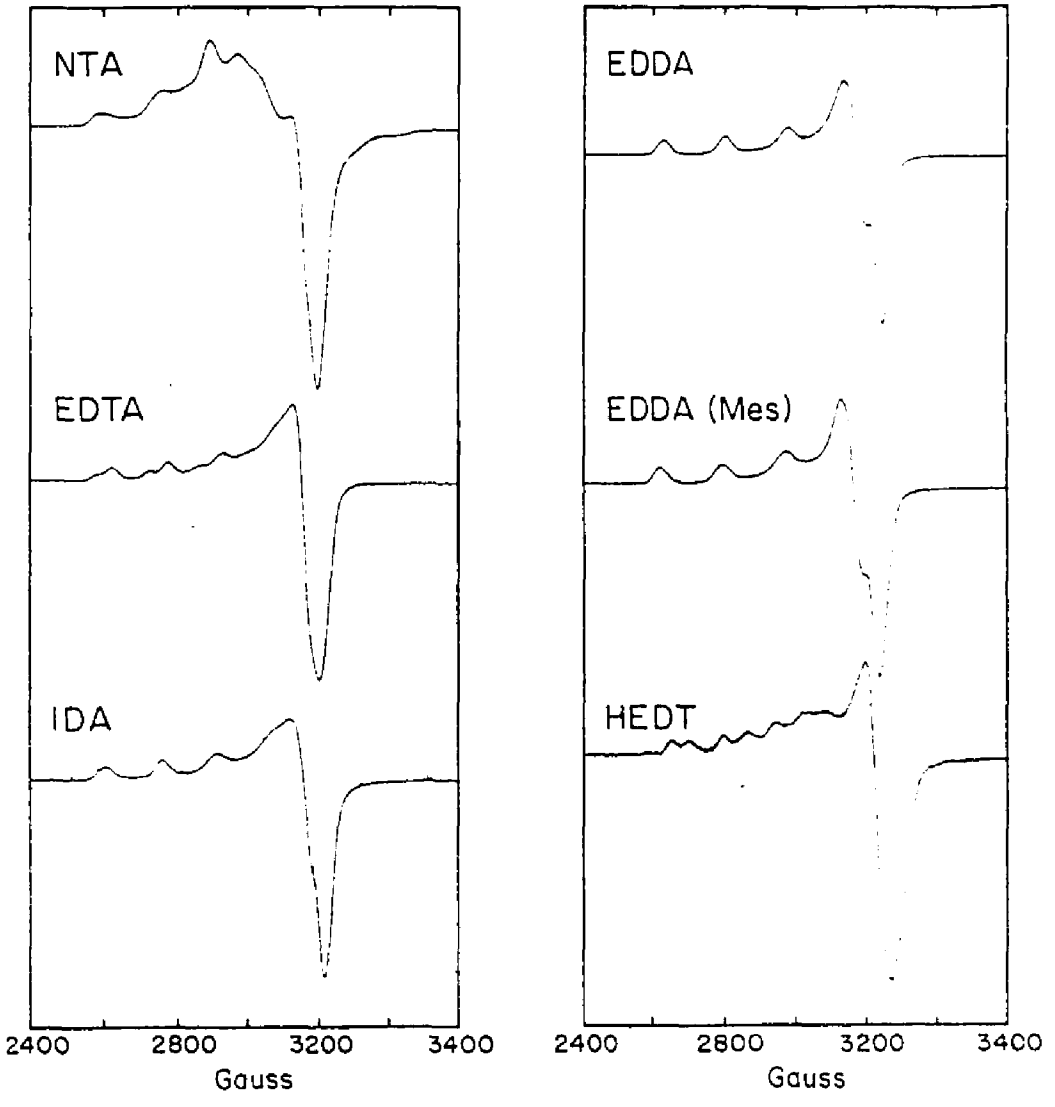

Figure 2.7: EPR spectra for the complexes of Cu(II) with the model ligands - EDDA, HEDT, EDTA, NTA and IDA

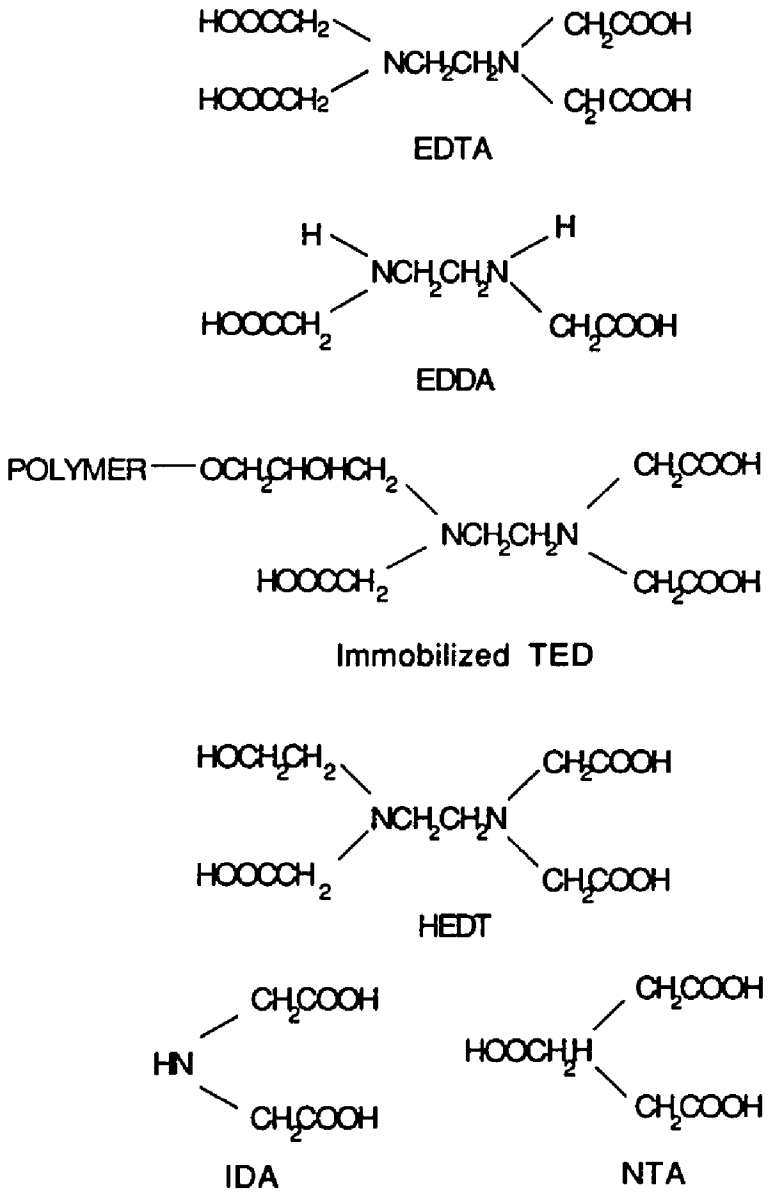

Figure 2.8: Structures of the model ligands EDDA, HEDT, EDTA, NTA and IDA and that for the "immobilized ligand" proposed by Pierce Chemical Co.

present. One of these matches the EDDA spectrum. The other is the HEDT spectrum. Because Cu(II) has a strong tendency to be four-coordinate, the third acetate group is only partially coordinated to Cu(II) under the conditions used for taking the EPR spectra. Careful inspection of the spectra for the commercial samples of the "immobilized ligand"-Cu(II) complex indicates a small but detectable signal which corresponds to the HEDT spectrum.

Discussion

The experimental evidence shows that the commercial "immobilized ligand" does not have the structure indicated by the manufacturer. Instead, it appears to be a mixture of ligands, with EDDA predominant. The EPR spectra provide the most direct evidence for this. However, the other experimental data are also consistent with this interpretation. The fact that the experimental capacities are lower than the theoretical capacities calculated from the nitrogen content indicates that some of the nitrogen is in a form that does not complex with Cu(II).

The observation that the experimental capacities are lower at pH 5.0 than at pH 7.0 suggests that there are ligands present which bind Cu(II) only at pH 7.0. From the measured complexation constant, EDDA would be expected to contribute to the Cu(II) binding capacity at both pH values. This discrepancy suggests that a weaker ligand is present. The ASV titration shows a significant amount of free copper

in solution before the end-point, which is also consistent with the presence of weaker ligands in addition to EDDA.

There is no evidence for weaker ligands in the EPR spectra. Since the spectra were run at pH 5.0 and 5.5, there should be no Cu(II) complexes of those ligands which bind Cu(II) at pH 7.0 but not at pH 5.0. The amount of weaker ligands that bind Cu(II) at pH 5.0 may be too small to show up on the EPR spectrum.

The conditional complexation constant at pH 5.0 is somewhat less than 6.0×10^9, the value calculated for Cu(II)-EDDA in solution at pH 5.0. This is certainly reasonable, since steric constraints imposed by the immobilization are likely to reduce the stability of the complex.

The formation of EDDA is consistent with the method for preparing the "immobilized ligand".[20] The first step is to react the surface of a carbohydrate with epichlorohydrin. The modified surface is then reacted with ethylenediamine. A very large excess of ethylenediamine is employed, to reduce the probability that a given ethylenediamine molecule will react with the surface at more than one site. In practice, this measure does not seem to be effective. Instead, once initially bound to the carbohydrate surface, the ethylenediamine seems to preferentially react at the other nitrogen. Thus when monobromoacetic acid is added to form the carboxymethyl groups on the nitrogen atoms, only

two positions are available. The reaction sequence that we propose is represented in Figure 2.9.

The weaker ligands that seem to be present could arise from ethylenediamine molecules that bind to three sites on the surface. Alternatively, they could form if the reaction with monobromoacetic acid does not go to completion.

Because the EPR spectrum of the Cu(II) complex of the immobilized TED sample provided by the referee is essentially identical to the spectrum of HEDT, we believe that this material is immobilized TED without a significant component of EDDA. The procedure for preparing both batches of the commercial material presumably differs from the literature procedure for preparing immobilized TED, such that, EDDA formation is promoted.

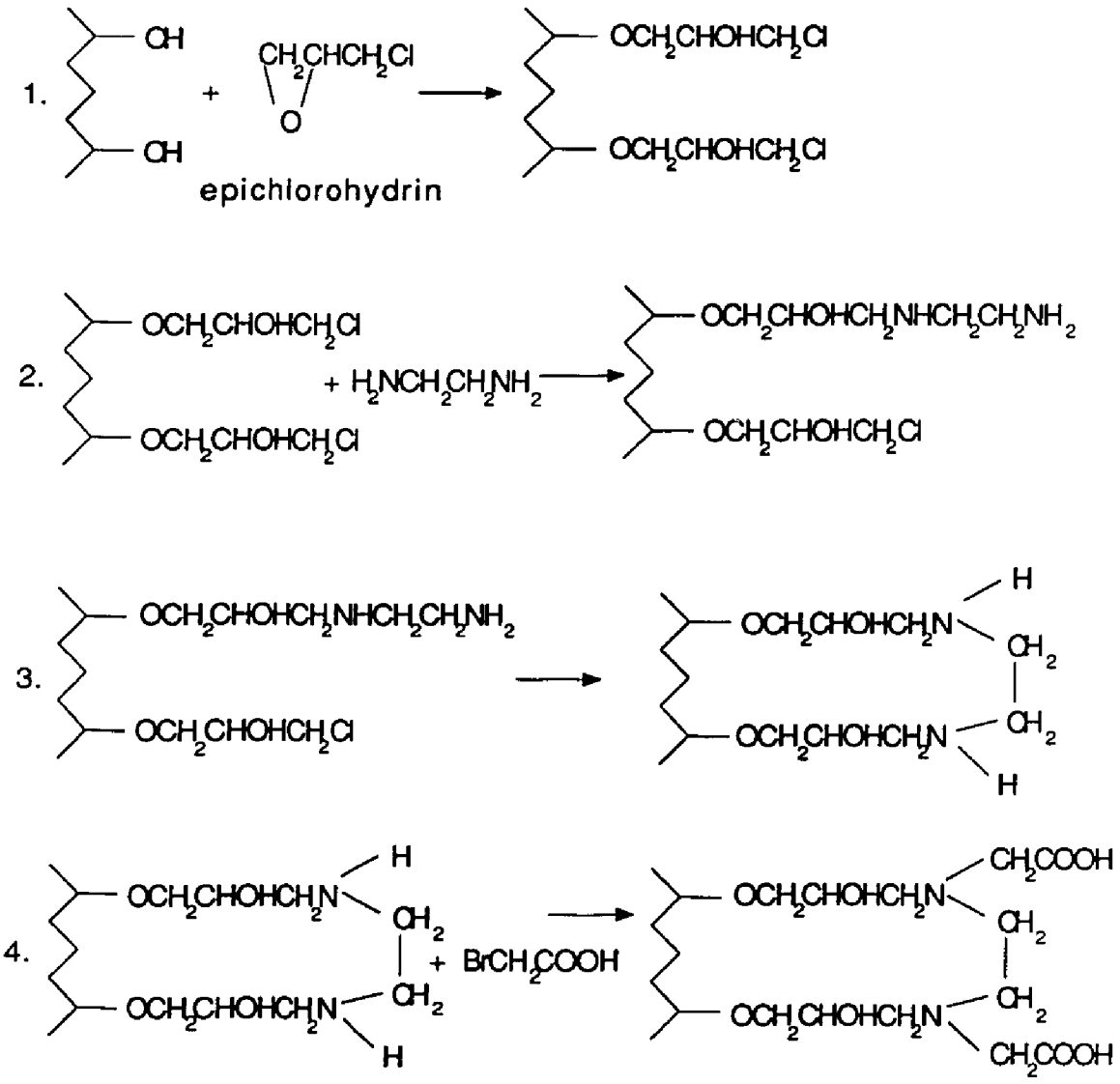

Figure 2.9: Reaction sequence proposed for the formation of the "immobilized ligand"

CHAPTER III

SENSORS BASED ON POLYMER SWELLING: BACKGROUND

Introduction

The goal of the second part of the thesis research was to develop a fiber optic chemical sensor (FOCS) based on polymer swelling. The basic principle is that, as the polymer swells in response to an analyte, it displaces a reflector. The displacement changes the amount or the intensity of the light reflected back through an optical fiber leading to a detector. The sensor consists of an electrical system, an optical system and a chemical system, as described in Chapter 1. This chapter describes how the chemical and the optical systems operate. The basic concept is illustrated in Figure 3.1.

The chemical system consists of a lightly crosslinked polymer. The polymer may be either neutral or ionic. Ionic polymers were examined in this research including Nafion membranes, sulfonated polystyrene membranes, Sephadex beads and Dowex 50W beads.

The optical system is composed of a beam splitter, optical fiber or fibers and a reflecting surface held in place on the surface of the polymer by a restoring force. The reflector is a polished metal strip. The system constructed to hold the reflector in place on the surface of

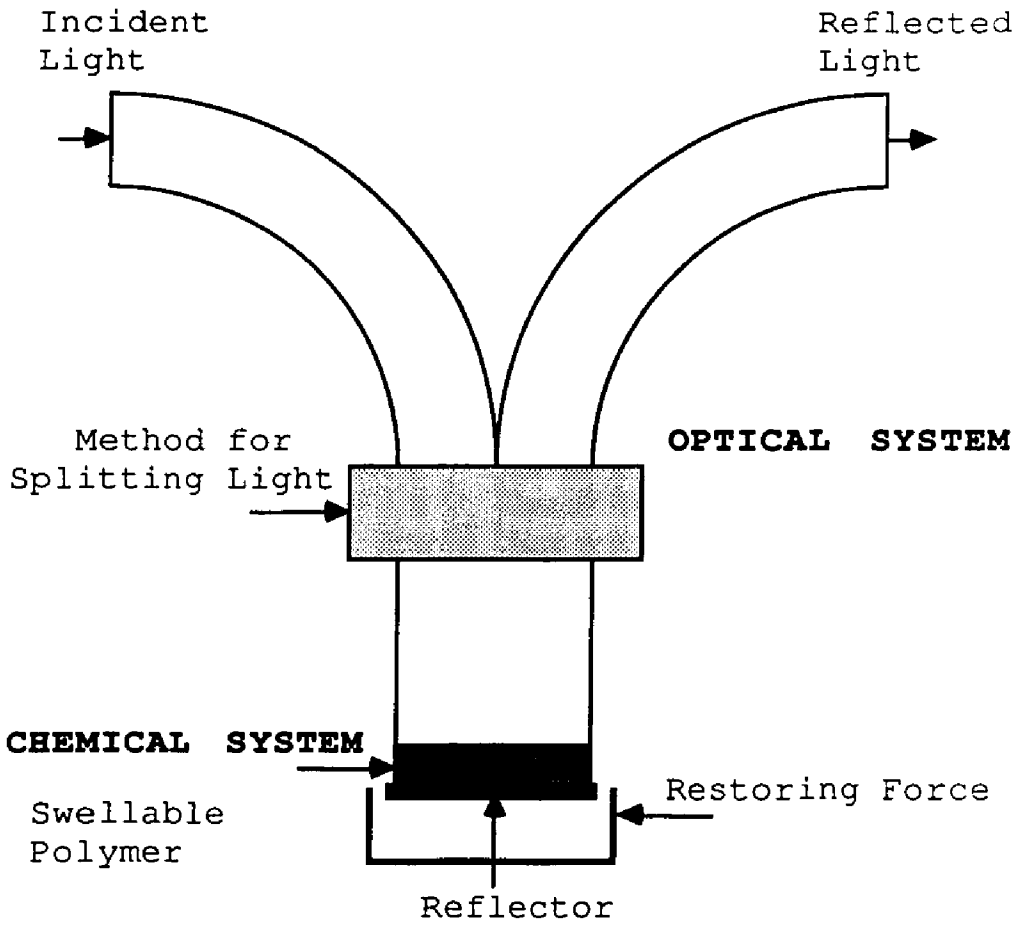

Figure 3.1: Basic concept of swelling based sensors

the polymer and to measure displacement of that reflector due to polymer swelling is detailed in Chapter 4.

This chapter will provide background information on polymer swelling and displacement optics, the two basic concepts exploited in the probe. Initially, the theory of polymer swelling for both neutral and ionic polymers is developed. Since ionic polymers were the focus of this research they are examined in more detail. The forces determining the degree of swelling and the equations governing these forces are explained. Then, the optical displacement method for measuring the change in the size of the polymer in response to an analyte is described.

Polymer Swelling

Neutral Polymers

Neutral polymers dissolve when they are placed in contact with compatible solvents. Crosslinking prevents polymers from dissolving. Instead they swell in compatible solvents until two opposing forces reach equilibrium. The force promoting swelling is the free energy of mixing with the solvent. The opposing force is the elastic retractive force of the crosslinks. Equilibrium is reached when the free energy of mixing is just balanced by the elastic free energy needed to stretch the network. This is the basis of the theory of polymer swelling developed in the classic text by Flory[28].

Factors Affecting Swelling of Neutral Polymers

The following changes in the polymer or solvent shift this equilibrium. A more highly compatible solvent increases free energy of mixing thus increasing the degree of swelling. The degree of swelling also decreases with an increase in primary molecular weight, i.e. the weight before crosslinks have been introduced. A greater number of crosslinks per unit molecular weight of the polymer or shortened crosslinks enhance the elastic retractive force, therefore reducing the degree of swelling.[28]

Ionic Polymers

Swelling is significantly increased when a neutral polymer is made ionic through the introduction of ionizable groups, because electrostatic repulsion between like charges on the ionic polymer tends to expand the matrix.[28]

A common example of an ionic polymer is a cation exchange resin. A cation exchange resin of the type used in this research in contact with a dilute salt solution is pictured in Figure 3.2. The resin has fixed ionizable groups which dissociate in the presence of water to yield fixed negative charges and free positive charges. The presence of additional free positive charges (counterions) and free negative charges (co-ions) is inevitable due to the presence of other electrolytes in the solvent (for example H^+ and OH^- from water and Na^+ and Cl^- when NaCl is added). The counterions shield the fixed charges, reducing the

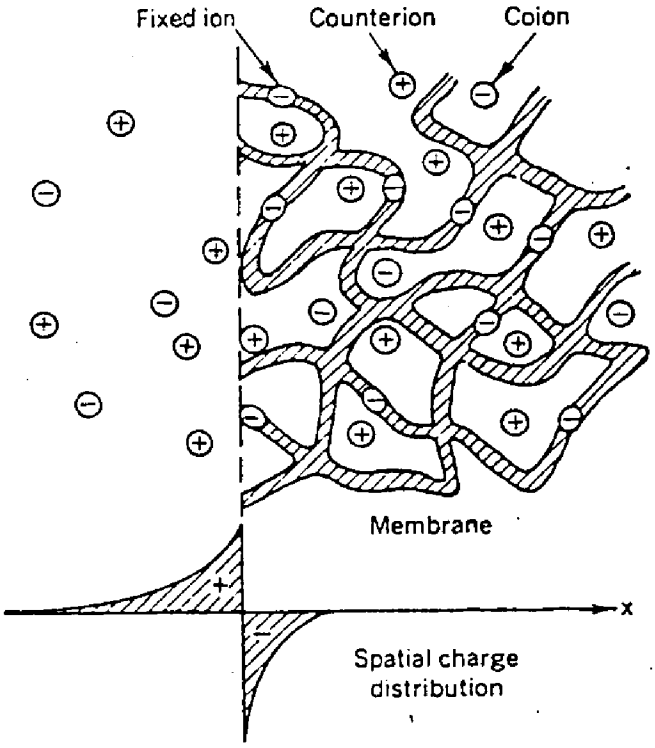

Figure 3.2: Cation exchange resin in contact with a dilute salt solution

electrostatic repulsion.[28]

Swelling of ionic polymers is the result of a combination of the solvation effects described for neutral polymers and the electrostatic repulsion effect unique to ionic polymer.

Electrostatic repulsion may also be viewed as an osmotic pressure effect. The resin has a higher concentration of ions than the solution in contact with it due to the high density of fixed charges in the resin. The difference in concentration between the resin and solution results in an osmotic pressure difference between the two phases which tends to drive solvent into the resin from the less concentrated solution.[28] This decreases the concentration of the ions in the resin which reduces the concentration difference between the two phases. In particular, it lowers the concentration of the counterions. This decreases the amount of shielding of the fixed negative charges in the resin. Thus, the magnitude of the electrostatic repulsion increases. Both the flow of solvent into the resin due to the osmotic pressure effect and the decrease in shielding of like charges result in swelling of the resin.

In Figure 3.2 the concentration of free positive ions is greater in the resin than in the solution. Conversely, the concentration of free negative charges is higher in the solution than in the resin. In order to

balance the concentration difference, cations flow into the solution from the resin and anions flow into the resin from the solution. The initial exchange of ions between the resin and the solution results in an excess of positive charge in the solution and an excess of negative charge in the resin. The result is a potential difference between the two phases known as the Donnan potential.[29] This potential prevents further diffusion of ions to equalize the concentrations in the resin and the solution.

Factors Affecting Swelling of Ionic Polymers

An increase in the number of fixed negative charges per repeating unit of the polymer increases the concentration difference between the two phases.[29] Thus, more solvent flows into the resin. An increase in the number of fixed charges also increases the electrostatic repulsion between like charges, since the average distance between charges decreases.

Any process that changes the number of fixed charges will affect the extent of swelling. Ionization of the functional groups on the resin increases the number of fixed charges.[30] A weak acid ion exchanger is an example of this effect. As pH changes, the extent of ionization changes which causes a change in the extent of swelling. This is the basis for ion detection using the polymer swelling concept.

Another major effect on swelling is the extent to

which counterions shield the fixed charges on the crosslinked polymer. More effective shielding results in less electrostatic repulsion and consequently, less swelling of the polymer. The degree of shielding depends on several factors. The main ones are the concentration and the charge of the counterion. These two factors are summed up in the ionic strength. Other factors like counterion size and degree of solvation also affect swelling.[28,30]

Swelling Equation

Flory derived the following equation to describe the swelling of ionic polymers based on the basic principles outlined above:[28]

$$q_m^{5/3} = \{[(i/2v_u S^{1/2})]^2 + [(1/2 - x_1)/v_1]\}/(v_e/V_o) \qquad 3\text{-}1$$

The individual terms in the equation are defined as follows:

- q_m is the equilibrium swelling ratio i.e. volume swollen polymer at equilibrium / volume unswollen polymer.
- i is the number of fixed charges per repeating polymer unit.
- v_u is the molar volume of the polymer repeating unit.
- S is the molar ionic strength.
- x_1 is the parameter expressing first neighbor interaction free energy, divided by kT, for solvent with polymer. Selectivity for neutral polymers is embodied in this

term.

v_1 is molar volume of the solvent.

v_e is the effective number of chains in a real network.

V_o is volume of the unswollen polymer network.

The first part of this equation expresses the swelling due to the electrostatic effect. The second part of the expression describes the swelling due to the solvation effect. Both parts of the equation include a term which represents the crosslinking factor.

The second term is not usually significant in systems involving ionic polymers. Instead, the electrostatic term dominates in systems involving ionic polymers. The electrostatic effect depends on the crosslinking term, v_e/V_o, the charge density, i/v_u, and the ionic strength, S. Consequently, if the charge density and the crosslinking are held constant, the swelling of the polymer will depend solely upon the ionic strength of the solution.

Optical Displacement Measurement

Introduction

Optical displacement is the method used to measure the change in the size of the polymer as it swells in response to an analyte (in this research the ionic strength). This section describes the optical displacement measurement for both a single and a dual fiber arrangement. The dual fiber arrangement may be extended to include

optical displacement measurements with a bundle of optical fibers.

Dual Fiber Arrangement

As the polymer swells it moves a reflector (a polished strip of metal) away from the ends of two optical fibers. One fiber (source fiber) carries light from a source to the reflector and the other fiber (detector fiber) receives the light reflected from the metal strip and carries it to a detector. As the distance between the reflector and the fibers changes, the amount of light received by the fiber leading to the detector changes. This is illustrated in Figure 3.3.

In Figure 3.3 the light reaching the reflector from the source fiber describes an acceptance cone, which depends on the numerical aperture of the fiber. The reflected light collected by the detector fiber also describes an acceptance cone. The amount of light actually observed by the detector depends on the overlap of these two cones.

When the fiber is very close to the target as in Figure 3.3a the amount of light reaching the detector fiber is small. However, as the reflector moves further away from the ends of the fibers the overlap region grows larger. Consequently, the amount of light collected by the fiber leading to the detector increases. This is illustrated in Figure 3.3b.

An additional factor determines the amount of light

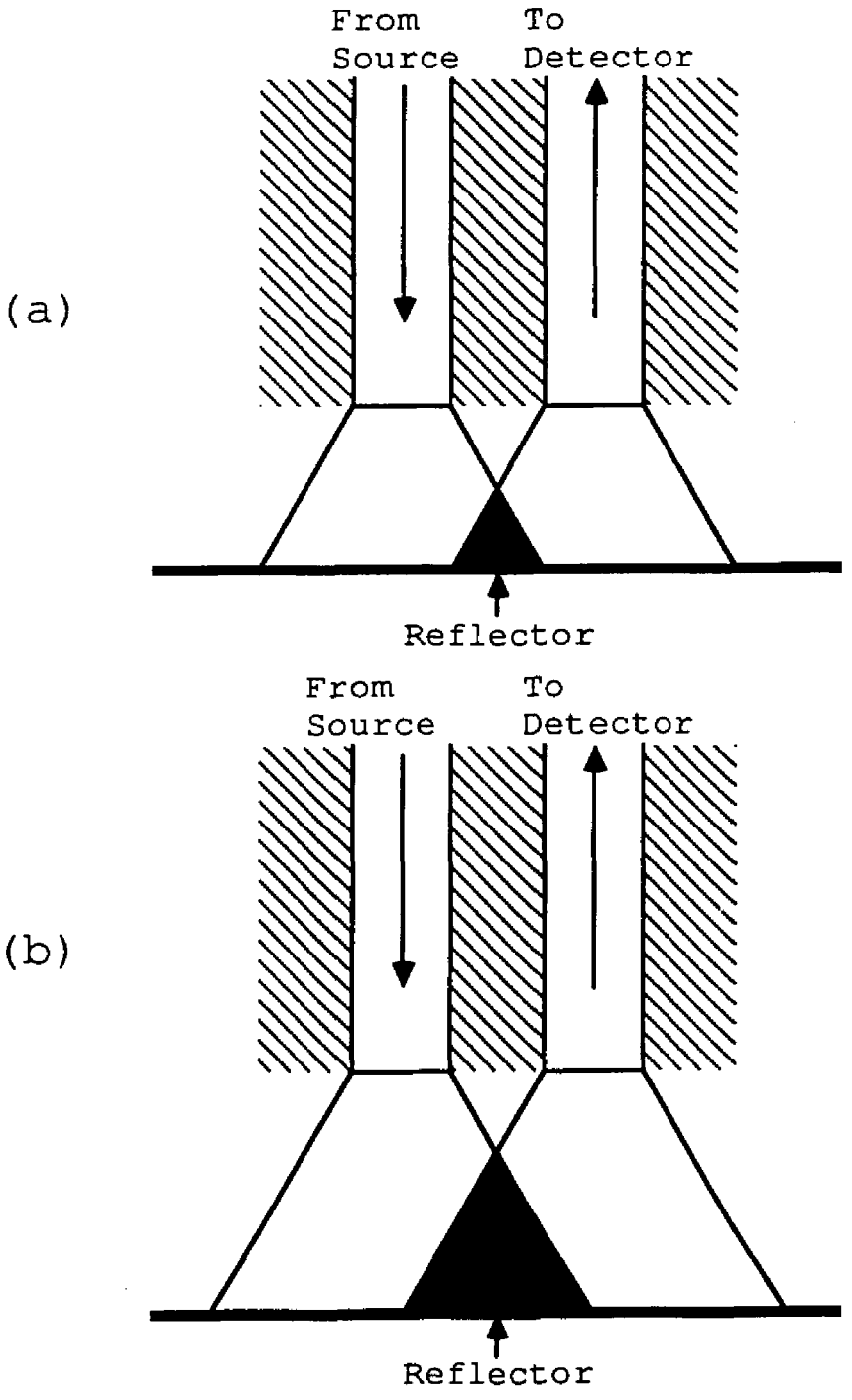

Figure 3.3: Variation in the region of overlap with the movement of a reflector in a dual fiber arrangement

reaching the detector. As the reflector moves further away from the ends of the fibers the light must travel a greater distance and therefore spreads further. The result is that the intensity of the light in the overlap region which reaches the detector decreases.

Therefore, when the two fibers are close to the reflector the region of overlap is small. As the fibers move away from the reflector the overlap increases but the intensity grows weak. The result is that the amount of light reaching the detector passes through a maximum point. To the left of the maximum the region of overlap of the cones is the limiting factor. To the right of the optimum the distance the light must travel to reach the detector fiber limits intensity. This is illustrated in Figure 3.4.[31] This curve was generated by varying the distance between the reflector and the ends of a dual fiber arrangement. Figure 3.4 shows data for two different distances between the two fibers. The displacement range over which the initial rise in signal and the maximum occur is determined by the diameter of the fibers, their numerical aperture and the distance between the two fibers (r).[32]

Instrumentation for optical displacement measurements has been developed by Mechanical Technology Inc. Latham, NY.[33] While their instrument demonstrates that the idea is operable it does not meet our needs, because it is designed for noncontact distance measurements.

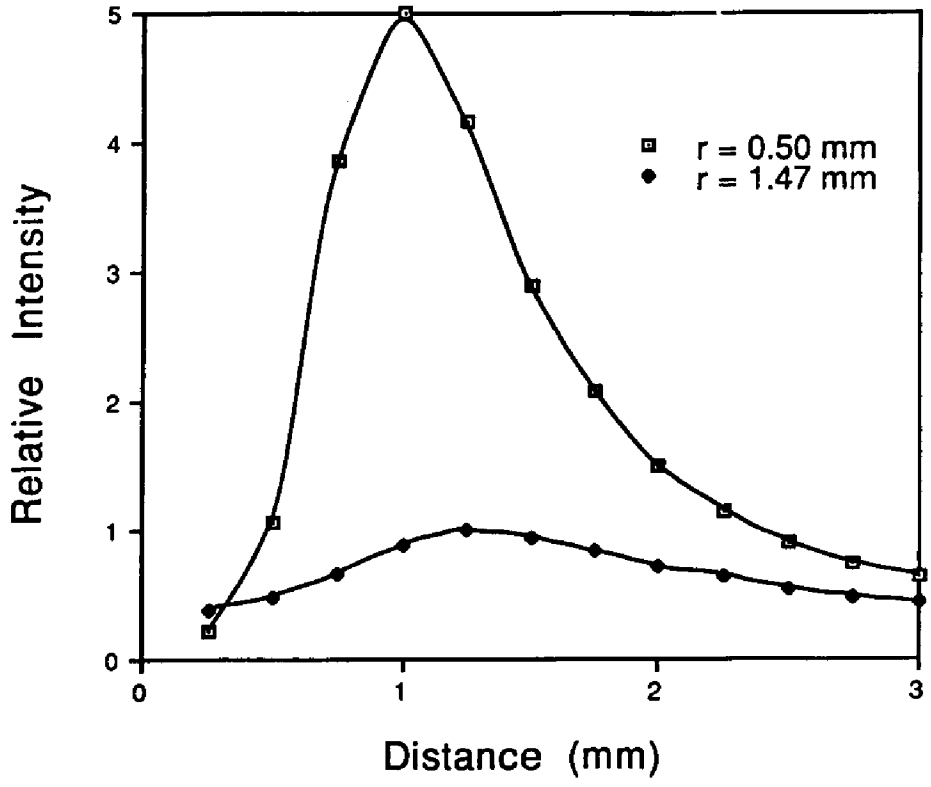

Figure 3.4: Displacement curve for the dual fiber arrangement

Single Fiber Arrangement

In a single fiber arrangement the same fiber that carries the light from the source to the reflector receives the reflected light and carries it to the detector. The light is separated via a fiber optic coupler. As the distance between the reflector and the end of the fiber changes, the intensity of the reflected light collected by the fiber changes. This is illustrated in Figure 3.5. When the fiber is very close to the reflector, as in Figure 3.5a, the intensity of the reflected light reaching the fiber is high. As the reflector moves away from the fiber, as in Figure 3.5b, the intensity of the reflected light decreases, because the beam of light spreads as it travels through space. This is illustrated graphically in Figure 3.5c.

Additional Factors

Two factors must be taken into account when implementing optical displacement into a swelling sensor system. The first is the diameter (or thickness for a cylinder) of the polymer. The second is the nature of the reflector.

The diameter determines whether the initial measurement is to the right or the left of the maximum intensity signal in the dual fiber arrangement. Therefore, this determines whether the signal increases or decreases as the polymer swells. It also determines the sensitivity of the measurement. As shown in Figure 3.4 the front slope of

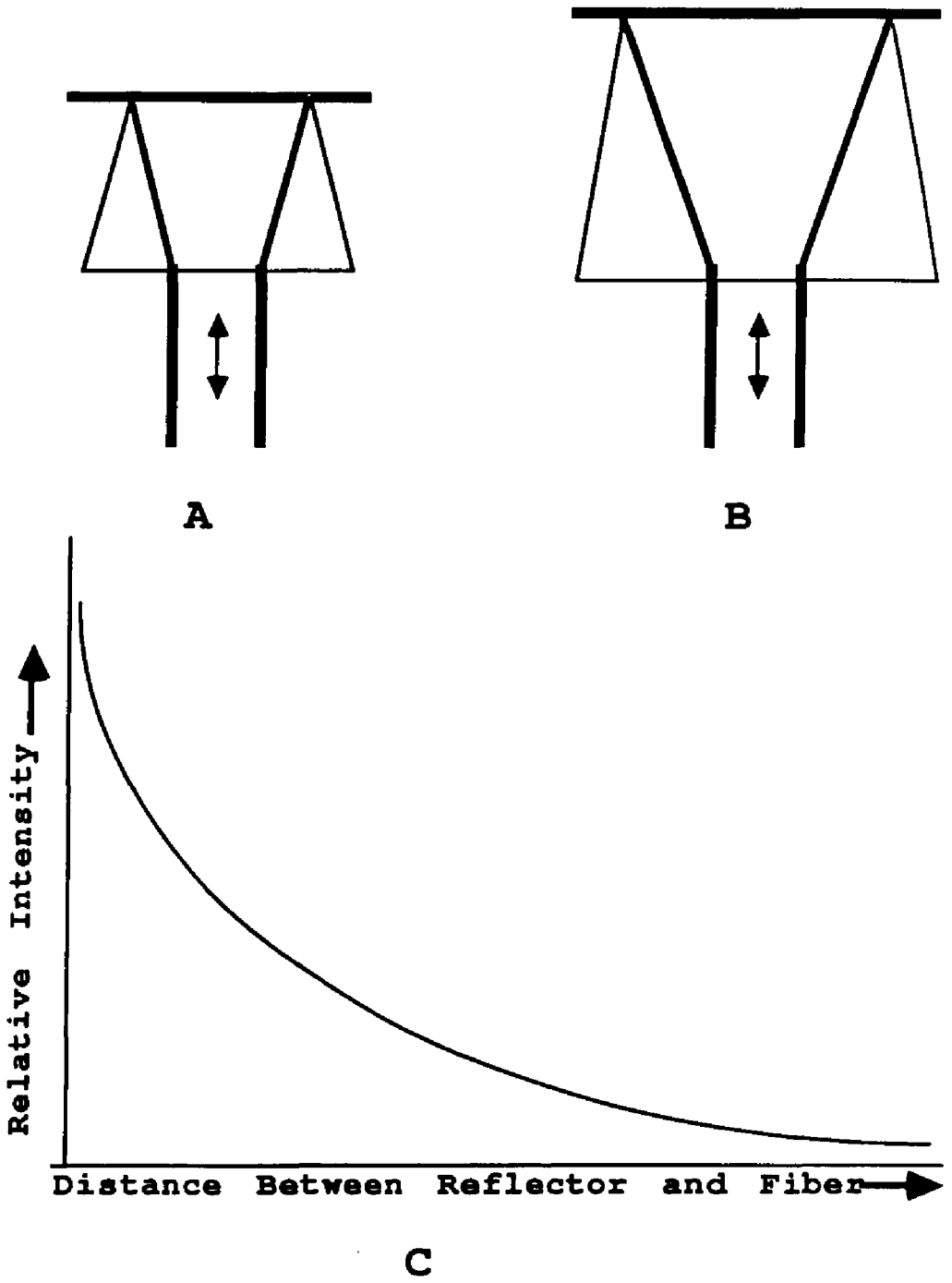

Figure 3.5: Variation in the reflected light collected with the movement of a reflector and the displacement curve for the single fiber arrangement

the curve rises more sharply than the back slope. Thus, the front slope is more sensitive than the back slope. In the single fiber arrangement, the diameter determines where the measurement falls on the curve. The measurement is more sensitive in a region where the change in the rise/change in the run is the greatest.

With regard to the second parameter, a specular reflector is preferred over a diffuse reflector. A diffuse reflector scatters light in all directions thus decreasing the amount of light available for the detector fiber to collect and reducing the slope of the intensity vs distance curve.

CHAPTER IV

SENSORS BASED ON POLYMER SWELLING: INSTRUMENTATION DEVELOPMENT

Introduction

The instrumentation for measuring the swelling of ion exchange resins and other immobilized reagents in response to various stimuli consists of the basic elements shown in Figure 4.1. This chapter describes the development of the optical system, which is composed of a beam splitter, optical fiber or fibers, a reflector and a restoring force. The optical system must allow the chemical system to swell selectively and reversibly in response to an analyte. This must then cause a measurable change in the reflected intensity. For this to happen the reflector must move freely in conjunction with the polymer as it swells and contracts.

Three fiber optic arrangements for splitting the beam of light incident on the reflector from the light reflected were investigated. Preliminary experiments involved a fiber optic bundle. Later experiments employed both a single fiber/fiber optic coupler combination and a dual fiber arrangement. While a fiber optic bundle collects light efficiently, the probe is rather bulky. The single fiber/fiber optic coupler combination is easily

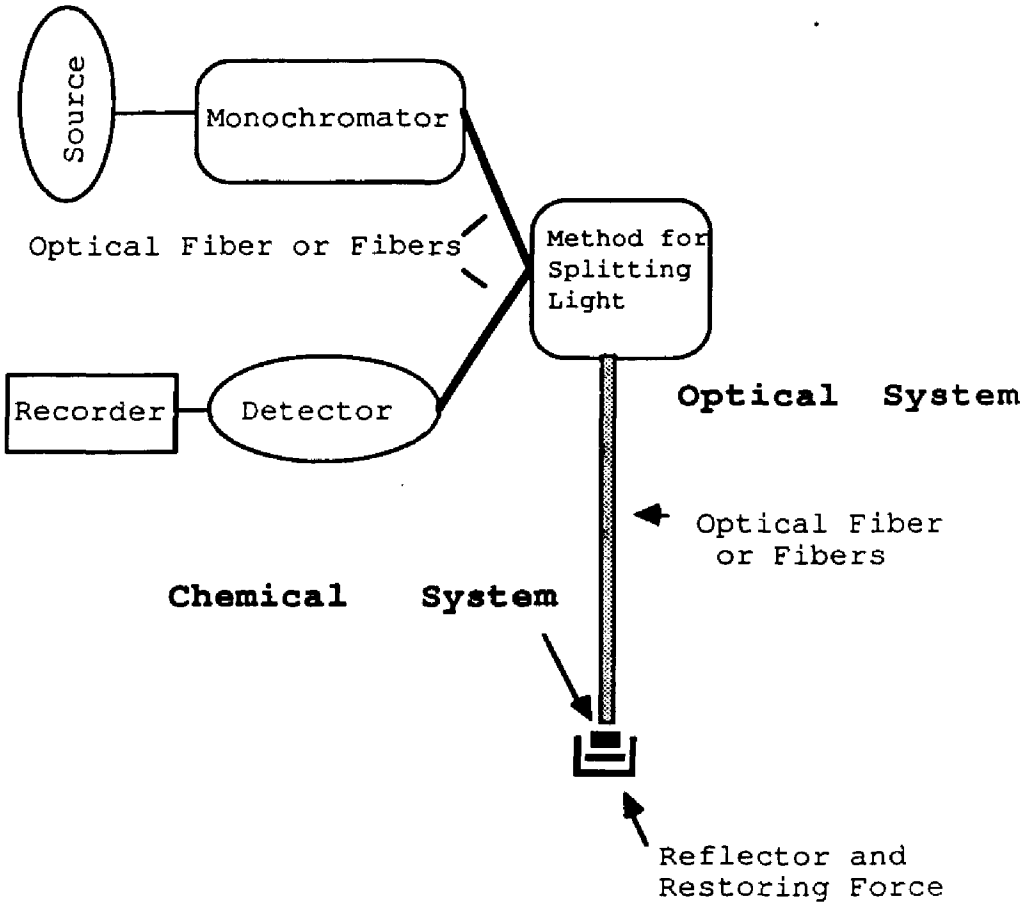

Figure 4.1: Basic elements for measuring swelling of ion exchange resins by optical displacement

miniaturized, but the amount of light collected is low. A dual fiber arrangement collects more light than the single fiber system and is still easily miniaturized.

Several different reflection arrangements were constructed for the optical system with each of the three fiber optic arrangements. This chapter describes these arrangements in detail along with other instrumentation used for this project.

Spectrofluorometer

Except for preliminary experiments, the monochromator, source, detector and recorder are part of an SLM 8000 spectrofluorometer. The SLM spectrofluorometer is a modular instrument which consists of an LH-450 xenon arc lamp, an OP-450 optical module, an MC 300 excitation monochromator with a concave holographic grating and a photomultiplier tube with a variable voltage supply for each of two channels. The emission monochromator was bypassed during all experiments. Fiber optics were coupled to the exit port of the excitation monochromator and to the detector using light-tight aluminum cylinders that fit over the lens housings in the sample chamber. The aluminum fittings are threaded to accept SMA connectors. Single optical fibers terminated with SMA connectors conduct light to and from the sample.

Preliminary experiments were performed on a fiber optic fluorometer built by Instrumentation Laboratories. It

consists of a tungsten halogen lamp, a source housing with a cooling fan and the capacity to hold filters, a photomultiplier tube housing with the capacity to hold filters, and a Heath SR-255B strip chart recorder. The detector and source housings are designed to accept a bifurcated fiber optic bundle which conducts light to and from the sample.

Fiber optic arrangements and reflection devices

Bundle

In preliminary experiments the goal was to measure optical change due to swelling of a film. This work was performed using a bifurcated fiber optic bundle (3 mm or 5 mm diameter) connected to the fiber optic fluorometer described above. Approximately half of the fibers form the branch that carries light from the source to the common end and the other half form the branch that carries light back to the detector. The fibers are randomly mixed at the common end which is immersed in the sample. A bifurcated bundle is pictured in Figure 4.2.

In many experiments a reflector was employed. The reagent phase was placed between the common end of the bundle and the reflector, as shown in Figure 4.2. The reflector is in direct contact with the reagent phase. Consequently, the measured parameter is the change in reflected intensity due to the change in the distance between the end of the bundle and the reflector due to

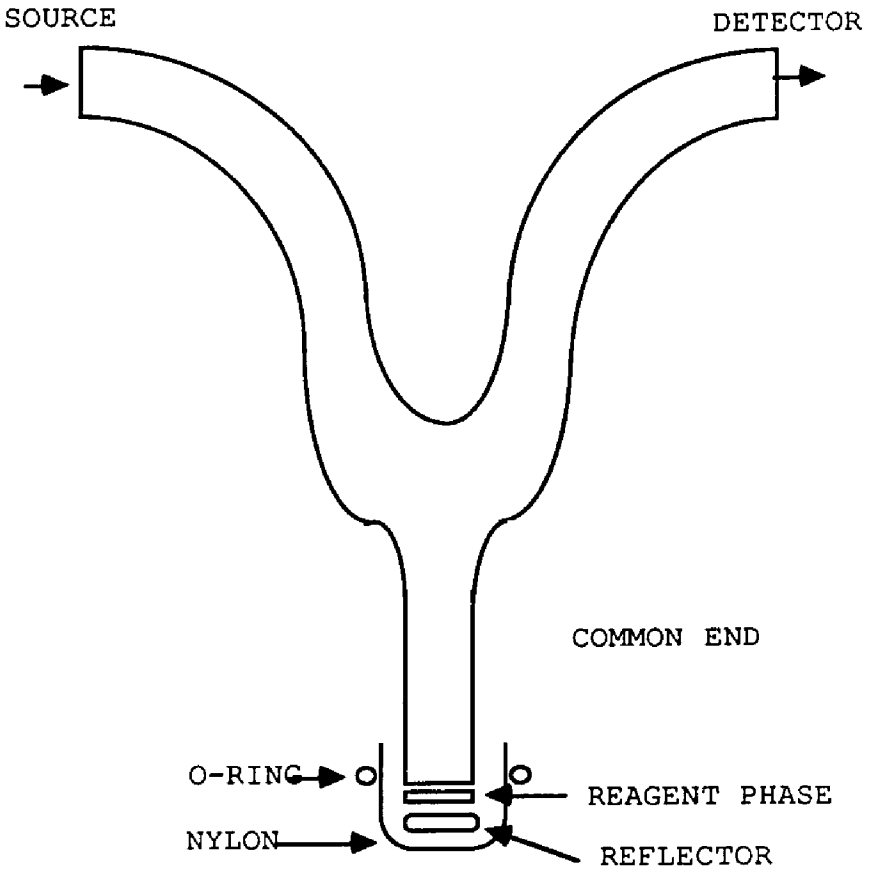

Figure 4.2: Bifurcated bundle system with reflector secured with nylon mesh and an o-ring

swelling of the reagent phase.

The reflector was a metallic grid (Polysciences, Inc. 3.05mm 1 x 100, 400) designed to support samples for electron microscopy. Both nickel and gold grids were used. The gold grids reflect more light than the nickel grids.

Initially the grid stuck to the reagent phase on the bundle without adding adhesive. However, mechanical stress due to swelling of the reagent phase as well as repeated changing of the sample solution caused the grid to fall off. To prevent this the grid was secured with a square of nylon mesh (cut from nylon pantyhose) and an o-ring. See Figure 4.2.

Single fiber

Once preliminary experiments with the bifurcated fiber optic bundle proved that swelling causes a change in reflected intensity, the sensor instrumentation was modified so that the polymer volume could be smaller. Initially, single fiber measurements were investigated. Therefore, all subsequent experiments were performed with the SLM fluorometer which is more readily coupled to single fibers.

A single fiber (200 micron core diameter, plastic-clad-silica, Ensign-Bickford, Avon, CT) terminated with SMA connectors (OFTI Billerica, MA and Ensign-Bickford Avon, CT) conducts light from a fiber optic coupler to the reflector and back, as shown in Figure 4.3. The fiber optic couplers (either 200 micron core diameter, plastic-on-silica from

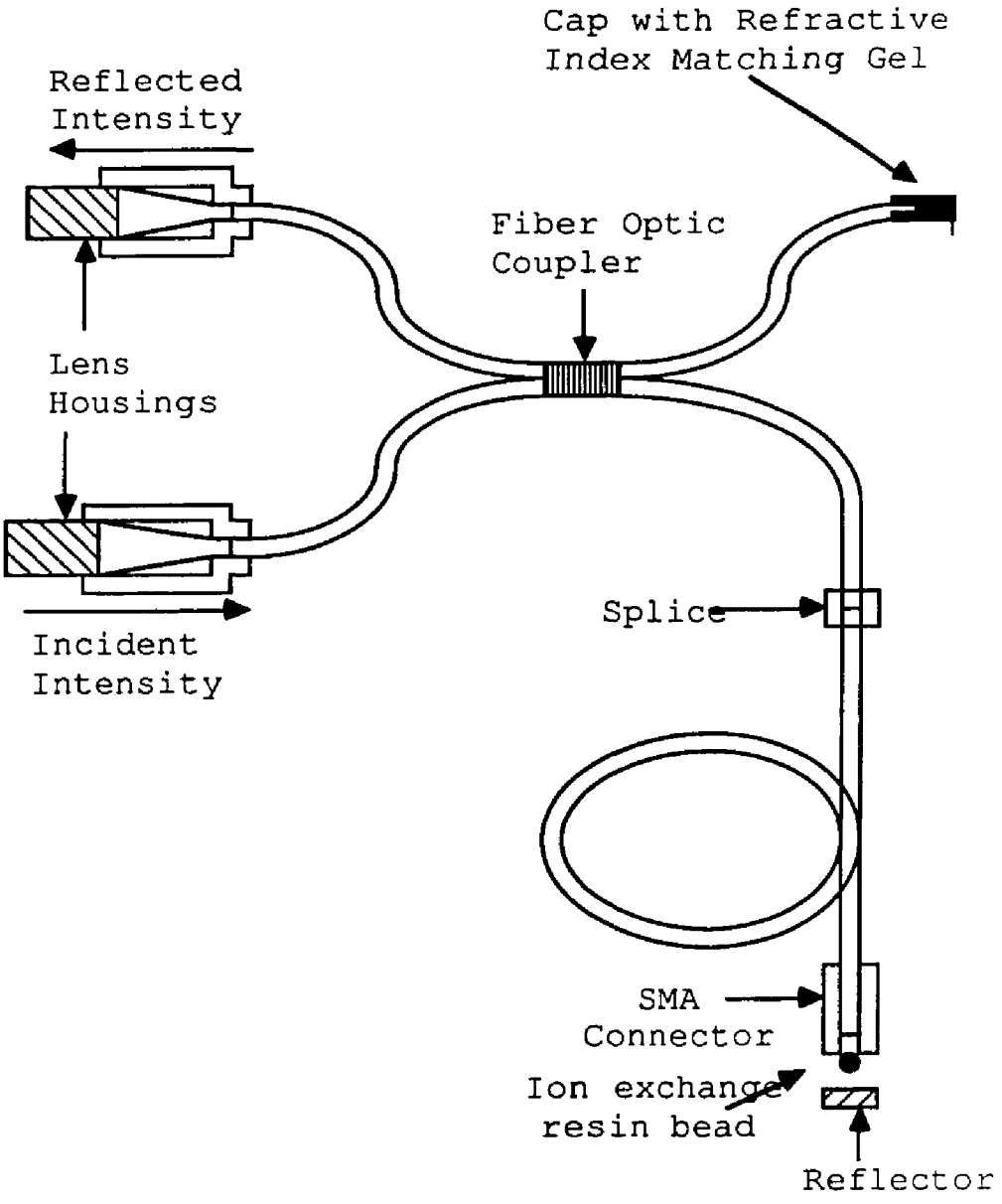

Figure 4.3: **Single fiber arrangment spliced to a fiber optic coupler**

Aster Inc. or 200 micron core diameter, glass-on-glass from ADC Westboro, MA) terminated at all four ends with SMA connectors served as a beam splitter to separate the light. The coupler fibers were terminated with SMA connectors so that they could be connected directly to the source and detector lens housings of the SLM fluorometer.

The coupler is actually two fibers which have been melted together until approximately half of the light in one fiber passes into the second fiber. The ratio of light intensity in one fiber compared to the other fiber is called the splitting ratio. The splitting ratio of the Aster coupler as a function of the wavelength was determined experimentally. The results are shown graphically in Figure 4.4. The splitting ratio for the Aster coupler is approximately 50% throughout the visible spectrum. The splitting ratio of the ADC coupler is also approximately 50% at all wavelengths in the visible spectrum.[34]

The coupler pictured in Figure 4.3 is joined via a splice bushing (Ensign-Bickford, Avon CT) to the single sampling fiber. Refractive index matching gel, a polyalpholefin compound (Petrarch), placed between the two fiber ends reduces unwanted background signal due to reflection at the interface.

In all experiments performed with the single fiber, the reagent phase was a polymer bead. In the first arrangement the bead was placed in the hole created when the

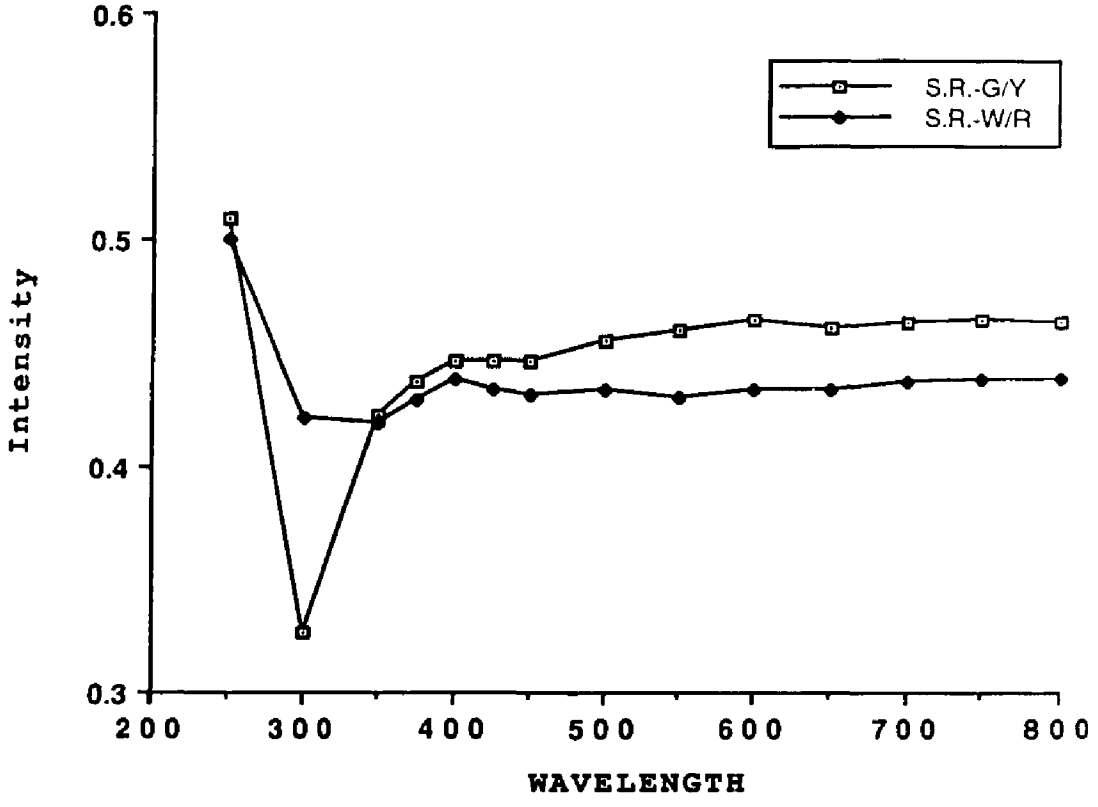

Figure 4.4: Splitting ratio of Aster fiber optic coupler

optical fiber is recessed slightly in the SMA connector terminating the fiber.

The various reflector systems designed in conjunction with this apparatus are pictured in Figure 4.5. In the first system (a) the reflector took the form of aluminum foil, a metal strip or the gold grid described previously. The reflector was held in place by an o-ring and a square of nylon pantyhose. The nylon and o-ring also served as a restoring force so that the reflector remains in contact with the bead as the bead shrinks. This was not successful. The nylon and o-ring did not allow the bead to swell. So, the reflector did not move. This system was only used with the fiber optic fluorometer.

In the next system (b) the reflector was attached directly to the bead, therefore, no restoring force was needed. The bead was held in the hole with index matching gel. The reflector (a small circle of aluminum foil punched out with a blunted needle) was held on to the bead with Lubriseal, Norland epoxy #68 (optically clear cement) or EPO-TEK epoxy (which allows the bead to swell). None were successful. The Lubriseal coats the bead preventing contact with aqueous solutions. The Norland epoxy does not hold when the bead swells. And the EPO-TEK epoxy, although initially promising, never cured despite several attempts. Painting a reflector onto the bead was also tried. Both a grey spray-paint and Liquid Paper (non-water soluble) were

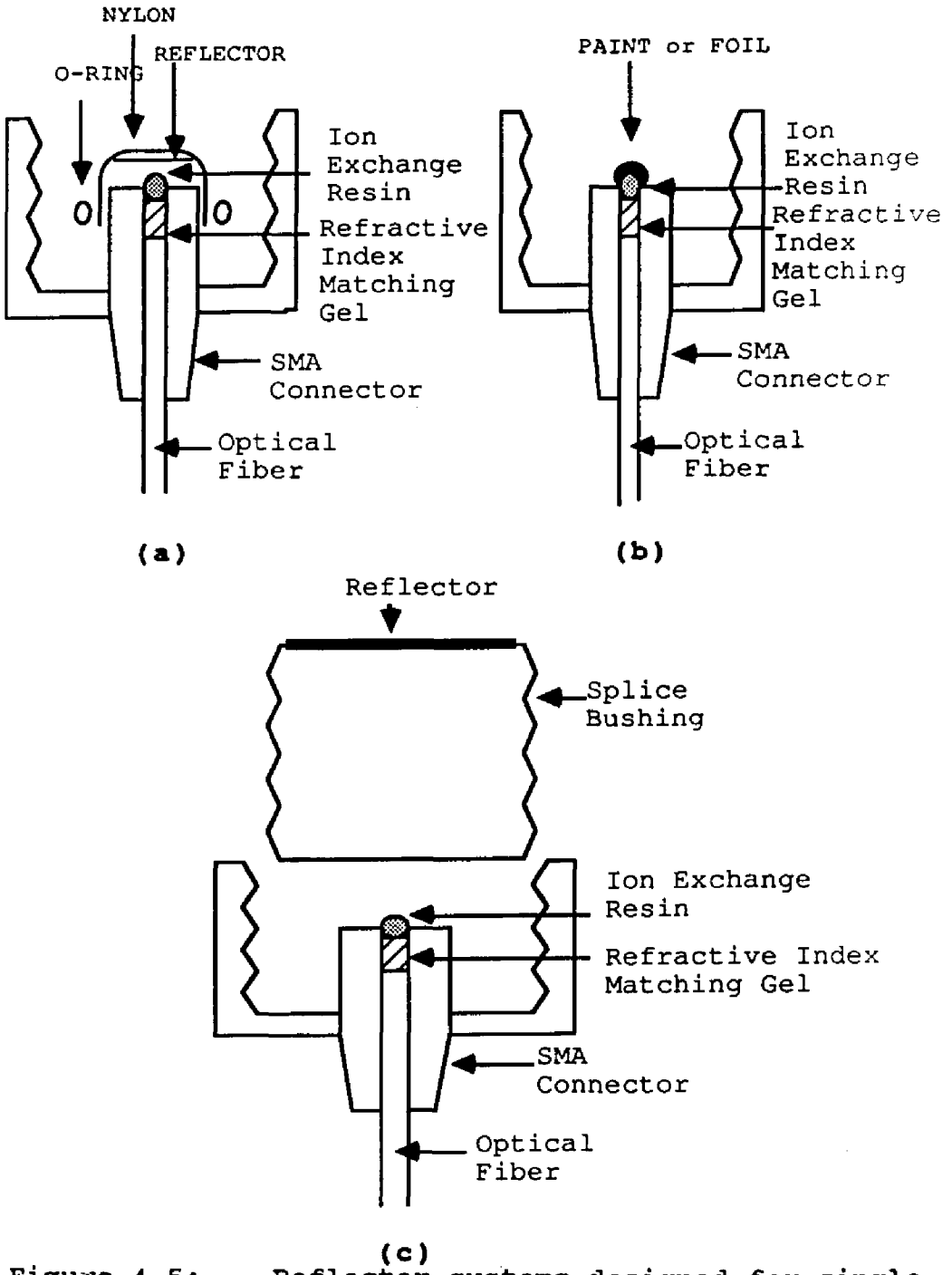

Figure 4.5: Reflector systems designed for single fiber arrangement-bead is in hole created when sample fiber is recessed slightly in the SMA connector

used. Since the bead absorbs the paint and swells, this idea was discontinued. System (b) was used only with the SLM fluorometer.

The final system (c) was successful. The reflector, aluminum foil, was attached to a bushing with EPO-TEK. The bushing was then screwed down onto the SMA connector so that it was in contact with the bead. Since the reflector position is fixed, the only parameter being measured is the change in the optical characteristics of the bead as it swells. This system was used only with the SLM fluorometer.

The next arrangement (shown in Figure 4.6) was developed so that the distance between the end of the fiber optic and the reflector would vary as the polymer swelled. The bead was placed in a depression drilled in the top of the SMA connector terminating the sampling fiber. The bead was initially held in place with index matching gel. However, since the bead tended to absorb the gel and swell, this was discontinued. It was discovered that the bead remained in place once the reflector was positioned on top of it.

The reflector is a rectangular ramp initially hinged at one end. The bead is placed between the hinge and the end of the fiber on the top of the SMA connector. This arrangement is more sensitive than when the fiber is between the hinge and the bead. At first, the reflector was hinged using Crazy Glue. However, this was too rigid. The

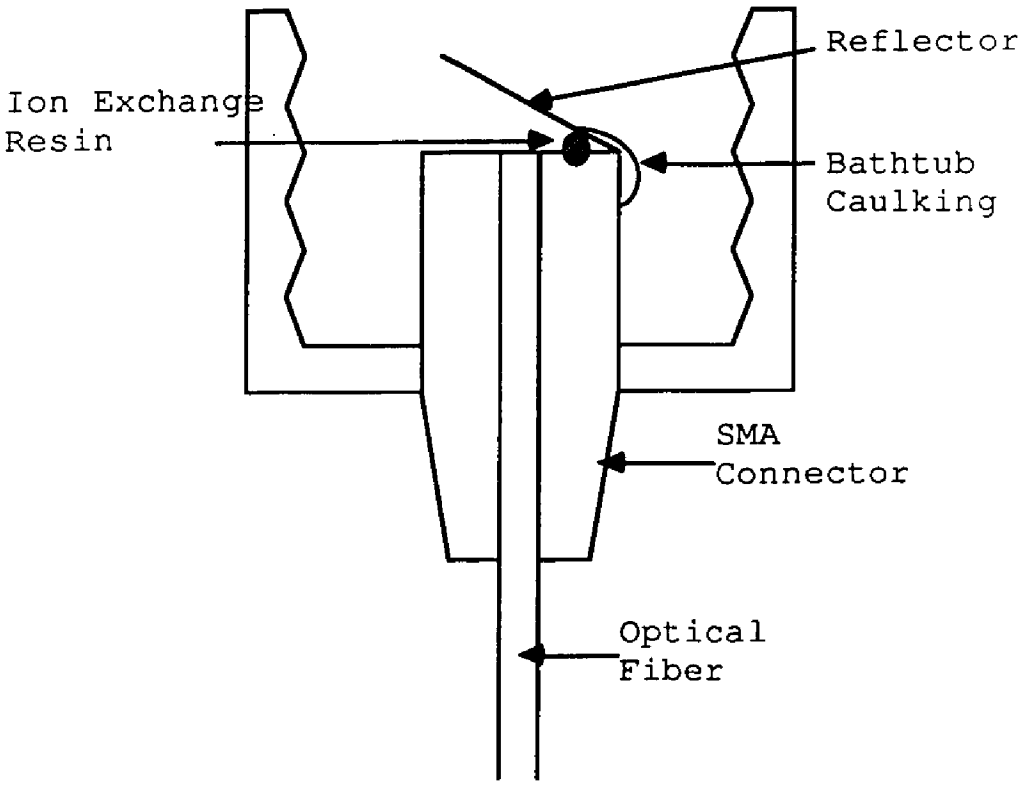

Figure 4.6: Reflector system designed for single fiber arrangement-bead is in depression drilled in top of SMA connector terminating sample fiber

alternative was tile caulking which was more flexible. Later, the reflector was not glued to the connector. Although a curved reflector was investigated, a flat polished strip of metal is the reflector of choice since the curved reflector was difficult to polish. The metal was polished with increasingly finer grades of sand paper from a fiber optic terminating kit until images were clearly reflected on the strip.

The next step was to develop a suitable way of restoring the reflector to its original position as the polymer shrinks. The approaches investigated appear in Figure 4.7. The first five all failed for various reasons.

The spongy foam in the first approach provided a force strong enough to hold the reflector in contact with the bead yet pliable enough to allow the reflector to move as the bead swelled. The foam was glued to a strip of metal which was suspended over the reflector by attaching it to a splice bushing. However, the foam absorbed the sample solution producing a "memory effect". When a new sample is placed in contact with sensing element the previous solution remains in the foam and in contact with the bead. Including a cap, as in approach two, to separate the foam from the solution did not work. Either the cap did not remove the foam from the bead enough to eliminate the memory effect or the cap added more weight than the swollen bead could displace.

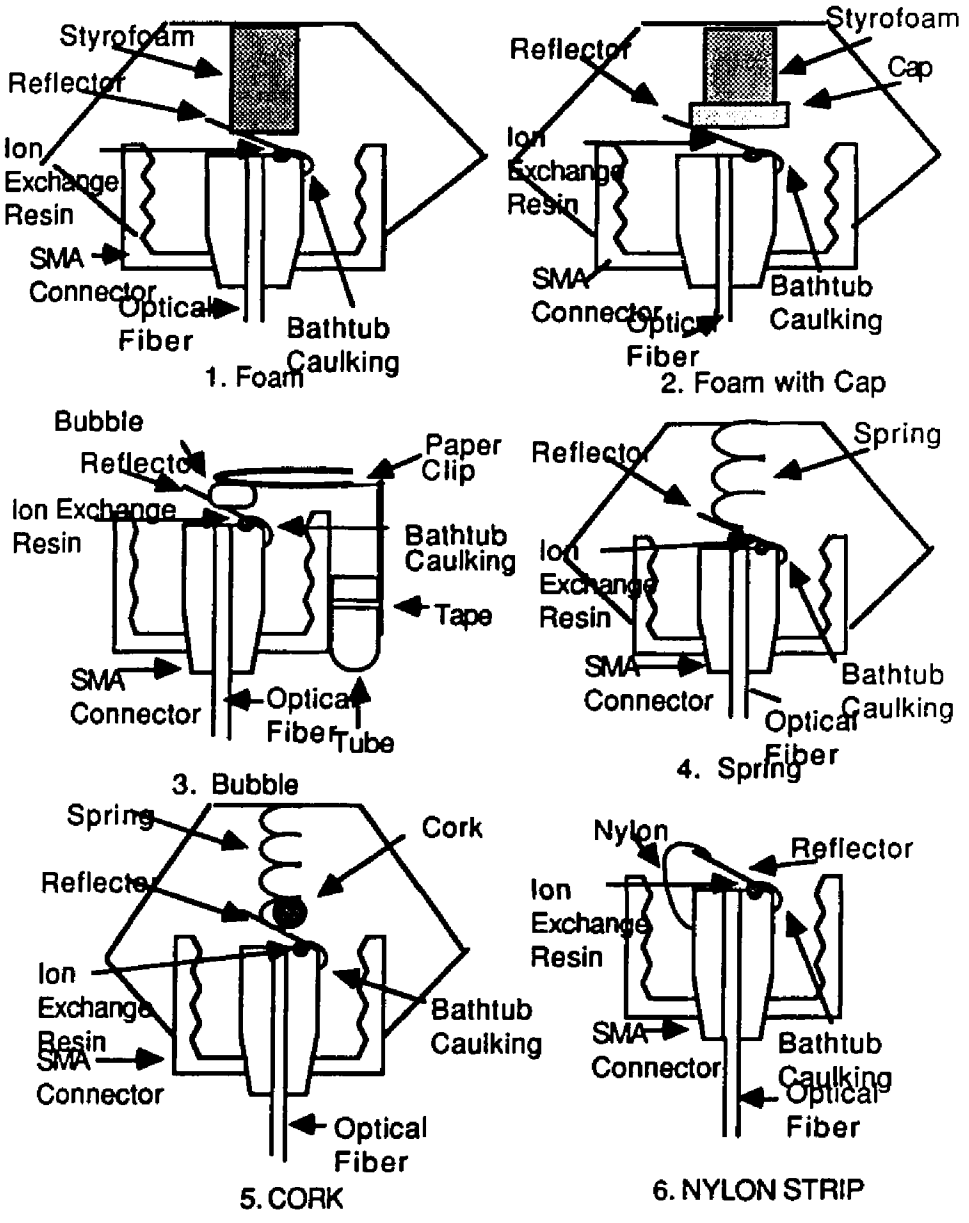

Figure 4.7: Restoring methods (designs 1-6) developed for reflector system designed for single fiber arrangement-bead is in depression drilled in top of SMA connector terminating sample fiber

Approach three involving air in a plastic bubble held in place by a paper clip also failed. The bubble held the reflector in place and allowed it to move as the bead swelled but it did not force the reflector to retract as the bead shrunk. A more rigid bubble may have alleviated this problem but then the swelling bead would not have been able to displace the reflector.

The spring arrangement in approach four was promising since it would not absorb the sample solution. However, a spring soft enough to allow the bead to displace the reflector was not available.

Approach five was to allow a cork ball caged in a spring attached to the SMA connector to float upward and hold the reflector against the bead. The cork did not absorb the sample solution. The bead could easily displace the cork and the cork forced the reflector to remain in contact with the bead as it contracted. However, the cork ball allowed the bead to fall out as the SMA connector and fiber were inverted. The cork ball was not up against the reflector until the SMA connector was inverted and in the sample.

The reflector was glued to the connector in designs one through five.

The sixth scheme was successful. A strip of nylon mesh was attached to the reflector and the SMA connector with Crazy Glue. The seventh and eighth designs improved on

this idea. These are pictured in Figure 4.8. In the seventh design the reflector was not hinged and two strips of nylon mesh held the reflector in place.

In the final arrangement the nylon mesh is held in place by hooks not glue. Two hooks are attached by a thin wire to a splice bushing which couples into the SMA connector. The third hook is glued to the reflector and holds the nylon mesh strip. The reflector is removed easily for polishing. The nylon is also changed easily when it stretches to the point where it is no longer useful. Because there is no glue, this arrangement should be applicable in organic media which would interact with many adhesives. The flat edge of the hook itself could be polished and used as the reflector.

Dual Fiber

While the single fiber arrangement was successful, intensity changes upon swelling were smaller than desired. The dual fiber arrangement, pictured in Figure 4.9, was the next improvement in the sensor design. One fiber brings light to the reflector and the second carries the reflected radiation to the detector. The two fibers are held in a single fiber SMA connector adapted to accommodate two fibers. The fibers were glued in place and clamped. The other ends of the two fibers were terminated with SMA connectors. The bead was placed perpendicular to the two fibers. The end of the probe is pictured in Figure 4.10.

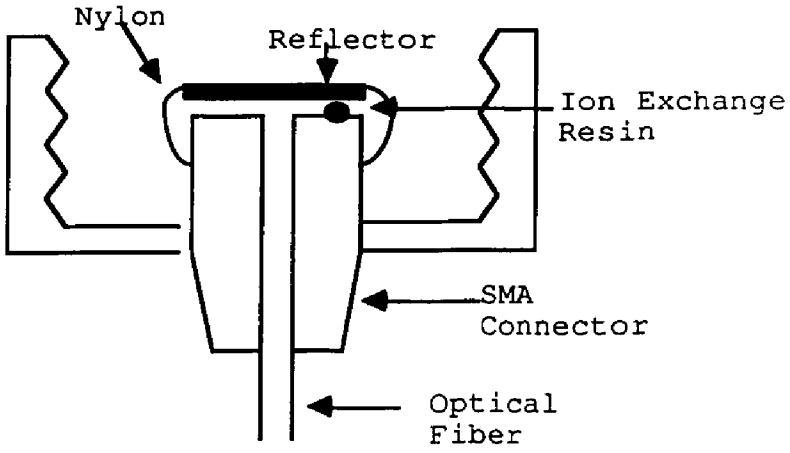

7. 2 Nylon Strips

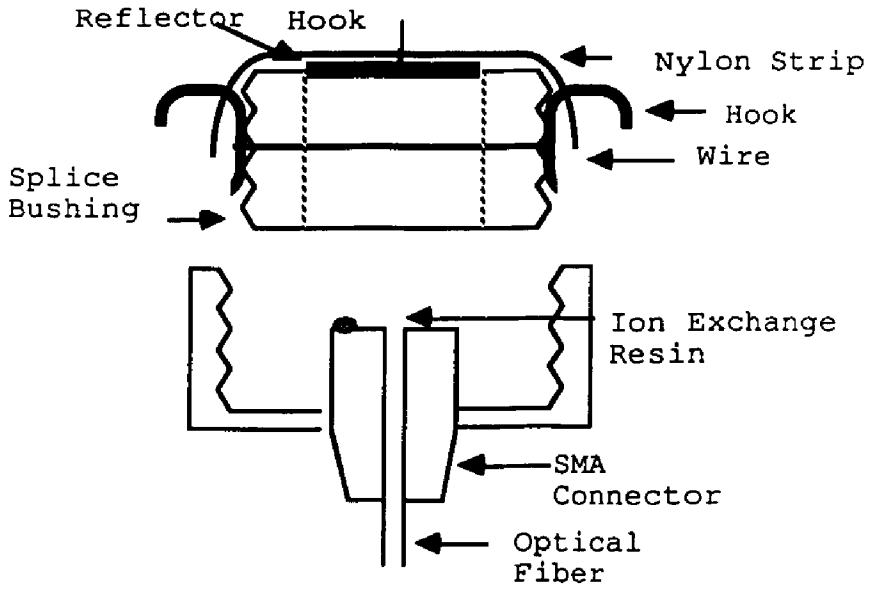

8. Nylon and Hooks

Figure 4.8: Restoring methods (designs 7 and 8) developed for reflector system designed for single fiber arrangement-bead is in depression drilled in top of SMA connector terminating sample fiber

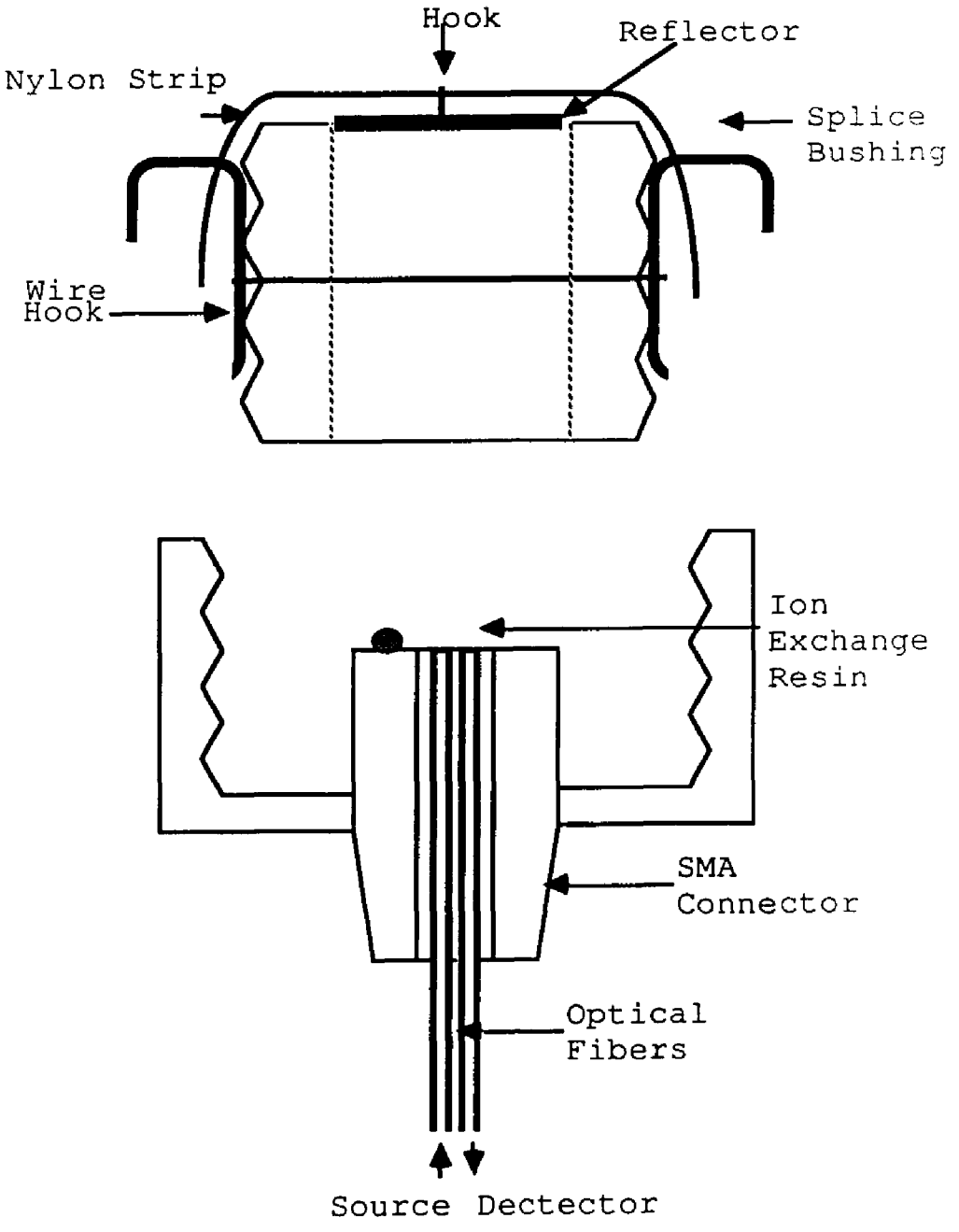

Figure 4.9: **Dual fiber arrangement with reflector and restoring design 8**

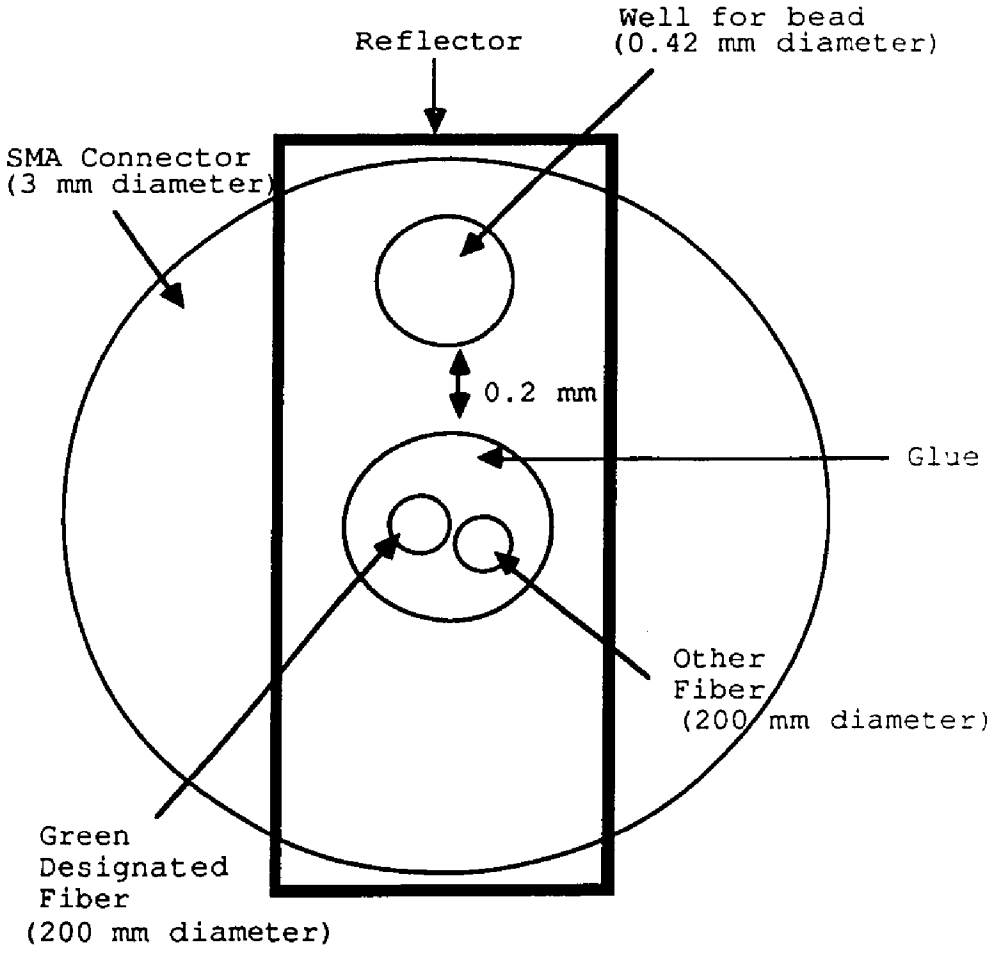

Figure 4.10: End view of dual fiber showing placement of green designated fiber in relation to the other fiber and the bead

Other arrangements are possible but were not investigated.

Other Instrumentation

An Orion Research Digital Ionalyzer/501 and a Ross combination electrode were employed to measure pH. A microscope (Carl Zeiss, Jena NR 271277), illuminator (American Optical Corp.), and dissecting tools were used to aid in placement and manipulation of the fiber optic, reflector assemblies and beads. A traveling microscope (David W. Mann Precision Instruments) and illuminator (Central Scientific Co.) were used to determine bead diameter. The 200 micron fiber was terminated with a kit (OFTI, Billerica, MA).

CHAPTER V

SWELLING BASED ION CONCENTRATION SENSOR

Introduction

An ionic strength sensor provides a convenient system for demonstrating that chemical sensors based on polymer swelling and optical displacement are feasible. Ionic strength sensors are of interest for two reasons. First, ionic strength measurements are important for sensing applications in media where ionic strength varies in an uncontrolled way such that a correction factor is required. An example of such an application could be the human body. Second, the relationship between the ionic strength of a solution and the swelling of crosslinked ionic polymers is well known. This relationship, defined by Flory[28], is outlined in Chapter 3. Third, a variety of crosslinked ionic polymers that can serve as sensing elements are commercially available in both membrane and bead form.

The swelling accompanying changes in ionic strength also provides a system for refining the instrumentation developed to measure the degree of polymer swelling by optical displacement.

This chapter will present the results of experiments to show the viability of swelling based sensors. The results of preliminary experiments involving polymer

membranes are presented. The results of experiments performed with the polymer beads, Dowex 50W and SP Sephadex, will be described in more detail. In particular, the effect of several parameters on swelling will be examined, including the degree of crosslinking of the polymer, the bead diameter, the salt concentration of the sample solution and the type of salt.

Ionic Polymer Membranes

Introduction

Preliminary investigations involved the ionic polymer membranes Nafion 117, 2-acrylamido-2-methyl-1-propane sulfonic acid polymer (AAMPS) crosslinked with N,N'-methylene-bis-acrylamide (BIS) and sulphonated polystyrene crosslinked with divinylbenzene (DVB).

Nafion is an uncrosslinked perfluorosulfonic acid polymer with crystallized regions which act as crosslinks.[35] The behavior of these crystallized regions and Nafion in general has been the subject of much investigation but is still not fully understood.[36-44] However, Nafion was tested first because it was readily available and easy to work with.

The other two membranes investigated, polystyrene and AAMPS, are covalently crosslinked and were prepared in the laboratory. Crosslinked polystyrene is usually prepared in bead form, however, membrane formulations do exist.

Initial investigations involved measuring the

optical change due to swelling in the films with changing salt solution concentration. This work was performed with the Nafion membranes. In other experiments a reflector was used. Consequently, the parameter measured was the change in the reflected intensity. The change is the result of the change in the distance between the end of the bundle and the reflector due to swelling of the membranes as the salt concentration is varied.

Experimental

Apparatus. The instrumentation used to measure the degree of polymer swelling is described in Chapter 4. The apparatus used to prepare the AAMPS and the sulfonated polystyrene crosslinked membrane polymers consisted of a constant temperature water bath, an oven, a petri dish, a desiccator, two metal plates, two rubber spacers, two glass slides and clamps, a UV lamp, and a flood lamp.

Reagents. Nafion 117 (5% solution in lower aliphatic alcohols) was purchased from Aldrich. Divinylbenzene (tech grade 55%), benzoyl peroxide (97%), ethylbenzene (99%), styrene (99%), chlorosulfonic acid (99%) 2-acrylamido-2-methyl-1-propane sulfonic acid (99%) and riboflavin were purchased from Aldrich. N,N'-methylene-bis-acrlyamide was from Sigma. Ammonium persulfate and KCl were purchased from Fisher Scientific. NaCl was purchased from JT Baker Chemical Co..

Procedures. Initially a 50 microliter aliquot of

the 5% solution of Nafion was delivered to the common end of the 5 mm bifurcated fiber optic bundle with a diameter of 5 mm. The bundle was clamped such that the common end was horizontal pointing upward. The alcohols evaporated leaving a thin film on the end of the bundle. The common end of the bundle was then placed in KCl solutions with various concentrations. The other two ends of the bifurcated bundle were connected to the source and detector of the fiber optic instrument as described in Chapter 4. The optical change due to swelling of the membrane with changing KCl solution concentration was measured.

Next, 15 microliters of 5% Nafion solution was placed on a 4 mm diameter concave-planar glass spacer to form a membrane. Each membrane was allowed to equilibrate in a different concentration KCl solution for more than 24 hours. Each membrane was then placed on the end of the fiber bundle and the optical change due to swelling of the membrane with changing KCl concentration was measured.

In another experiment Nafion membranes were formed on the end of a 3 mm diameter fiber optic bundle. In this instance a 10 microliter aliquot of 5% Nafion solution was delivered to the common end of the bundle. Also, Nickel and Gold grid reflectors were employed. A square of nylon mesh and an o-ring held the grid in place on the side of the film exposed to the solution. The change in reflected intensity with changing KCl concentration was measured.

Two different ways of forming sulfonated polystyrene membranes crosslinked with DVB were investigated. The first followed a procedure published by Zundel.[45] In the second method the film is formed in a petri dish. 965 microliters styrene and 35 microliters DVB were mixed together in 1 ml ethylbenzene with 0.01 g benzoyl peroxide as the initiator. 570 microliters of this mixture was delivered to the petri dish. A watch glass was placed over the petri dish and held down by a beaker containing 400 ml water to reduce monomer evaporation. The entire assembly was placed in a 70°C to 90°C oven. The ethylbenzene evaporates leaving a crosslinked polystyrene film.

The film was sulfonated by adding 2 ml chlorosulfonic acid to the petri dish. The dish was covered with a watch glass and placed in a desiccator for approximately 1.5 hours. The petri dish was intermittently lightly agitated causing evolution of HCl vapor. Then the dish was exposed to the air for approximately 0.5 hours to completely remove the HCl. The sulfonation reaction appears in Figure 5.1.

A 4.9% crosslinked AAMPS polymer film was prepared by polymerizing 2-acrylamido-2-methyl-1-propanesulfonic acid in the presence of the crosslinking agent N,N'-methylene-bis-acrylamide (BIS). 1350 microliters of a 1.93 M solution of AAMPS and 1200 microliters of a 0.15 M solution of BIS were delivered to a 8.8 cm diameter petri dish to form a

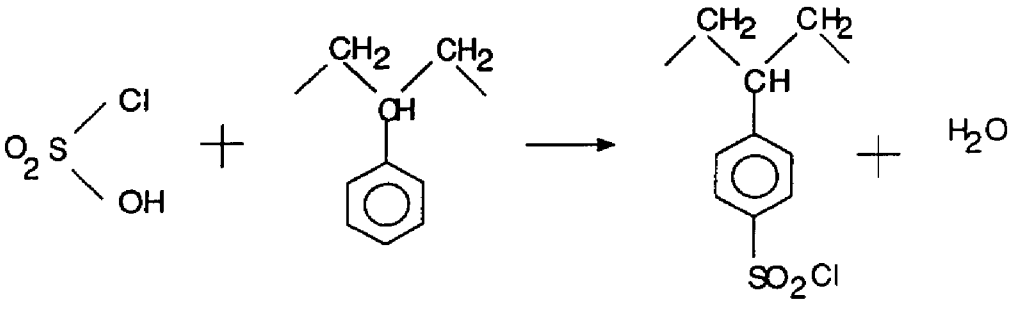

SULFONATION

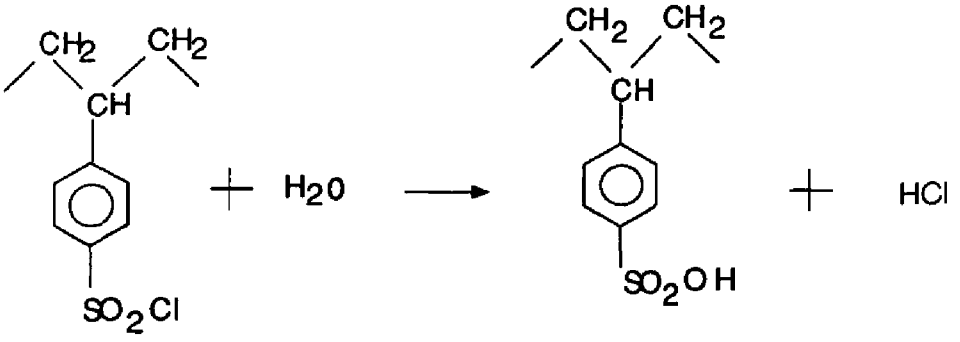

HYDRATION

Figure 5.1: Sulfonation reaction of polystyrene film

0.009 cm thick film. To prevent quenching of the free radical polymerization mechanism both solutions were made with water that was deoxygenated by nitrogen bubbling. Riboflavin 0.4 g and ammonium persulfate 0.4 g were added to the petri dish to initiate polymerization. The reaction was photocatalyzed with either a UV lamp or a flood lamp. Similar procedures for preparing polyacrylamide crosslinked with BIS have been described in the literature.[46,47]

The gel was swollen with water and a 3 mm diameter disk of the film was cut out with a disposable pipet. The disk was placed on the 3 mm fiber optic bundle. The polymer and the gold grid reflector were held in place with a square of nylon mesh and an o-ring. The change in the reflected intensity with increasing NaCl concentration was measured.

Results and Discussion

No optical change with changing KCl concentration was evident when Nafion membranes were formed directly on the 5 mm diameter fiber optic bundle. Erratic optical changes with changing KCl concentration were noted in the Nafion films formed on the glass spacers. It is believed the changes were not due to the variations in KCl concentration but to differences in the films formed for the individual KCl solutions. There was also no change in reflected intensity due to changing KCl concentration when the nickel and gold grid reflectors were added. A visual test of swelling on a large plug of Nafion indicated that

while Nafion swells in water there was no visible change in salt solution.

The experimental results indicate that Nafion does not follow the theory developed by Flory. Nafion is not a crosslinked polymer. The amount of swelling is controlled by the crystallized regions in the polymer,[36] and the behavior of these crystallized regions is poorly understood. Flory's theory outlined in Chapter 3 does not consider the swelling behavior of polymers such as Nafion which have these regions.

Another possible explanation for the lack of change in the swelling of Nafion with changing salt concentration is that the change in swelling was too small to measure with the available instrumentation. Only one in every eight monomer units of Nafion is sulfonated while conventional resins are close to 100% sulfonated.[40] As explained in Chapter 3 a decrease in the number of fixed charges per repeating unit ionized decreases the degree of swelling.

Another difficulty with Nafion is that the amount of the crystallized regions is unknown. Consequently, a parameter comparable to the percent crosslinking can not be calculated. Since the extent of crosslinking has a direct effect on the degree of swelling, the amount of crosslinking or effective crosslinks must be known to control swelling. Because a polymer with controllable crosslinking was required, both sulfonated polystyrene and AAMPS were

investigated.

The sulfonated polystyrene films crosslinked with DVB formed were too brittle and delicate to be of practical use. This material is typically formed in beads and is not readily prepared as a film.

Reflected intensity varied with NaCl concentration for the BIS crosslinked AAMPS film. The reaction was reversible but not consistent. The change in intensity was less than 20% when the salt concentration was increased to 1 M.

Preliminary work with polymer films indicated that the basic premise was viable but a better medium was required. The films were difficult to prepare in a controlled manner. Also, the change in the reflected intensity with changing salt concentration was too small.

Ionic Polymer Beads

Introduction

Another alternative examined was ionic polymers in bead form. The specific polymer beads tested were Dowex 50W and Sulfopropyl Sephadex (SP Sephadex). The bead polymers were investigated in more detail, because they proved to be more useful as sensing elements.

The first bead polymer examined was Dowex 50W, a sulfonated polystyrene crosslinked with divinylbenzene (DVB). Dowex 50W is a cation-exchange resin typically used in chromatographic columns. Resins used in these columns

are highly crosslinked to avoid rupture of the column due to swelling when solvent is introduced. The most common percentage crosslinking is 8%. Resins with degrees of crosslinking as low as 2% are available, however. Dowex 50W was chosen because the degree of crosslinking was known and beads with a range crosslinking percentages were available commercially.

The second bead polymer investigated was SP Sephadex, a sulfonated dextran crosslinked with epichlorohydrin. SP Sephadex is a strongly acidic cation exchanger used primarily for the chromatography of proteins. SP Sephadex was chosen because preliminary investigations indicated that the polymer swelled more than Dowex in the same solutions. The degree of crosslinking is not, however, reported in the product information.

The variables that affect the swelling of ionic polymer beads and thus the response of swelling based salt concentration and ionic strength sensors have been described by Flory and are outlined in Chapter 3. Several of these parameters were held constant using a single type of polymer. They include the molecular weight, the number of fixed charges ionized per repeating unit, the nature of the counter ion and the crosslink length. In addition, the nature of the solvent was held constant by using deionized water in all experiments.

The parameters varied were the percent crosslinking

of the polymer, the polymer bead size, the concentration of the salt solution and the type of salt in the sample solution. The effects of these variables were systematically evaluated by independently varying each one.

The effect of percent crosslinking was examined using 2, 4 and 8% crosslinked Dowex beads. The bead size was varied for the Dowex resin with the percent crosslinking that exhibited optimum swelling properties. The beads were grouped as small, medium and large.

Finally, the response for several different salts was examined, using the Dowex 50W and SP Sephadex beads that exhibited optimum swelling properties. The salts investigated were NaF, NaCl, KCl, $CaCl_2$ and Na_2SO_4.

The total amount of reflected light detected by the assembly was affected by three instrumental parameters: the number of fibers in the probe, the arrangement of the optical fibers carrying light from the source and bringing light to the detector and the wavelength of light involved. These parameters were also varied.

The experiments performed to test the viability of the swelling based ion concentration sensor are detailed in this Chapter along with the effect of the variables on the sensor response.

Experimental

Apparatus. The apparatus for measuring the displacement of the reflector due to the swelling of the

polymer and for measuring the bead diameter is described in Chapter 4. Both designs seven and eight were employed.

Reagents. Dowex 50W-X8 100-200 mesh ionic form H^+ was purchased from Baker. Thomas (8690-B10) Lubriseal standard formula was used. NaF, KCl, $CaCl_2$ were purchased from Fisher Scientific. $CaCl_2$, Na_2SO_4 and NaCl were from JT Baker Chemical Co.. Dowex 50W-X2, Dowex 50W-X4, Dowex 50W-x8 50-100 mesh cation exchange resins and C-50-120 SP Sephadex were from Sigma.

Procedures. The 2% Dowex beads were separated into three size groups, small (0.33 - 0.43 mm), medium (0.44 - 0.54 mm) and large (0.55 -0.65 mm). The SP Sephadex beads were also separated into size groups but experiments are only reported for beads with 0.43 - 0.47 mm diameters. The SP Sephadex beads in the other size groups showed no response.

The groupings were determined by visual observation under a microscope. The actual diameters of the beads were determined after the beads had been employed in the sensor probe. Some of the beads were lost or destroyed before the diameter could be determined. When the saved beads were measured, it was discovered that a few of the beads were placed in an incorrect group. In the body of this thesis, the actual bead diameter is indicated if known. When the exact diameter is not known, a size range is estimated.

The diameters of the beads were measured in the

following manner. The bead was swollen in distilled water, then placed on a glass slide. One edge of the bead was lined up with the crosshairs of the traveling microscope and the position in millimeters was recorded. The glass slide was moved until the opposite edge of the bead was lined up with the crosshairs and the position of the bead was again recorded. The difference in the position of the bead was the diameter. The beads were dried and stored.

Dissecting tools were used to place the bead polymers in the hole drilled in the SMA connector. The process was observed with a microscope.

The size of the hole drilled in the SMA connector was determined by filling the hole with modelling clay, removing it and measuring the depth and width of the model as the diameter of the beads were measured. The hole was 0.42 mm wide and 0.20 mm deep.

Displacement of the reflector as a function of ion concentration in all experiments was determined in the following manner. The dual or single fiber, bead and reflector assembly was placed into distilled water first, then into a 1 M salt solution. This process was repeated until the intensity readings stabilized. Then, the assembly was immersed into increasingly concentrated salt solutions ranging from 0.001 to 1 M. The displacement of the reflector due to the swelling of the polymer was measured. The sample was stirred at a slow to moderate rate. The

reflector was removed and polished when necessary and the nylon mesh was replaced when needed.

The swelling of the polymer was reversible in salt solutions ranging in concentration from 0.00001 (distilled water) to 1.0 M. The absolute change in intensity as a function of ionic strength was not reproducible but the normalized reflected intensity change was reproducible. For this reason, the normalized reflected intensity changes as a function of salt concentration were reported.

The following standard conditions apply unless otherwise indicated. A 2% Dowex or an SP Sephadex bead was immersed in NaF solutions. A dual fiber probe was employed. The green designated fiber (the green taped fiber of the ADC coupler used with the single fiber assembly and the green taped fiber of the dual probe) carried light from the source. The displacement was measured at 400 and 500 nm.

In some experiments, design number seven described in Chapter 4, was employed and the assembly and sample were surrounded by a black box. In other experiments design eight was used. The assembly and sample were not placed into the black box, but the experiment was performed at night in a darkened room.

Results

Response to ion concentration. The most sensitive response to salt concentration is shown in Figures 5.2 and 5.3 at 400 and 500 nm, respectively. It was observed with

the 2% crosslinked (0.33 mm) Dowex bead sensor. The reflected intensity decreases with increasing NaF concentration. The reflected intensity has been normalized to 100% for distilled water. The experiment was performed with design 8 at night in a darkened room. A 40% change in the normalized reflected intensity was noted at 500 nm while a 48% change in the normalized reflected intensity was seen at 400 nm. The majority of the change occurs in a narrow region from 0.100 to 1.00 M.

Similar response was observed for the SP Sephadex bead (0.47 mm) sensor as shown in Figure 5.4 and 5.5 at both 400 and 500 nm, respectively. The reflected intensity has been normalized to 100% for distilled water. The experiment was performed at night in a darkened room with design eight. At 500 nm the average change in the normalized reflected from 0.00001 to 1.00 M was 83%. The average change at 400 nm from 0.00001 to 1.00 M was 93%. The largest change was from 0.001 to 0.100 M.

Dual versus single fiber probe. The first factor varied was the number of fibers in the sensor probe. The response of the single fiber probe is shown in Figure 5.6. The experimental conditions are similar to those for the dual fiber probe presented in Figures 5.2 and 5.3. Both experiments were performed with a 2% Dowex bead and design eight. The diameter of the 2% Dowex bead used in the dual fiber experiment was 0.33 mm. The estimated diameter range

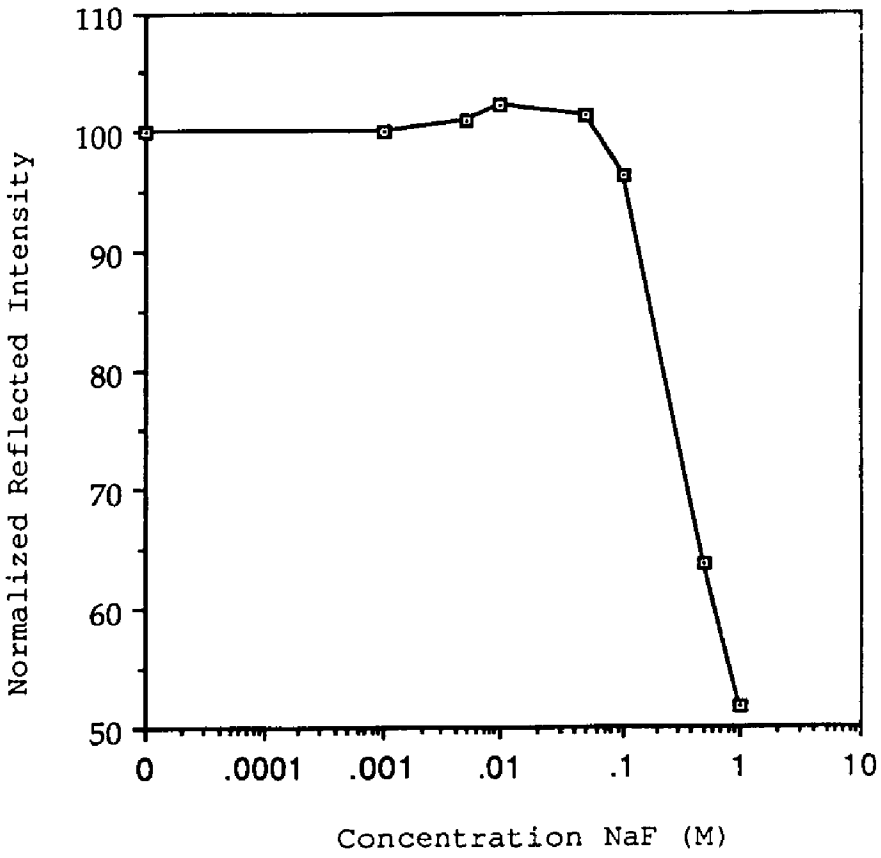

Figure 5.2: Response of a 0.33mm 2% Dowex bead dual fiber sensor at 400nm

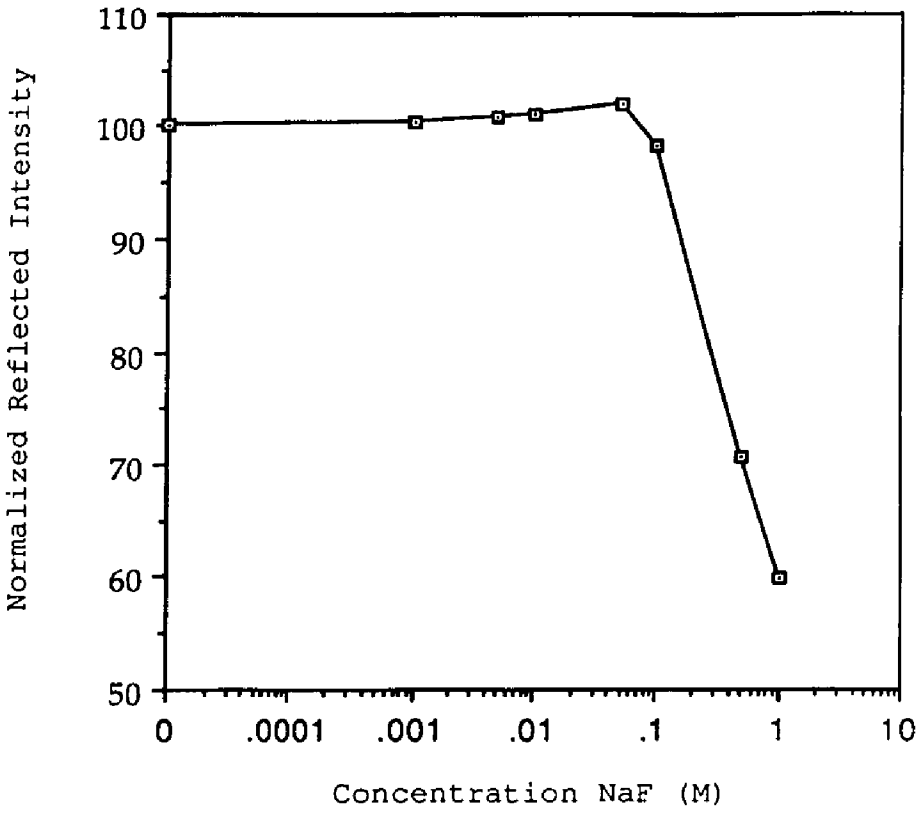

Figure 5.3: Response of a 0.33 mm 2% Dowex bead dual fiber sensor at 500nm

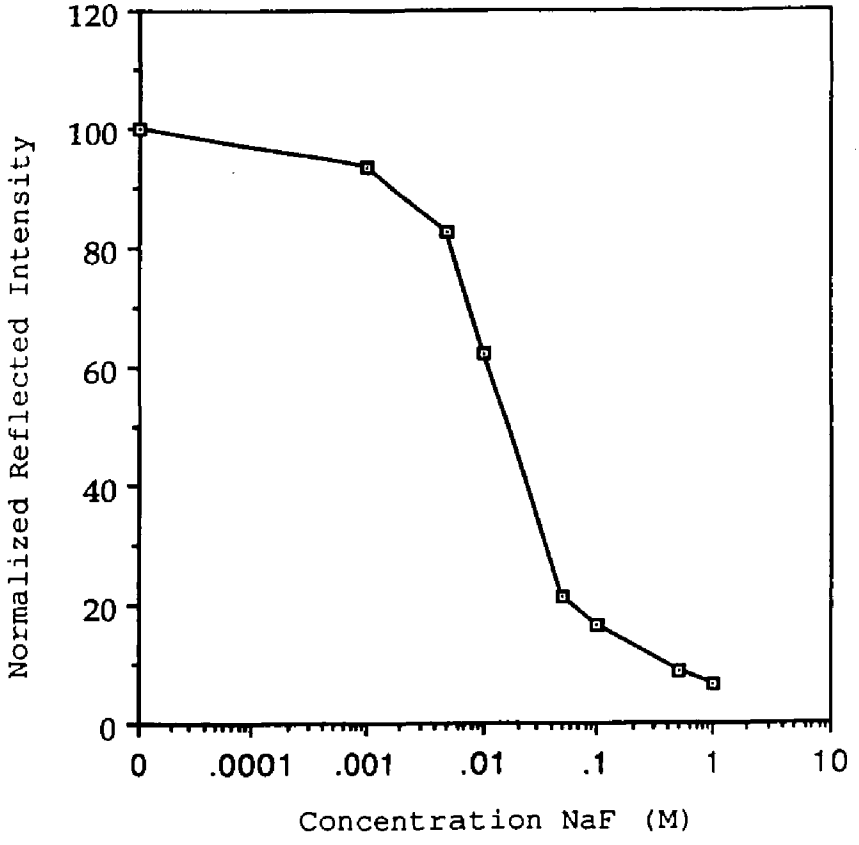

Figure 5.4: Response of a 0.47 mm SP Sephadex bead dual fiber sensor at 400 nm

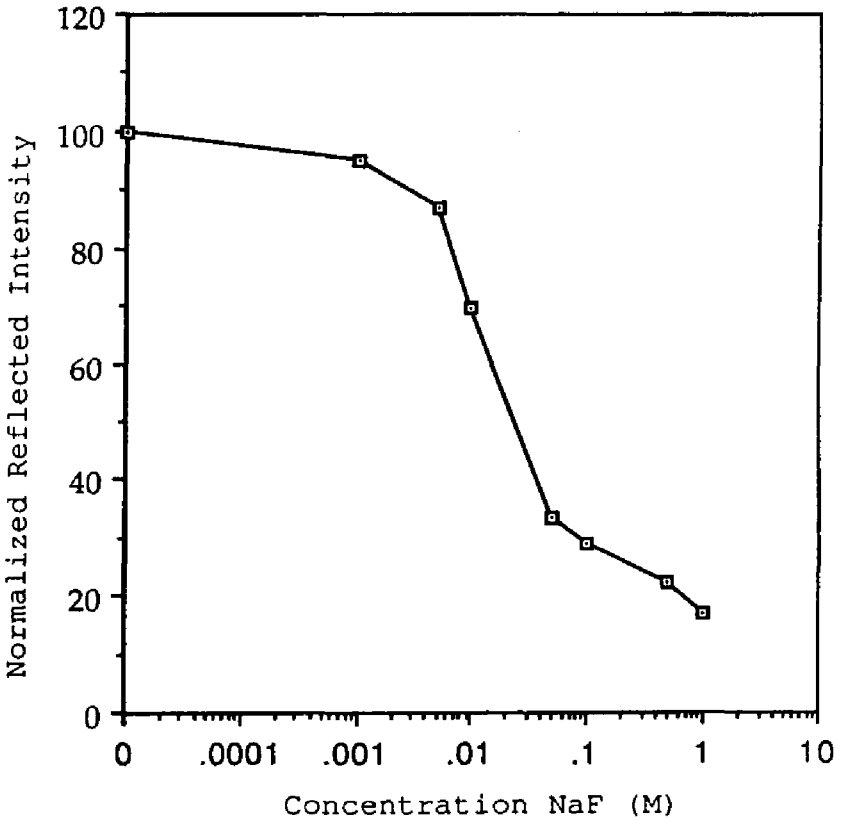

Figure 5.5: Response of a 0.47 mm SP Sephadex bead dual fiber sensor at 500 nm

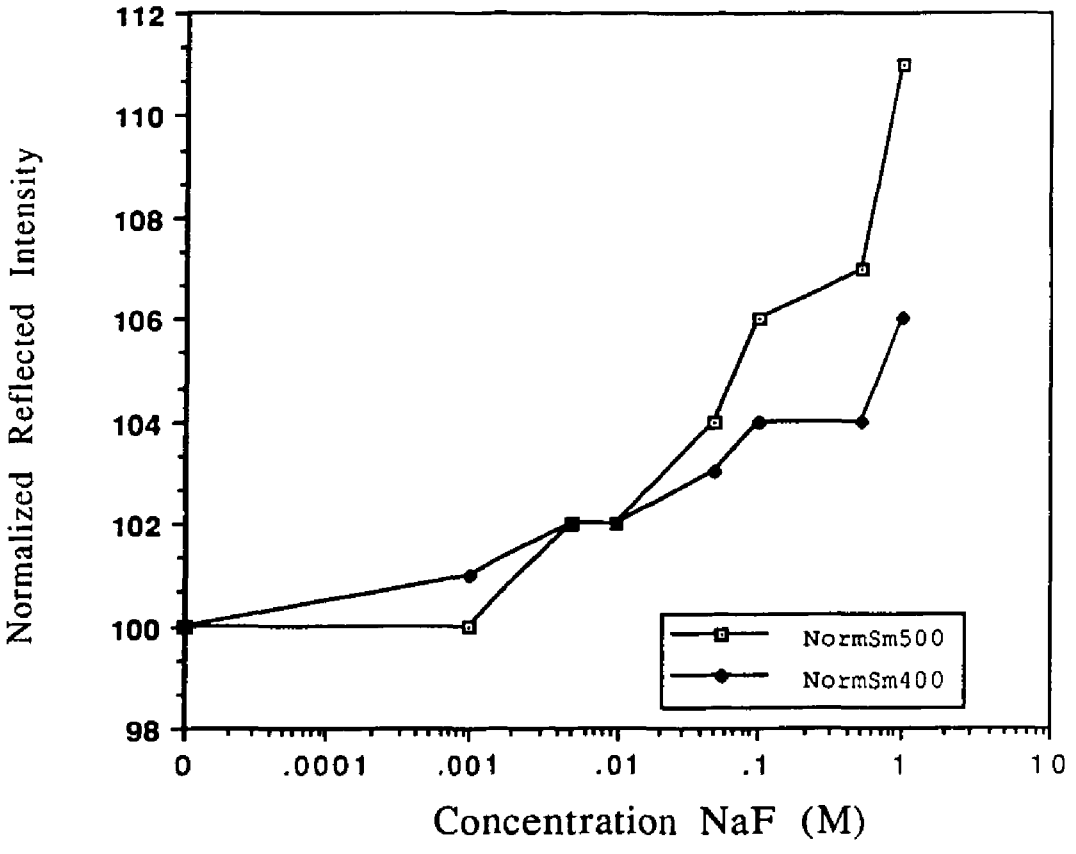

Figure 5.6: Response of a 2% Dowex bead (0.33 - 0.43 mm) single fiber sensor at 400 and 500 nm

for 2% Dowex bead used in the single fiber experiment was 0.33 - 0.43 mm. The experiments were performed at night in a darkened room. The reflected intensities were normalized to 100% for distilled water.

The normalized reflected intensity measured by the single fiber probe increased as the log of the molarity increased. The percent change was 6% at 400 nm and 11% at 500 nm for concentration changes from 0.000010 to 1.00 M.

Green to detector versus green to source. The next variable investigated was the difference in the two fibers which brought light to the detector and from the source. In the single fiber probe this variable took the form of the splitting ratio of the fiber optic coupler. This parameter was described in Chapter 4. The two fibers in the dual fiber probe were compared. An SP Sephadex bead with an estimated diameter range of 0.43 - 0.47 mm was used. The experiment was performed in a black box with design seven. The intensity was normalized to 100% for distilled water.

The arrangement with the green designated fiber to the source produced a 30% change at 500 nm and a 39% change at 400 nm for a 100 fold change in molarity. This is illustrated in Figure 5.7. The probe with the green taped fiber coupled to the detector produced a change of 21% at 500 nm and 31% at 400 nm for a 100 fold change in concentration. This is illustrated in Figure 5.8.

Response versus wavelength. The third instrumental

variable investigated was the relationship between the wavelength and the response of the sensor probe. The results of this experiment appear in Figure 5.9. The response is given for the visible range from 325 to 800 nm. The diameter of the SP Sephadex bead was 0.43 mm. The experiment was performed at night in a darkened room with design eight.

Percent crosslinking. The effect of the percent crosslinking on the swelling of the Dowex polymer bead is shown in Figure 5.10 for 500 nm and in Figure 5.11 for 400 nm. The percent crosslinking varies from 2 to 8 percent. The diameters of the 2, 4 and 8% crosslinked Dowex beads were 0.45, 0.36 and 0.42 mm, respectively. The reflected intensity was normalized to 100% for distilled water. The analysis was performed at night in a darkened room with design eight.

As the percent crosslinking increased, the change in the normalized reflected intensity decreased. This was consistent with expectations. According to Flory's equation for polymer swelling, presented in Chapter 3, the equilibrium swelling ratio to the 5/3 power is inversely proportional to the term representing the percent crosslinking. Pepper demonstrated this relationship with DVB crosslinked polystyrenes.[48]

The 8% crosslinked bead sensor did not show any change in reflected intensity with ion concentration. The

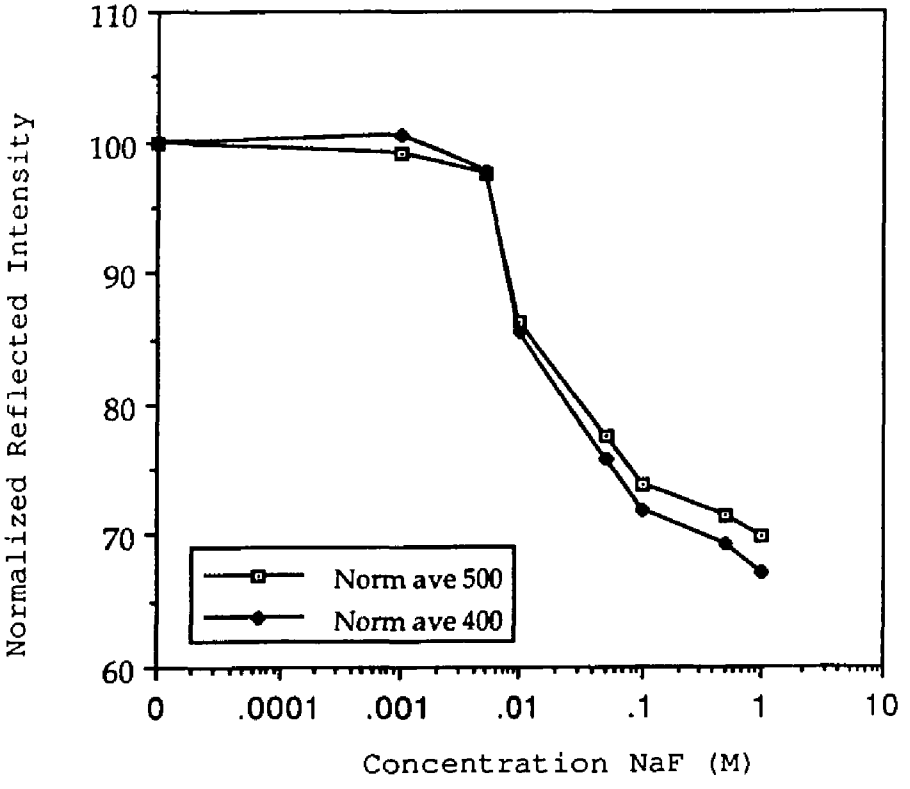

Figure 5.7: Response of a SP Sephadex bead (0.43 - 0.47 mm) dual fiber sensor with the green designated fiber carrying light from the source

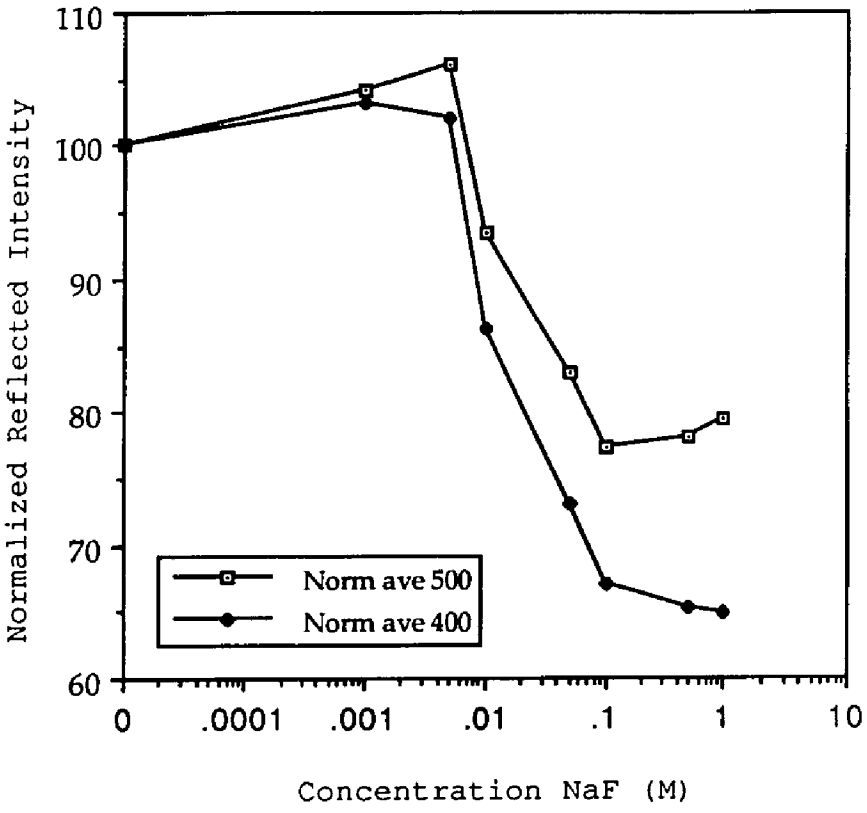

Figure 5.8: Response of a SP Sephadex bead (0.43 - 0.47 mm) dual fiber sensor with the green designated fiber carrying light to the detector

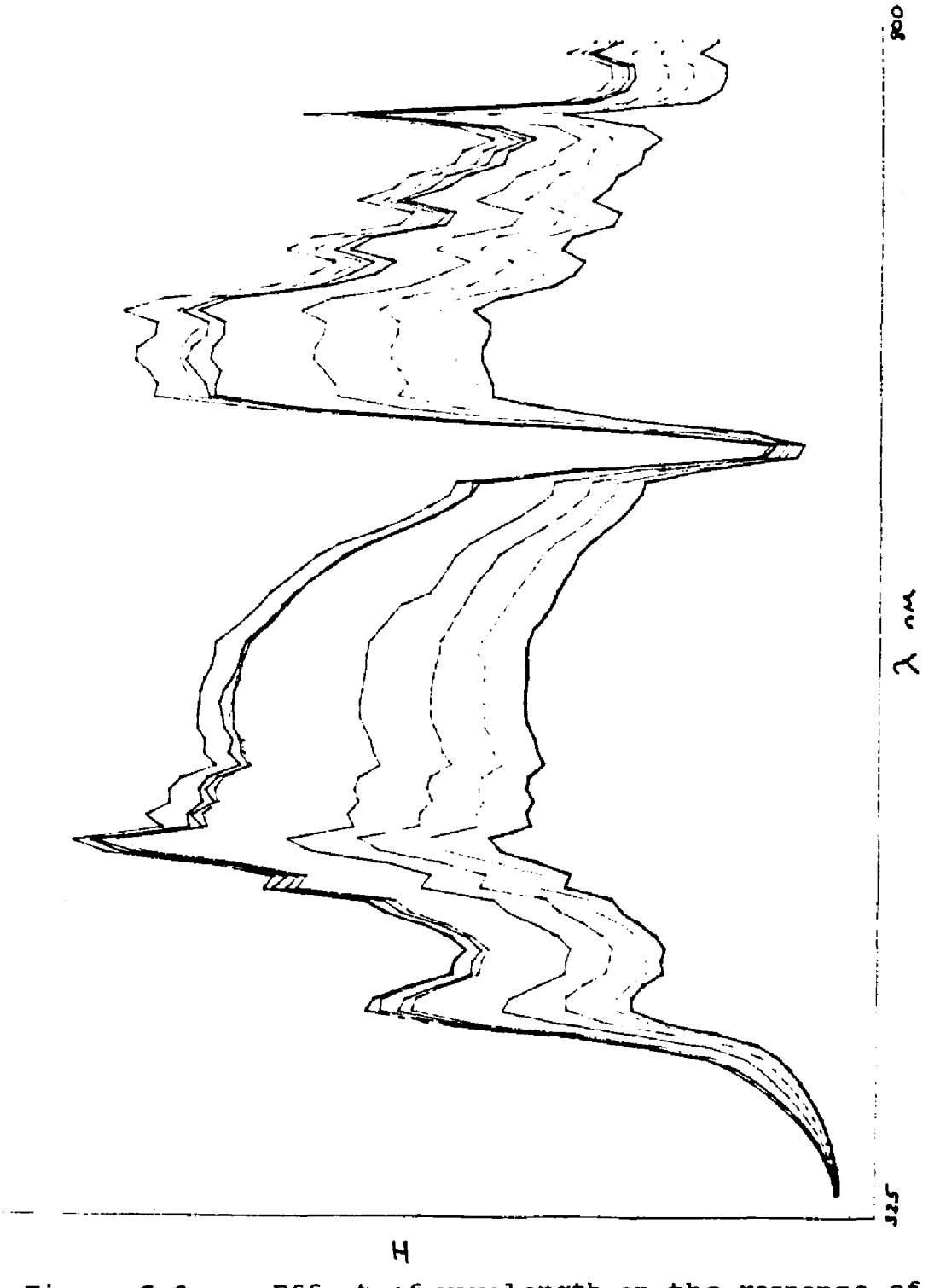

Figure 5.9: Effect of wavelength on the response of a 0.43 mm SP Sephadex bead dual fiber sensor as a function of ion concentration

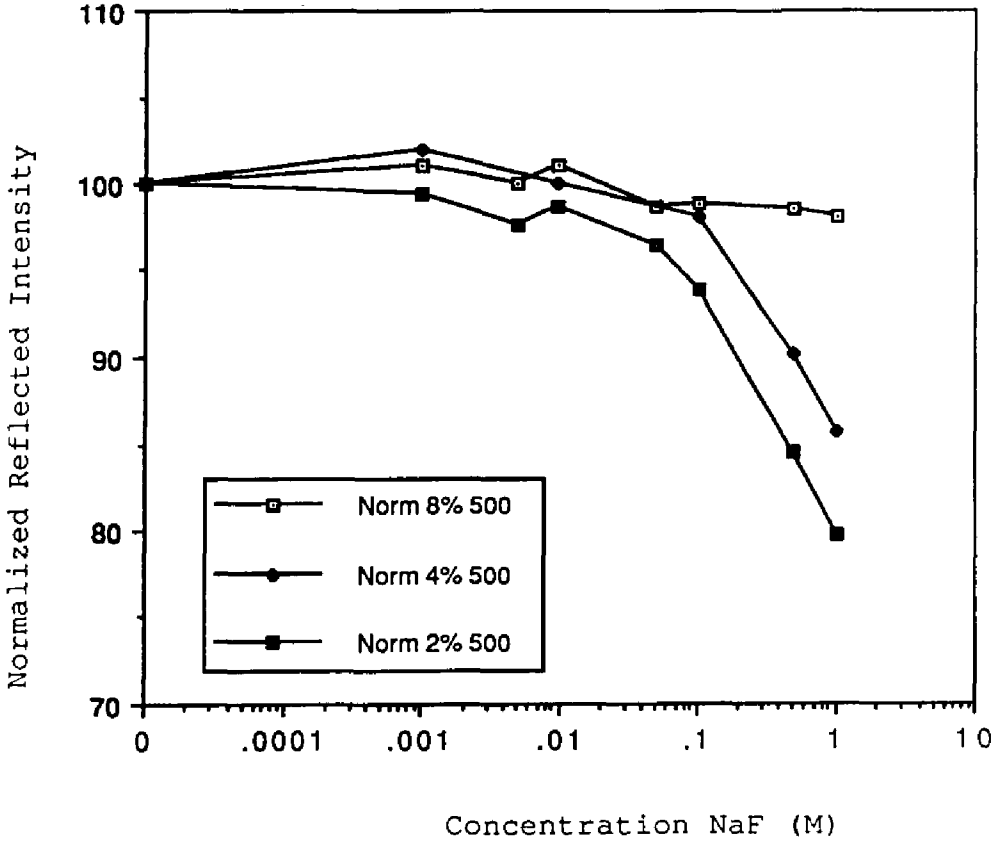

Figure 5.10: Effect of crosslinking on the response of a Dowex bead dual fiber sensor as a function of ion concentration at 500 nm

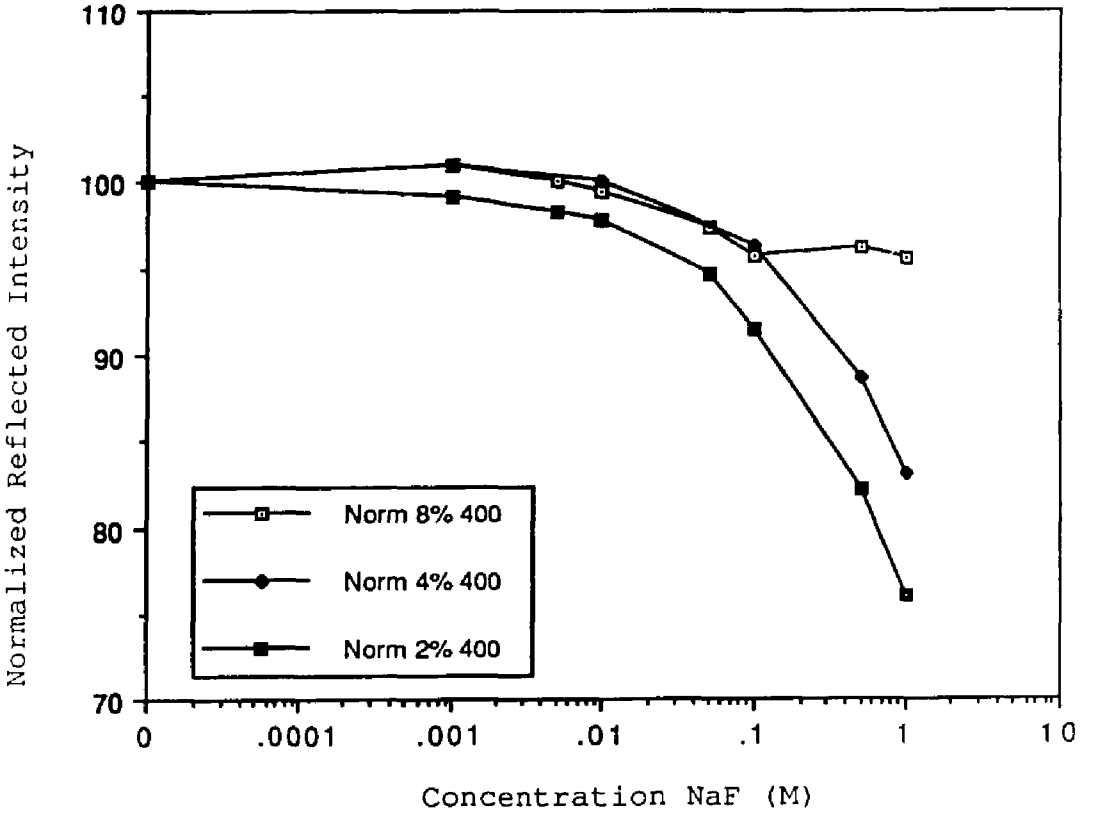

Figure 5.11: Effect of crosslinking on the response of a Dowex bead dual fiber sensor as a function of ion concentration at 400 nm

reflected intensity did change as a function of ion concentration with the 4% and 2% crosslinked bead sensors. At 500 nm the normalized reflected intensity decreased 15% and 20%, respectively, as the log of the molarity increased. At 400 nm the normalized reflected intensity decreased 17% and 24%, respectively, as the ion concentration increased.

Bead diameter. The response of the 2% crosslinked Dowex bead sensor as a function of bead diameter is given in Table 5.1 at 500 nm and in Table 5.2 at 400 nm. Reflector design number seven was employed and the experiment was performed in a black box. The diameters of the 2% Dowex beads were 0.41, 0.43 and 0.57 mm, respectively. The percent changes in the reflected intensity with ion concentration were 41%, 35% and 23% at 500 nm and 43%, 40% and 23% at 400 nm for the 0.41, 0.43 and 0.57 mm beads. The change in normalized reflected intensity as a function of ion concentration decreased as the bead diameter increased.

A better example of the relationship between bead size and the change in the normalized reflected intensity as a function of ion concentration is shown in Table 5.3. Table 5.3 compares a 0.33 mm and a 0.45 mm 2% Dowex bead sensor. The data for the 0.33 mm bead sensor was taken from Figures 5.2 and 5.3. The data for the 0.45 mm bead sensor was taken from Figures 5.10 and 5.11.

The effect of bead diameter was also examined with the single fiber arrangement. The results of this

Concentration NaF (M)	Normalized Reflected Intensity at 500 nm		
	0.41 mm	0.43 mm	0.57 mm
0.00001	100.0	100.0	100.0
0.00100	102.0	97.4	97.9
0.05000	97.5	93.6	99.2
0.10000	91.7	86.9	99.4
1.00000	58.6	65.1	77.0

Table 5.1: Effect of bead diameter on the response of 2% Dowex bead dual fiber sensor as a function of ion concentration at 500 nm

Concentration NaF (M)	Normalized Reflected Intensity at 400 nm		
	0.41 mm	0.43 mm	0.57 mm
0.00001	100.0	100.0	100.0
0.00100	101.8	95.5	97.7
0.05000	95.8	89.7	100.2
0.10000	90.5	81.0	100.8
1.00000	56.9	60.3	77.2

Table 5.2: Effect of bead diameter on the response of 2% Dowex bead dual fiber sensor as a function of ion concentration at 400 nm

Concentration NaF (M)	Normalized Reflected Intensity			
	0.33 mm		0.45 mm	
	500 nm	400 nm	500 nm	400 nm
0.00001	100.0	100.0	100.0	100.0
0.00100	100.3	99.9	99.4	99.2
0.00500	100.8	100.9	97.6	98.2
0.01000	101.0	102.2	98.6	97.8
0.05000	102.0	101.4	96.4	94.7
0.10000	98.3	96.3	93.9	91.5
0.50000	70.7	63.7	84.5	82.2
1.00000	59.9	51.8	79.7	76.0

Table 5.3: Effect of bead diameter on the response of 2% Dowex bead dual fiber sensor as a function of ion concentration

experiment are shown in Table 5.4. The ADC coupler and design number eight were used. The experiment was performed at night in a darkened room with 2% Dowex beads. The diameter of one bead was 0.45 mm. The estimated diameter range of the other bead was 0.33 - 0.43 mm. The normalized reflected intensity increased as the log of the molarity increased. The change in the normalized reflected intensity was slightly greater for the 0.45 mm bead than it was for the 0.33 - 0.43 mm bead. At 500 nm the change in the normalized reflected intensity was 11% for the 0.33 - 0.43 mm bead and 15% for the 0.45 mm bead. At 400 nm the changes were 6% and 15%, respectively.

Salt type. Finally, the salt type was varied. Both a 0.33 mm 2% crosslinked Dowex bead and a 0.45 mm SP Sephadex bead were studied. The experiment was executed with reflector design number eight at night in a darkened room.

The change in the normalized reflected intensity as a function of salt concentration for the Dowex bead sensor is shown in Figure 5.12 at 500 nm and Figure 5.13 at 400 nm. Note that the concentration range in these plots extended to 1.00 M salt. The changes in the normalized reflected intensity for the Dowex bead sensor from 0.00001 or distilled water to 1.00 were 75% for KCl, 73% for NaCl, 33% for CaCl2 and 40% for NaF at 500 nm and 69% for KCl, 62% for NaCl, 37% for CaCl2 and 48% for NaF at 400 nm. The changes

Concentration NaF (M)	Normalized Reflected Intensity			
	0.33 - 0.43 mm		0.45 mm	
	500 nm	400 nm	500 nm	400 nm
0.00001	100	100	100	100
0.00100	100	101	101	101
0.00500	102	102	102	102
0.01000	102	102	105	105
0.05000	104	103	104	106
0.10000	106	104	108	108
0.50000	107	104	112	112
1.00000	111	106	115	115

Table 5.4: Effect of bead diameter on the response of 2% Dowex bead single fiber sensor as a function of ion concentration

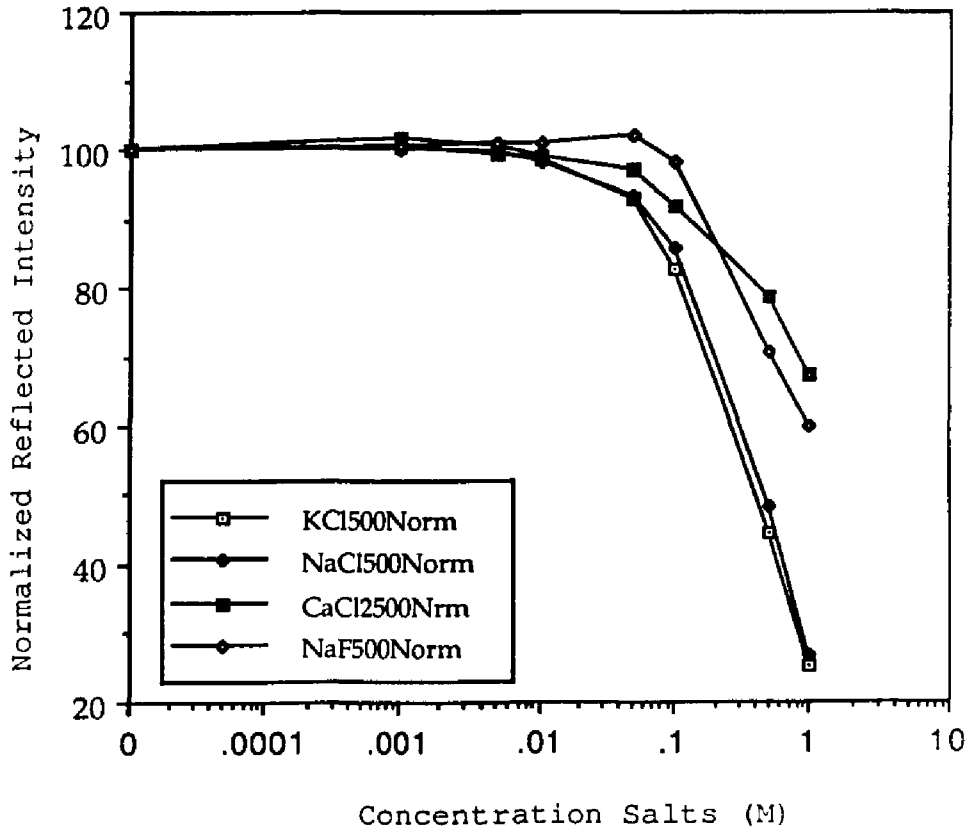

Figure 5.12: Effect of salt type on the response of a 0.33 mm 2% Dowex bead dual fiber sensor as a function of ion concentration at 500 nm

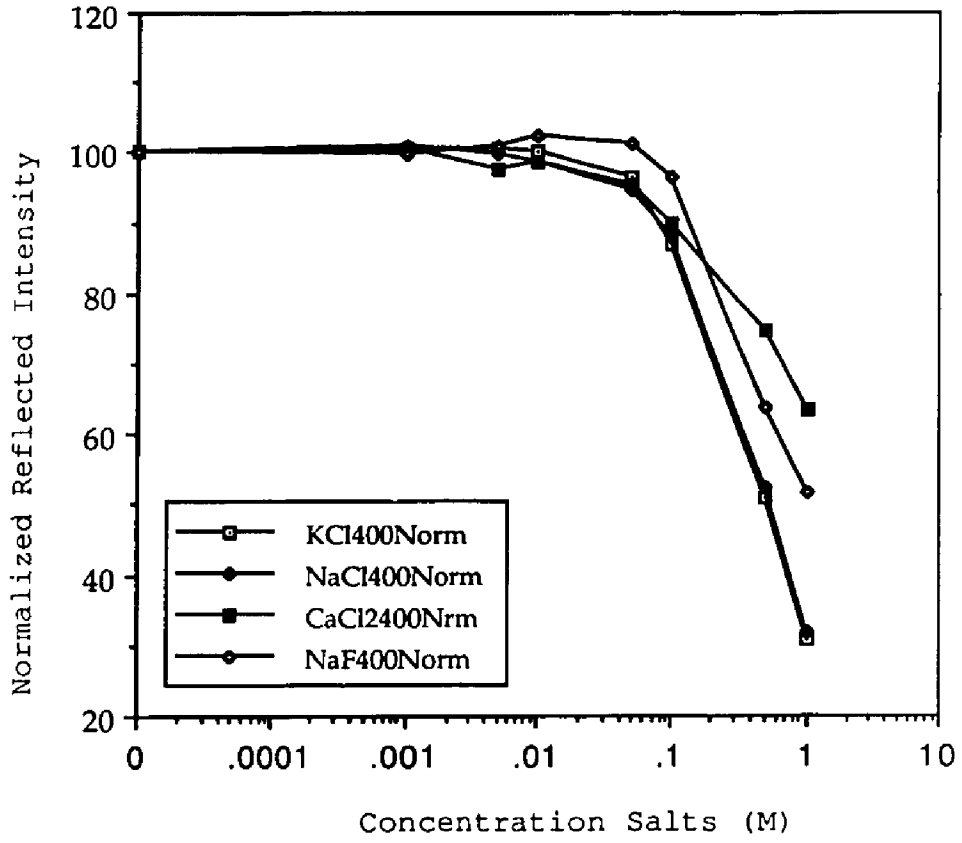

Figure 5.13: Effect of salt type on the response of a 0.33 mm 2% Dowex bead dual fiber sensor as a function of ion concentration at 400 nm

in the normalized reflected intensity for the Dowex bead sensor from 0.00001 to 0.100 were 17% for KCl, 14% for NaCl, 8% for CaCl2 and 2% for NaF at 500 nm and 13% for KCl, 12% for NaCl, 10% for CaCl2 and 3% for NaF at 400 nm.

The changes in the normalized reflected intensity as a function of the salt concentration for the SP Sephadex bead sensor are presented in Figure 5.14 at 500 nm and Figure 5.15 at 400 nm. Note that the concentration range in these plots extended to 0.100 M salt. The change in the normalized reflected intensity for the SP Sephadex bead sensor from 0.00001 to 0.100 was 45% for Na2SO4, 49% for NaCl and 52% for KCl at 500 nm and 51% for Na2SO4, 56% for NaCl and 59% for KCl at 400 nm.

Figure 5.16 shows the change in the normalized reflected intensity as a function of the square root of the ionic strength for the SP Sephadex bead sensor at 400nm and 500 nm. Figure 5.17 shows the change in the normalized reflected intensity as a function of the square root of the ionic strength for the Dowex bead sensor at 400 and 500 nm. The reflected intensity values are the same but the log of the molarity of the salts has been converted to the ionic strength.

Discussion

Ion concentration. The observed data are consistent with the expected characteristics of optical displacement sensing. For an isotropically illuminated optical

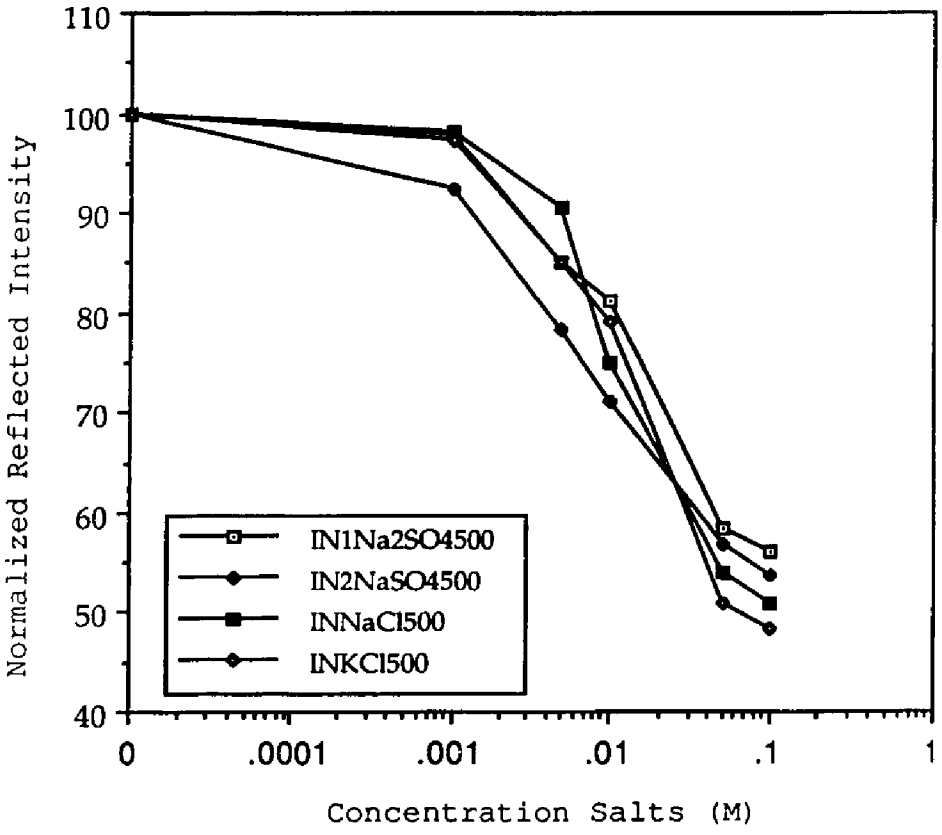

Figure 5.14: Effect of salt type on the response of a 0.45 mm SP Sephadex bead dual fiber sensor as a function of ion concentration at 500 nm

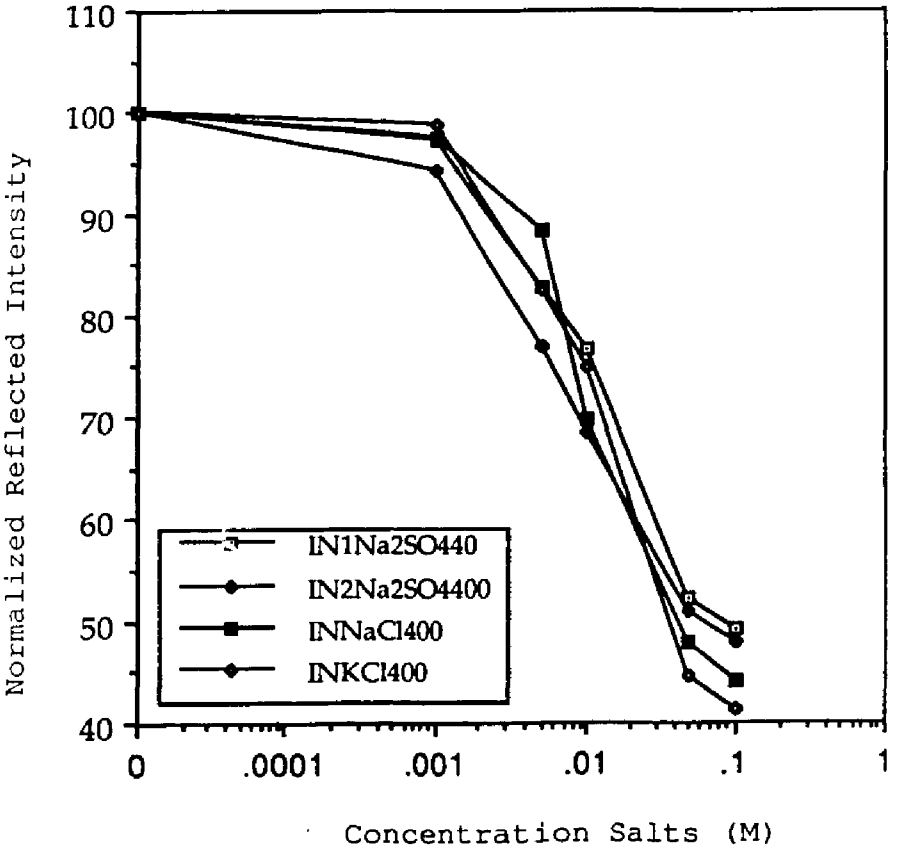

Figure 5.15: Effect of salt type on the response of a 0.45 mm SP Sephadex bead dual fiber sensor as a function of ion concentration at 400 nm

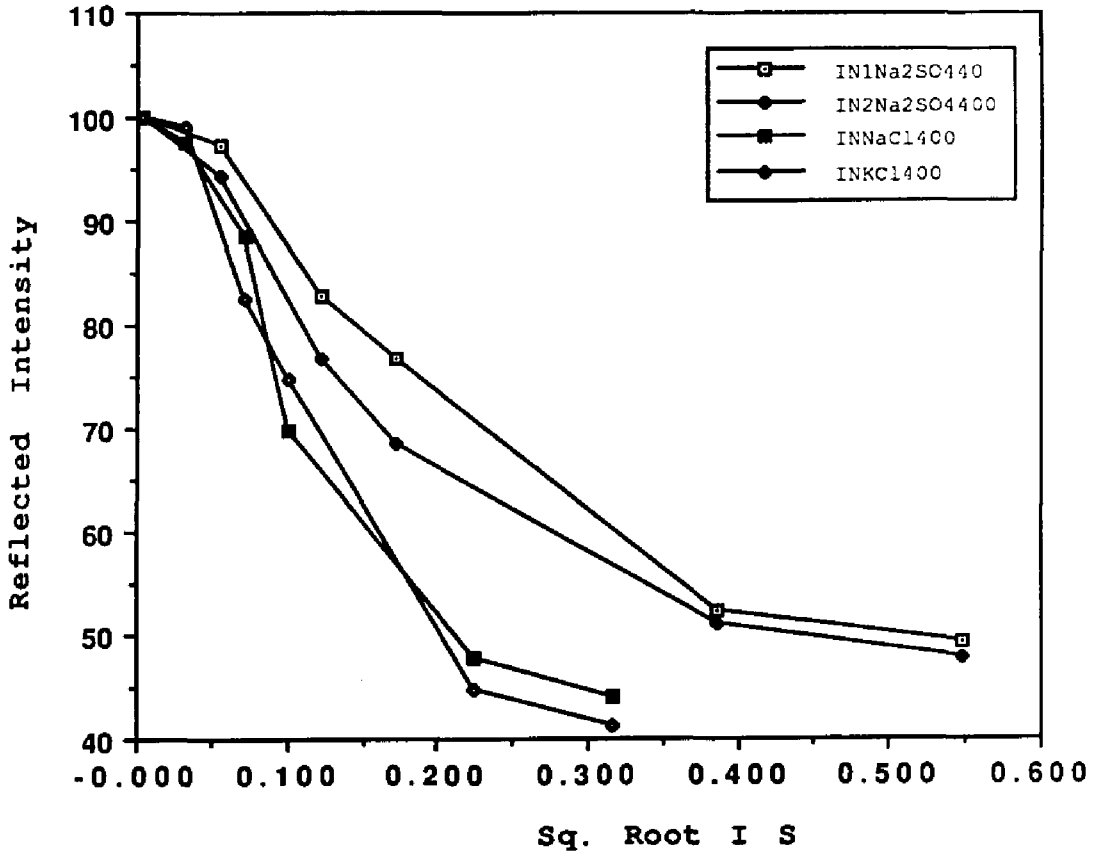

Figure 5.16: Effect of salt type on the response of a 0.45 mm SP Sephadex bead dual fiber s sensor as a function of the square root of the ionic strength

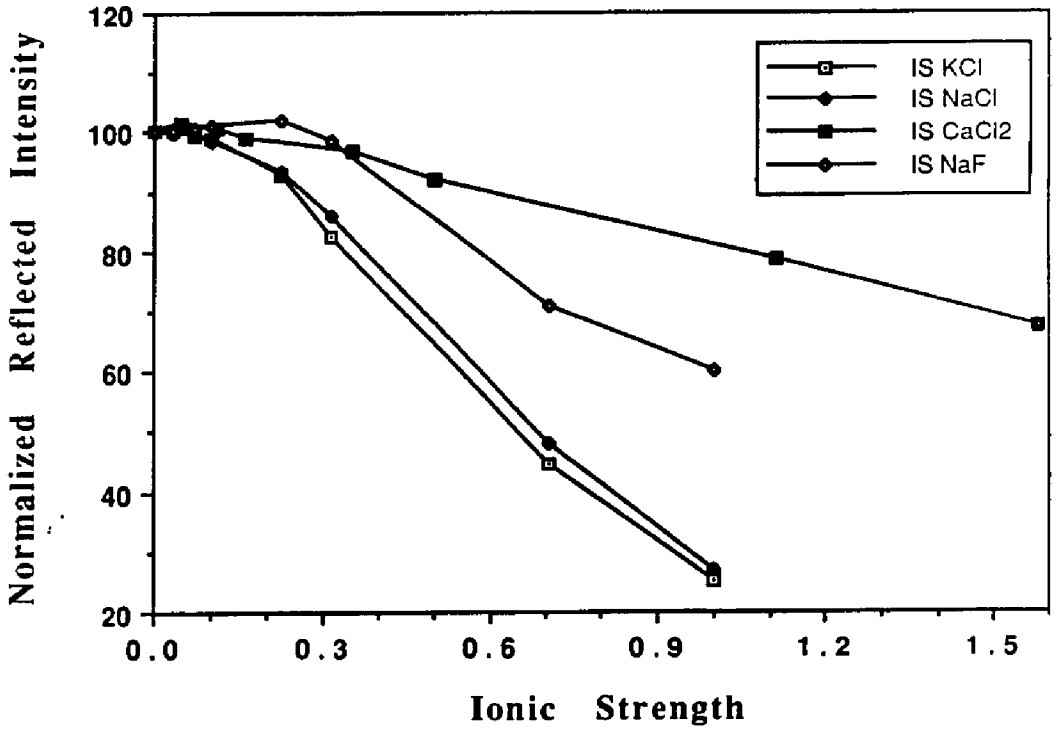

Figure 5.17: Effect of salt type on the response of a 0.33 mm 2% Dowex bead dual fiber sensor as a function of the square root of the ionic strength

displacement sensor with fibers that are immediately adjacent, the maximum in the power vs. displacement curve occurs at a distance of 400 micrometers[32]. The actual value will be influenced by factors such as the numerical aperture of the fiber and the distance between the fibers and is unknown for this work. However, 400 micrometers serves as a good estimate for interpreting the observed data. Note that this maximum occurs at a smaller distance between the fibers and the reflector than the maximum shown in Figure 3.4. The data in Figure 3.4 were taken for fibers that had not been stripped of buffer. This increases the distance between the fibers which in turn causes the power maximum to shift to larger displacements[32]. Figure 3.4 may be modified to include the displacement curve for adjacent fibers (r=200 micrometers) where the maximum occurs at 400 micrometers. The modified Figure 3.4 appears in Figure 5.18.

The actual displacement in this system may be estimated by subtracting the depth of the depression in the SMA connector (0.20 mm) from the diameters of the beads swollen in distilled water. Since the range of bead diameters employed extended from 0.33 - 0.65 mm, all but the largest of the beads had a response on the sensitive front slope of the displacement curve.

The decrease in reflected intensity with increasing ion concentration with the 2% crosslinked Dowex bead sensor indicated the response was on the more sensitive front slope

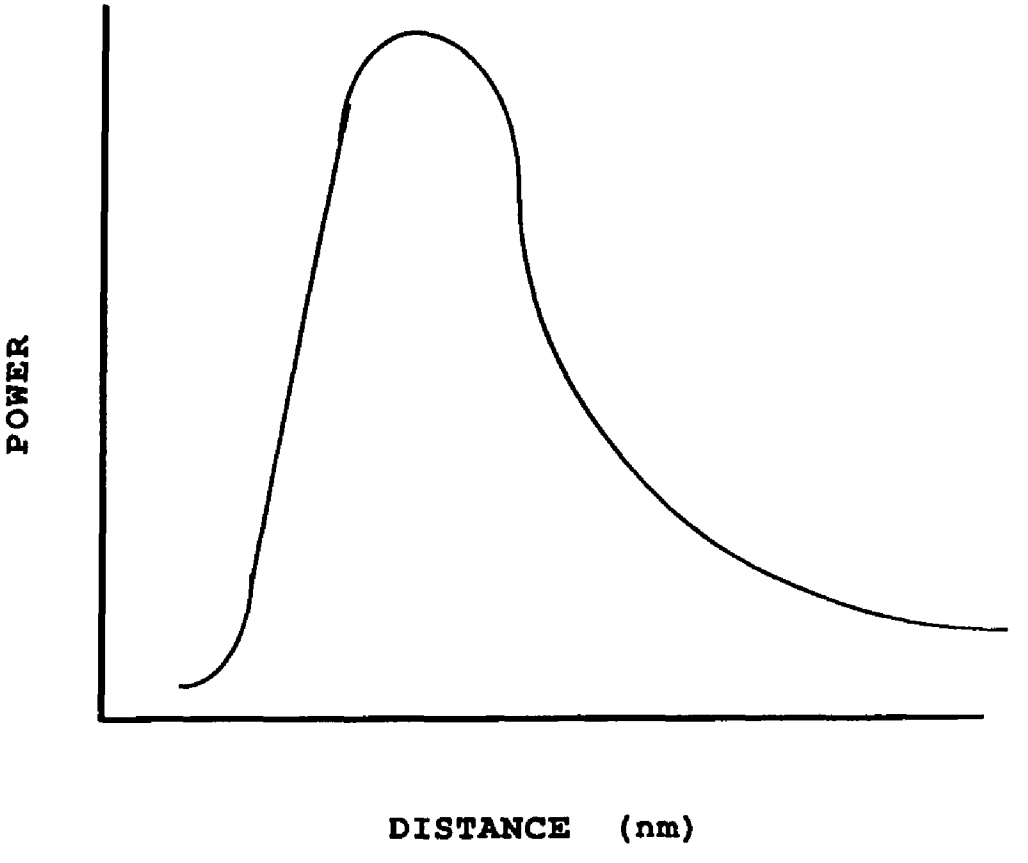

Figure 5.18: Theoretical displacement curve for adjacent fibers (r=200 micrometers)

of the displacement curve. A similar response was shown for the SP Sephadex sensor for the same reason. However, the intensity decrease was greater and occurred over a larger range of ion concentration, 0.001 to 1.00, than it did with the Dowex sensor. The larger change was expected since SP Sephadex is more compatible with water than Dowex 50W.

Dual versus single fiber probe. In the single fiber probe the increase in the normalized reflected intensity with increasing salt concentration was expected. As the concentration increased the bead shrunk and the intensity of light reflected increased. The was illustrated in Figures 3.5 and 3.6.

The dual fiber probe was preferred over the single fiber probe for two reasons. First, it is apparent in Figure 5.6, that the single fiber response was more erratic than the dual fiber response. Second, the change in the normalized reflected intensity for the same range of ion concentration is smaller. The relative change is smaller with single fiber measurements since a large background signal due to reflection at the interfaces is inherent in single fiber measurements.

Green to detector versus green to source. The change for the green taped fiber to the detector was smaller than that for the green taped fiber to the source. This effect was due to the relative positions of the two fibers in relation to the bead. The two fibers are close to

parallel with the green designated fiber slightly closer to the bead. This is illustrated in Figure 4.10. The ramp reflector complicates interpretation of the effect. Also, the normalized reflected intensity was more erratic with the green taped fiber to the detector. For this reason experiments were performed with the green taped fiber to the source.

Response versus wavelength. The absolute intensity response of the probe follows that of the instrumentation employed in the instrument. The normalized response was not affected by the wavelength dependence of the PMT or other instrumental effects. The numerical aperture of the optical fiber, however, is dependent on wavelength.

Percent crosslinking. The pattern of behavior for the Dowex bead sensor as the percent crosslinking increased was expected. As the crosslinking increased the bead became more rigid. Thus, the bead swelled less and the change in the reflected intensity with increasing ion concentration decreased. The difference in the response was not as large as expected, however. It is believed that this is because the bead sizes were not all the same. As shown in Tables 5.1-5.3 as the bead size increased the change in the normalized reflected intensity decreased.

To maximize response, it is necessary to establish the least amount of crosslinking necessary to maintain bead shape. If the crosslinking of the bead is decreased beyond

this point, the bead deforms instead of moving the reflector in contact with it.

Bead diameter. It was expected that the bead diameter would have an effect on the amount the normalized reflected intensity changed with ion concentration. The diameter of the bead in distilled water is the upper limit on the change in reflected intensity. The position of the upper limit on the displacement curve determines the magnitude of the change in reflected intensity. This is illustrated in Figure 5.18. The greatest change in reflected intensity per change in distance to the reflector is on the straight line portion of the front slope. The smallest change is when the fibers are very close to the reflector and at the maximum point in the displacement curve.

The Dowex 50W beads with diameters in the range from 0.33 - 0.43 mm gave the maximum response, while those in the range from 0.55 - 0.65 mm produced the least change in reflected intensity. After taking the depression in the SMA connector into account, the upper limits of the smaller and the larger beads are 0.13 - 0.23 mm and 0.35 - 0.45 mm, respectively. This places the response of the smaller bead on the straight line portion of the front slope and the response of the larger bead on the peak in the displacement curve.

The diameter of the SP Sephadex bead in distilled

water (0.43 - 0.47 mm) would place the response on the straight line portion of the front slope in the displacement curve. The SP Sephadex bead diameter which produced the greatest change in reflected intensity was larger than the Dowex 50W bead diameter which produced the greatest change. A possible explanation for this is that the Dowex 50W beads are more rigid than the SP Sephadex beads. So, the diameter of the SP Sephadex beads in distilled water may not be a good representation of the upper limit of the change in the reflected intensity.

While it was determined that the bead diameter has a definite effect on the reflected intensity, the best bead diameter was not determined. The range of diameters explored was limited to the bead diameters purchased. Finding the optimum bead size will be the subject of future work.

The relationship between the absolute intensity and the bead size could not be established, since the response had to be normalized to remove differences in the response due to placement of the bead, reflector fouling, source changes and reflector placement.

Salt type. The two bead sensors examined respond differently to salt concentration. The SP Sephadex bead sensor showed a linear relationship between the normalized reflected intensity and the log of the salt concentration from 0.001 M to 0.100. The normalized reflected intensity

changed as a function of the log concentration of the salt with Dowex bead sensor as well. The range, however, was smaller and shifted to the higher concentration end. The range extended from 0.100 to 1.00 M.

There was no apparent change in the response when the salt type was changed with the SP Sephadex bead sensor. A change was expected for the Na_2SO_4 solutions, since the concentration of the positive ion in the salt is double that of the other salts. The change may not be apparent since the concentration is only doubled and the concentrations are plotted on a log scale.

The Dowex bead sensor did appear to show some change in the reflected intensity with salt type. The same general trend was followed but the percent change in the response was different. It is believed this difference was not real for CaCl2 and NaF. NaCl and KCl showed no difference. It was noted at the conclusion of the experiment that the CaCl2 solutions caused the Dowex bead to fall apart. This changed the position of the reflector for the remainder of the experiment. The bead diameter was no longer a reasonable measure of the distance between the reflector and the ends of the fibers. The reason for the bead falling apart is unknown. It may be due to site bridging effects occurring with multiply charged ions. The reflected intensity change for the NaF solutions was determined after the CaCl2 solutions came into contact with the Dowex bead. Thus, the

reflector position was also changed for these measurements.

The SP Sephadex and the Dowex bead sensors did not show the relationship between swelling and the square root of the ionic strength as outlined by Flory and described in Chapter 3. Ohmine and Tanaka did note a relationship between the amount of swelling of an acrylamide gel and the valency of the positive ion of the salt They compared NaCl and $MgCl_2$.[49]

CHAPTER VI

SWELLING BASED pH SENSOR

Introduction

The second step in developing a new approach to sensing is to show that the method can be used to detect specific ions. This is most easily accomplished by demonstrating response to pH. Many pH sensors have been developed based on both electrochemical and optical principles. They are used extensively in almost every phase of chemistry as well as in other fields. However, all of the available pH sensors require periodic recalibration and do not operate unattended for extended lengths of time. Therefore, there is a niche for a polymer swelling based pH sensor if the ruggedness advantage can be realized in practice.

The sensing element in the pH sensor was the crosslinked polymer bead carboxymethyl Sephadex (CM Sephadex). It is a carboxylated dextran crosslinked with epichlorohydrin. The percent crosslinking of CM Sephadex was not reported in the product information. The polymer bead is a weakly acidic cation exchanger typically used in chromatographic columns. CM Sephadex was chosen because the Sephadex based beads employed in the ion concentration

sensor in Chapter 5 showed desirable swelling properties.

The variables that affect polymer swelling have been described in Chapter 3. Several of these variables were investigated in Chapter 5. The knowledge gained from these investigations was applied to this sensor. The critical variable which specifically affects pH measurements is the ionic strength of the solution. The experiments performed to investigate this parameter are detailed in this Chapter.

Experimental

Apparatus

The apparatus for measuring the displacement of the reflector due to swelling of the polymer and for measuring the bead diameter was described in Chapter 4. Design eight was employed in all experiments. An Orion Research Digital Ionalyzer/501 and a Ross combination electrode were used to measure pH.

Reagents

C-50-120 CM Sephadex was purchased from Sigma. NaCl and anhydrous sodium acetate were purchased from JT Baker Scientific. Glacial acetic acid was from VWR Scientific Inc..

Procedures

The polymer beads were handled in the same manner as described in Chapter 5. The displacement of the reflector as a function of pH was determined in the same manner as was the displacement as a function of ion concentration in

Chapter 5. Initialization was accomplished by immersing the bead first in a solution with pH 3.5 and then a solution with pH 6.0. These were the high and low ends of the range explored. The reflected intensity was normalized to 100 percent for pH 6.0.

The sample solutions were acetate buffers ranging in pH from 6.0 to 3.5. Initially, the ionic strength of these solutions was controlled by varying the concentrations of the acetic acid and the sodium acetate. The pH is varied by changing the ratio of the acid to the base. Later, the ionic strength was controlled by adding NaCl.

None of the beads used in the experiments were saved. The beads fell apart before they could be stored. In some instances a similar bead was saved. Of these beads the average diameter was 0.42 mm.

The standard parameters were as follows. A dual fiber arrangement was employed where the green fiber carried light from the source to the reflector. The displacement was measured at 500 nm.

Results and Discussion

Response versus pH

The normalized reflected intensity as a function of pH is shown in Figure 6.1. As the pH increased from 3.5 to 6.0 the normalized reflected intensity increased on average

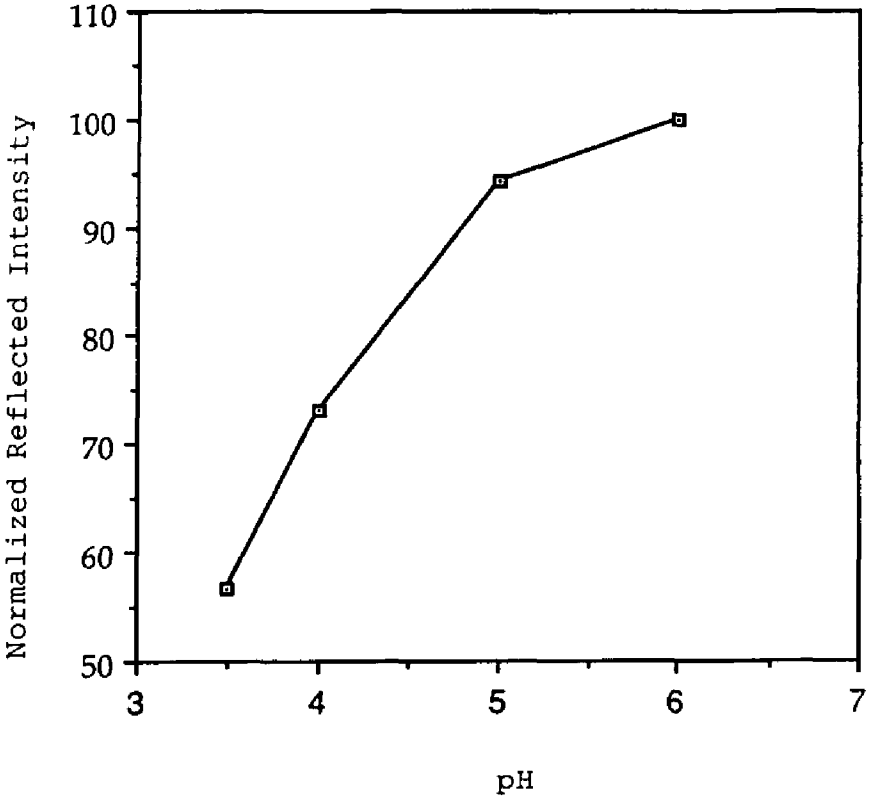

Figure 6.1: Response of the CM Sephadex bead dual fiber sensor as a function of pH at 0.01 ionic strength

43%. The ionic strength of the solutions was 0.01. The normalized reflected intensity changes are slightly greater than 10% for a pH change of 1.0 unit. If the source is stable to 1 part in 1000, this means that a change of 0.01 pH unit can be detected.

As the pH increased the concentration of H^+ ions in solution decreased which caused the CM Sephadex bead to swell. When the bead swelled the distance to the reflector increased, resulting in an increase in observed intensity as expected.

The diameter of the bead in distilled water places the response of the sensor on the straight line portion of the displacement curve. However, the CM Sephadex beads are not rigid and the diameter of the bead in distilled water may not be a good representation of the upper limit of the change in reflected intensity.

The sensor appeared to be most useful from 5.0 to 3.5 pH, since this was where the greatest change in reflected intensity occurred. The response did not level off. This indicated that the sensor could be useful at even lower pH's. This was not explored.

Ionic strength effect

The effect of ionic strength on the normalized reflected intensity is shown in Figure 6.2 at two ionic strengths, 0.100 and 0.010. The average change in the

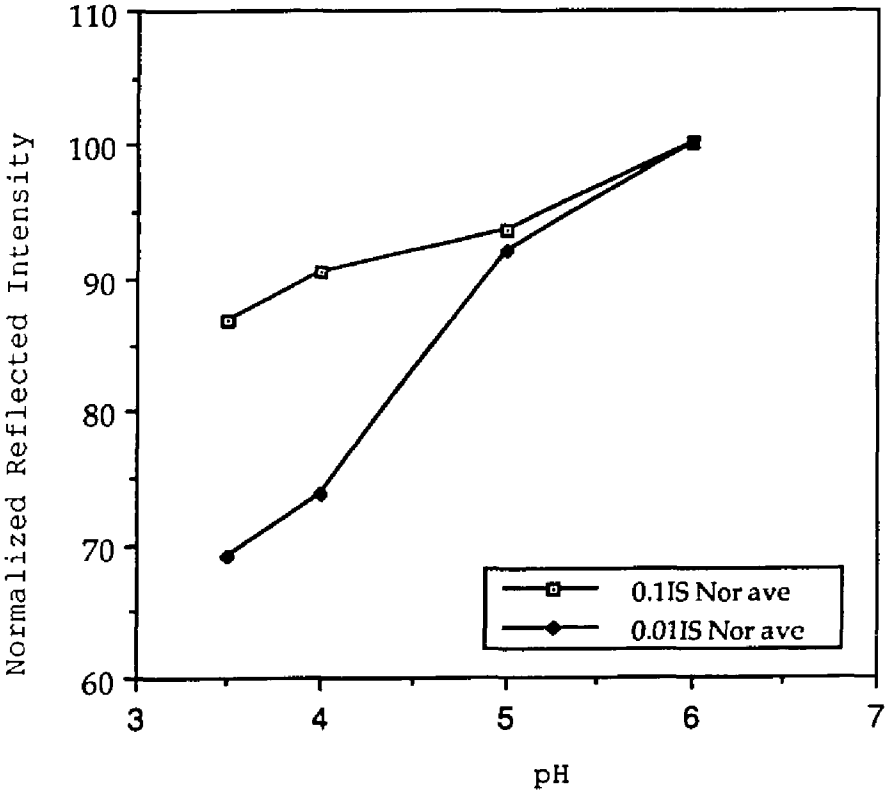

Figure 6.2: Effect of ionic strength on the response of the CM Sephadex bead dual fiber sensor as a function of pH

normalized reflected intensity at 0.100 ionic strength was 13% and at 0.010 ionic strength 30%.

The difference in the percent change in the normalized reflected intensity for 0.010 ionic strength in Figure 6.1 and Figure 6.2 is probably due to the different beads used in each experiment. The exact diameters of the beads were not known.

As the ionic strength increased the percent change in the normalized reflected intensity decreased. The ionic strength overpowers the response due to the pH change and the normalized reflected intensity remained relatively constant. As shown in Figure 5.16 with the SP Sephadex bead sensor, the normalized reflected intensity began to level out at 0.100 ionic strength for NaCl. This indicated that the bead had contracted as much as possible. Any increase in ionic strength beyond this point resulted in only small changes in the normalized reflected intensity.

The effect of lowering the ionic strength to 0.001 was also investigated. The results although not shown were erratic which indicated that the buffer capacity was not high enough to stabilize the pH measurement.

CHAPTER VII

CONCLUSION AND FUTURE WORK

The commercial product marketed as tris(carboxymethyl)ethylenediamine referred to in the context of this dissertation as "immobilized ligand" was shown to be ethylenediaminediacetic acid. While the various experiments performed support this finding, the conclusive evidence is found in the EPR spectra. While the characterization of the "immobilized ligand" is valuable to those in the scientific community presently using it for protein separation and metal preconcentration, it was not demonstrated that the "immobilized ligand" incorporates selectivity for anions into a FOCS. Before this can be accomplished, a method for measuring the anions selected must be developed.

Fiber optic chemical sensors based on swelling and optical displacement have been shown to be viable. They offer several advantages over conventional FOCS. There are several areas, however, where improvements in the subsystems comprising the sensor must be made before the sensor may be used in a practical sense.

The electrical subsystem is more than adequate for remote sensing applications since the spectrometer remains

in the protected environment of the laboratory and may service several sampling sites. However, by replacing the expensive and rather bulky spectrometer with light emitting diodes (LEDS) and photodiodes the entire sensor can be made inexpensive and portable.

The optical subsystem requires the most improvement. While the reflector assembly developed was adequate for showing that the concept was viable, it is crude at best. With the knowledge attained in this research and with the aid of a mechanical engineer, a better configuration has been developed. This arrangement appears in Figure 7.1. In this design the bead is held in contact with the non reflecting side of the reflector by a permeable membrane. As the bead swells the reflector compresses the spring which moves the reflector closer to the ends of the fibers. A spring has replaced the nylon and hooks and the reflector has been removed from the solution. This will prevent fouling of the reflector. It is also possible in this configuration to adjust the position of the reflector and the fibers, which is not possible in my design. A dual fiber arrangement is still employed, since this arrangement was found to offer the best combination of sensitivity and small size.

Once the engineering problems of the optical subsystem have been solved, the flexibility of the chemical subsystem may be fully realized. The first step is to

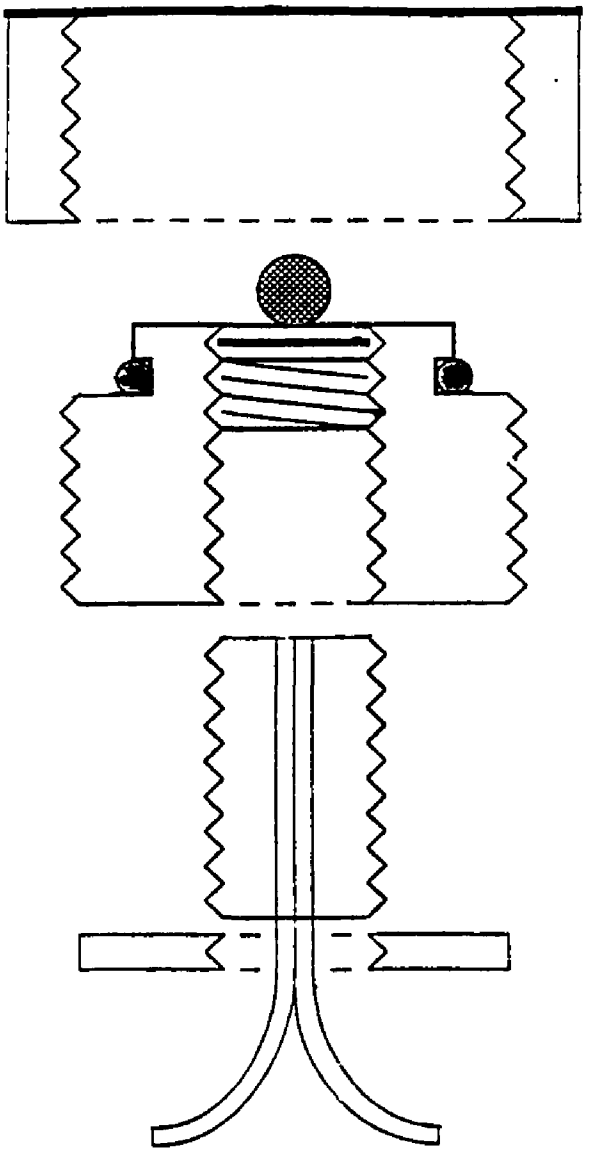

Figure 7.1: The future reflector/restoring system (design 9)

prepare the immobilized reagent phases in house so that parameters such as crosslinking and bead diameter can be controlled. The second step is to make the sensor specific for a variety of analytes. Both an immobilization substrate and a selection of modifiers are required. Suitable substrates include, polyvinylalcohol (PVOH), dextrans and polystyrene. Some possible modifiers include, N-(2-hydroxyethyl) ethylenediamine-triacetic acid (HEDT) for the detection of trace metal ions based on the charge of the ion and crosslinked cyclodextrans for the detection of organic molecules based on size. In fact any modifier-analyte combination may be incorporated into a sensor as long as the interaction effects the swelling of the polymer. Highly selective biomolecules such as penicillinase may be a modifier. Pencillinase catalyzes the reaction of penicillin to form penicillionic acid which is accompanied by a change in pH. As shown in this dissertation a pH change causes a change in the swelling of the polymer. Another possibility is no modifier at all. Unmodified PVOH may be used for the detection of water in organic solvents based on the solubility of PVOH in polar solvents such as water.

FOCS based on polymer swelling and optical displacement are far from competing in the market place with electrochemical or even other FOCS at the moment. However, it is believed by this investigator that one day they will

be a practical alternative to sensors based on more conventional techniques.

REFERENCES

1. Horn, D. Fiber Optic 1989, 16-41.

2. Seitz, W. R. in "CRC Critical Reviews in Analytical Chemistry" 1988, 19, 135-173.

3. Seitz, W. R. in "Biosensors: Fundementals and Applications" Oxford Science Publications Oxford University Press, 1987, 599-616.

4. Angel. S. M. Spectroscopy 1987, 2, 38-48.

5. Wolfbeis, O. S. Fresenius Zeitscrift Analytical Chemistry 1986, 325, 387-392.

6. Bowen, H. J. M. et al "Environmental chemistry Volume II" Royal Society of Chemistry, 1982, 90.

7. Horvath, D. J. "Trace Substances and Health" P.M. Newman, M. Dekker, 1976, 319.

8. Lehinger, A. L. "Principles of Biochemistry" Worth Publishers, 1982, 703.

9. Manahan, S. "Environmental Chemistry 2nd Edition" Willard Grant press, 1975, 185.

10. Narayanaswarmy, R; Sevilla, F. Analyst 1986, 111, 1085-1088.

11. Urbano, E.; Offenbacher, H.; Wolfbeis. O. S. Analytical Chemistry 1984, 56, 427-429.

12. Zhujun, Z; Mullin, J. L.; Tang, Y.; Seitz, W. R. in "Biosensors International Workshop" 1987, 229-234.

13. Hirschfeld, T.; Deaton, T.; Milanowich, F.; Klainer, S. M.; Fitzsimmons, C. "EPA report AD-89-F-2A074" 1984.

14. Narayanaswamy, R.; Russell, D. A.; Sevilla, F. Talanta 1988, 35, 83.

15. Japan Auto Parts Industries Association Nippondenso Co., Ltd. "Japan Kokai Tokkyo Koho JP 58,211,643 [83,211,643]" 1983, abstract 100:87796u.

16. Japan Auto Parts Industries Association Nippondenso Co., Ltd. "Japan Kokai Tokkyo Koho JP 58,211,641

[83,211,641]" 1983, abstract 100:87797v.

17. Sharp Corporation "Japan Kokai Tokkyo Koho JP 58 10,643 [83 10,643]" 1983, abstract 99:24525v.

18. Yamashita, K. (Matsushita Electric Industrial Co., Ltd.) "Japan Kokai Tokkyo Koho JP 61 44,340 [86 44,340]" 1986, abstract 104:209269e.

19. Nitto Electric Industrial Co., Ltd. "Japan Tokkyo Koho JP 82 10,370" abstract 97: 129595e.

20. Porath, J.; Carlsson, I.; Olsson, I.; Belfrage, G. Nature 1975, 258, 598-599.

21. Porath, J.; Olin, B. Biochemistry 1983, 22, 1621-1630.

22. Porath, J.; Olin, B.; Granstrand, B. Archives of Biochemistry and Biophysics 1983, 225, 543-547.

23. Lonnerdal, B.; Keen, C. L. Journal of Applied Biochemistry 1982, 4, 203-208.

24. Andersson, L. Journal of Chromatography 1984, 315, 167-74.

25. Heineman, W. R.; Mark, H. B.; Wise, J. A.; Roston, D. A. in "Laboratory Techniques in Electroanalytical Chemistry" Dekker, New York, 1984, 512.

26. Saari, L. A.; Seitz, W. R. Analytical Chemistry 1984, 56, 810-814.

27. Young, C. M.; Greenaway, F. T. Macromolecules 1986, 19, 484-486.

28. Flory, P. J. "Principles of Polymer Chemistry" Cornell University Press, New York, 1953.

29. Kesting, R. E. "Synthetic Polymeric Membranes: A Structural Perspective Second Edition" John Wiley and Sons, New York, 1985.

30. Helfferich, F. "Ion Exchange" McGraw Hill Book Co., Inc., New York, 1962.

31. Mingqi, B. private communication

32. Cook, R. O.; Hamm, C. W. Applied Optics 1979, 18, 3230-

3241.

33. Kissinger, C. Measurements and Control in product information from Mechanical Technology Incorporated, April 1988.

34. Bauer, R. "Development of a Glucose Sensor Based on Competitive Binding and Laser Excited Fluorescence" University of New Hampshire Dissertation, 1989.

35. Lindheimer, A.; Molenat, J.; Gavach, C. Journal of Electroanalytical Chemistry 1987, 216, 71-88.

36. Yeo, R. S. Journal of Applied Polymer Science 1986, 32, 5733-5741.

37. McCain, G. H.; Covitch M. J. Journal of the Electrochemical Society:Electrochemical Science and Technology 1984, 131, 1350-1352.

38. Narebska, A.; Wodzki, R.; Erdmann, K. Die Angewandte Makromolekulare Chemie 1983, 111, 85-95.

39. Lopez, M.; Kipling, B.; Yeager, H. L. Analytical Chemistry 1976, 48, 1120-1122.

40. Szentirmay, M. N.; Martin, C. R. Analytical Chemistry 1984, 56, 1898-1902.

41. Yeo, R. S.; Chan, S. F.; Lee, J. Journal of Membrane Science 1981, 9, 273-283.

42. Narebska, A.; Wodzki, R. Die Angewandte Makromolekulare Chemie 1982, 107, 51-60.

43. Yeager, H. L.; Steck, A. Analytical Chemistry 1979, 51, 862-865.

44. Steck, A.; Yeager, H. L. Analytical Chemistry 1980, 52, 1215-1218.

45. Zundel, G. "Hydration and Intermolecular Interaction: Infrared Investigations with Polyelectrolyte Membranes" Academic Press, NY, 1969, 232-243.

46. Hicks, G. P.; Updike, S. J. Analytical Chemistry 1966, 38, 726-730.

47. Fawcett, J. S.; Morris, C. J. O. R. Separation Science

1966, 1, 9-26.

48. Pepper, K. W. Journal of Applied Chemistry 1951, 1, 124-132.

49. Ohmine, I.; Tanaka, T. Journal of Chemical Physics 1982, 77, 5725-5729.